

NASA TECHNICAL NOTE



NASA TN D-7996

NASA TN D-7996

CASE FILE
COPY

NUMERICAL ANALYSIS AND PARAMETRIC STUDIES
OF THE BUCKLING OF COMPOSITE ORTHOTROPIC
COMPRESSION AND SHEAR PANELS

Jerrold M. Housner and Manuel Stein

Langley Research Center

Hampton, Va. 23665



NATIONAL AERONAUTICS AND SPACE ADMINISTRATION • WASHINGTON, D. C. • OCTOBER 1975

1. Report No. NASA TN D-7996	2. Government Accession No.	3. Recipient's Catalog No.	
4. Title and Subtitle NUMERICAL ANALYSIS AND PARAMETRIC STUDIES OF THE BUCKLING OF COMPOSITE ORTHOTROPIC COMPRESSION AND SHEAR PANELS		5. Report Date October 1975	6. Performing Organization Code
		8. Performing Organization Report No. L-10083	10. Work Unit No. 505-02-51-01
7. Author(s) Jerrold M. Housner and Manuel Stein		11. Contract or Grant No.	13. Type of Report and Period Covered Technical Note
9. Performing Organization Name and Address NASA Langley Research Center Hampton, Va. 23665		14. Sponsoring Agency Code	
		12. Sponsoring Agency Name and Address National Aeronautics and Space Administration Washington, D.C. 20546	
15. Supplementary Notes			
16. Abstract <p>A computer program is presented which has been developed for the combined compression and shear of stiffened variable thickness orthotropic composite panels on discrete springs; boundary conditions are general and include elastic boundary restraints. Buckling solutions are obtained by using a newly developed trigonometric finite-difference procedure which improves the solution convergence rate over conventional finite-difference methods. The classical general shear-buckling results (in terms of universal orthotropic parameters), which exist only for simply supported panels over a limited range of orthotropic properties, have been extended to the complete range of these properties for simply supported panels and, in addition, to the complete range of orthotropic properties for clamped panels. The program has also been applied to parametric studies which examine the effect of filament orientation upon the buckling of graphite-epoxy panels. These studies included an examination of the filament orientations which yield maximum shear or compressive buckling strength for panels having all four edges simply supported or clamped over a wide range of aspect ratios. Panels with such orientations had higher buckling loads than comparable, equal-weight, thin-skinned aluminum panels. Also included among the parameter studies were examinations of combined axial compression and shear buckling and examinations of panels with rotational elastic-edge restraints.</p>			
17. Key Words (Suggested by Author(s)) Buckling Orthotropic plates Finite differences Filamentary composite plates		18. Distribution Statement Unclassified - Unlimited Subject Category 39	
19. Security Classif. (of this report) Unclassified	20. Security Classif. (of this page) Unclassified	21. No. of Pages 102	22. Price* \$ 5.25

NUMERICAL ANALYSIS AND PARAMETRIC STUDIES OF THE BUCKLING OF COMPOSITE ORTHOTROPIC COMPRESSION AND SHEAR PANELS

Jerrold M. Housner and Manuel Stein
Langley Research Center

SUMMARY

A computer program has been developed for the combined compression and shear of stiffened variable thickness orthotropic composite panels on discrete springs; boundary conditions are general and include elastic boundary restraints. Buckling solutions are obtained by using a newly developed trigonometric finite-difference procedure which improves the solution convergence rate over conventional finite-difference methods. The trigonometric finite-difference procedure introduces two new parameters into the solution. These parameters can be computed by the program or selected by the user. The validity of the program has been substantiated by comparisons with existing solutions, and a program listing, input description, and sample problem are provided.

The classical general shear-buckling results (in terms of universal orthotropic parameters), which exist only for simply supported panels over a limited range of orthotropic properties, have been extended to the complete range of these properties for simply supported panels and, in addition, to the complete range of orthotropic properties for clamped panels. The program has also been applied to parametric studies which examine the effect of filament orientation upon the buckling of graphite-epoxy panels. These studies included an examination of the filament orientations which yield maximum shear or compressive buckling strength for panels having all four edges simply supported or clamped over a wide range of aspect ratios. Panels with such orientations had higher buckling loads than comparable, equal-weight, thin-skinned aluminum panels. Also included among the parameter studies were examinations of combined axial compression and shear buckling and examinations of panels with rotational elastic-edge restraints.

INTRODUCTION

The use of filamentary composite materials in aircraft and space structures offers a potential for weight savings over conventional (all metal) construction. Also, composites introduce added versatility into the design process by allowing the structure to be better tailored to meet the design criteria. One such design criterion is the prevention of compressive and shear buckling in panels of laminated construction. In laminated

panels the stiffness properties can be tailored by controlling the filament orientation in each lamina.

A considerable amount of literature exists on the buckling of flat isotropic and orthotropic panels under various boundary conditions. (See refs. 1 to 6.) Few results exist, however, for finite aspect-ratio panels, especially for shear buckling of orthotropic panels. General results for shear buckling, in terms of universal orthotropic parameters, exist only for simply supported panels over a limited range of orthotropic parameters. (See ref. 6.) Several general-purpose computer programs exist which could be employed to obtain results for panels with general boundary conditions under general loading states (refs. 7 to 9). These programs, however, tend to be expensive to use in performing parameter studies; therefore, a program which is suitable for performing parametric buckling studies of orthotropic flat rectangular panels was developed and is employed in this paper.

The present computerized analysis is applicable to the combined compression and shear buckling of stiffened, variable-thickness, flat rectangular orthotropic panels on discrete springs; boundary conditions are general and include elastic boundary restraints. Calculation of the flexural stiffnesses of a laminate from the properties of filament-reinforced laminas is automatically performed. The analysis makes use of a newly developed trigonometric finite-difference procedure. In contrast to conventional (polynomial) finite differences, trigonometric differences take advantage of the sinusoidal form of the buckle pattern to achieve converged solutions with fewer degrees of freedom, hence reducing computer time. The analysis has been validated by many comparisons with solutions in the literature and has been used to produce a variety of additional orthotropic and some isotropic panel results.

The classical general results for the shear buckling of simply supported orthotropic panels are extended in this paper to cover the complete range of orthotropic parameters. Also, the general results for the shear buckling of clamped panels over the complete range of orthotropic parameters have been calculated and are presented herein. In addition, it is of practical interest to present results which consider the effects of filament orientation upon the buckling strength of laminated composite panels. Consequently, parameter studies are presented for graphite-epoxy panels of various aspect ratios, boundary conditions, and in-plane loadings over a wide range of filament orientations, and those orientations which led to maximum buckling loads are identified. Finally, results are presented for the shear buckling of simply supported isotropic panels, each with a central stiffener.

SYMBOLS

a,b	dimensions of rectangular plate parallel to X- and Y-axes, respectively
$A^{(r)}$	coefficients defined by equation (C3)
C_x, C_{yx}	correction factors defined in equations (B4) and (B5)
D	isotropic plate flexural stiffness
D_3	$= D_{12} + 2D_{66}$
$D_{11}, D_{22}, D_{12}, D_{66}$	orthotropic plate flexural stiffnesses
$e_{ij}^{(r)}$	elements of matrix defined by equation (C2)
EI	flexural stiffness of discrete stiffener
E_1, E_2	Young's moduli of fibrous reinforced material parallel to fibers and transverse to fibers, respectively
G_{12}	shear modulus of fibrous reinforced material
h	core thickness of sandwich plate
I_1, I_3	row designations of boundaries ① and ③ (see fig. 2(a))
J_2, J_4	column designations of boundaries ② and ④ (see fig. 2(a))
k_ℓ	discrete lateral spring stiffness
k_R	uniformly distributed rotational spring stiffness
k_S	shear-buckling load coefficient $\frac{b^2 N_{xy}}{\pi^2 \sqrt[4]{D_{11} D_{22}^3}}$
k_x, k_y	stiffness of rotational springs which resist moments acting about Y- and X-axes, respectively

K_{ij}	plate stiffness terms defined by equation (A13)
M, N	total number of rows and columns of finite-difference stations, respectively
M_e, N_e	total number of rows and columns of finite-difference stations at which equilibrium is satisfied
M_x, M_y, M_{xy}	bending moments in plate (see fig. 1)
N_x, N_y, N_{xy}	in-plane loads (see fig. 1)
$\bar{N}_x, \bar{N}_y, \bar{N}_{xy}$	shear-buckling stress coefficients respectively $\frac{b^2 N_x}{\pi^2 D_{11}}, \frac{b^2 N_y}{\pi^2 D_{11}}, \frac{b^2 N_{xy}}{\pi^2 D_{11}}$
$\hat{N}_x, \hat{N}_y, \hat{N}_{xy}$	buckling parameters respectively $\frac{b^2 N_x}{E_1 t^3 \left[1 - \left(\frac{h}{t}\right)^3\right]}, \frac{b^2 N_y}{E_1 t^3 \left[1 - \left(\frac{h}{t}\right)^3\right]}, \frac{b^2 N_{xy}}{E_1 t^3 \left[1 - \left(\frac{h}{t}\right)^3\right]}$
N_{x_0}, N_{xy_0}	buckling loads for pure axial compression and pure shear, respectively
\bar{p}	buckling eigenvalue (see eq. (13))
r_x, r_y, r_{xy}	change of $\bar{N}_x, \bar{N}_y, \bar{N}_{xy}$ with \bar{p} , respectively (see eq. (13))
R_x, R_{xy}	ratio of N_x/N_{x_0} and N_{xy}/N_{xy_0} , respectively
S_{ij}	spring-stiffness terms defined by equation (A17)
t	total thickness of sandwich plate
$\bar{t}_x, \bar{t}_y, \bar{t}_{xy}$	values of N_x, N_y, N_{xy} when $\bar{p} = 0$
w	displacement of panel in positive z -direction
x, y, z	panel coordinates shown in figure 1

α_{ij}	curvature terms defined in equation (A14)
β	ratio of panel width to buckle length in an infinitely long panel
$\gamma_1, \gamma_2, \gamma_3$	coefficients defined by equation (7) or (8)
δU	internal virtual work
δV_N	virtual work of in-plane loads
δV_S	virtual work of discrete springs
Δ_x, Δ_y	finite-difference mesh spacings in x- and y-directions, respectively
$\hat{\Delta}_x, \hat{\Delta}_y$	trigonometric finite-difference coefficients as defined in equation (10)
Δ_x^*, Δ_y^*	trigonometric finite-difference terms defined in equation (A24)
θ	filament orientation (see fig. 2(a))
Θ, B	universal orthotropic parameters defined in equations (15) and (16)
λ_x, λ_y	trigonometric parameters defined through equation (10)
ν_{12}	major Poisson ratio relating contraction normal to filament direction to extension parallel to filament direction
$\xi_x, \xi_y, \eta_x, \eta_y$	functions defined by equations (A6) to (A9)
χ_{ij}	twist terms defined in equation (A16)
ψ_{ij}	curvature terms defined in equation (A15)

Comma preceding a subscript denotes differentiation with respect to the subscript.

ANALYSIS

Assumptions

The buckling analysis of linear elastic orthotropic plates has been carried out under the following assumptions:

1. Coupling between bending and extensional deformation is neglected. (In practice this assumption implies a midplane symmetric laminated panel.)
2. Coupling between bending and twisting deformation is neglected. (In practice this assumption implies a balanced laminate.)
3. The deformations of the panel obey the Kirchhoff hypothesis (see ref. 10).
4. The nonlinear strain-displacement relationships used to obtain (linear) buckling equations are

$$e_x = u_{,x} + \frac{1}{2}(w_{,x})^2$$

$$e_y = v_{,y} + \frac{1}{2}(w_{,y})^2$$

$$\gamma_{xy} = u_{,y} + v_{,x} + w_{,x}w_{,y}$$

where e_x , e_y , and γ_{xy} are the strains and u , v , and w are the displacements in x -, y -, and z -directions, respectively.

5. The in-plane loads, N_x , N_y , and N_{xy} , are uniformly distributed along the appropriate edges of the plate.

6. Discrete stiffeners have no torsional stiffness and are symmetrically disposed with respect to the neutral surface of the panel.

Governing Equations

The internal virtual work of the panel during buckling may be expressed as

$$\delta U = \int_0^b \int_0^a (M_x \delta w_{,xx} + M_y \delta w_{,yy} + 2M_{xy} \delta w_{,xy}) dx dy \quad (1)$$

where a and b are the dimensions of the panel parallel to the X - and Y -axes, respectively, and δ is the variational operator. Also,

$$\left. \begin{aligned} M_x &= D_{11}w_{,xx} + D_{12}w_{,yy} \\ M_y &= D_{12}w_{,xx} + D_{22}w_{,yy} \\ M_{xy} &= 2D_{66}w_{,xy} \end{aligned} \right\} \quad (2)$$

The sign conventions of the bending moments are given in figure 1, and the flexural stiffnesses, D_{11} , D_{12} , D_{22} , and D_{66} , given in reference 11, are about a unique neutral plane which has the property that matrix $[B]$, which represents coupling between bending and extension, is null with respect to this plane. As given by reference 12, the virtual work of the applied in-plane loads is given by

$$\delta V_N = \int_0^a \int_0^b (N_x w_{,x} \delta w_{,x} + N_y w_{,y} \delta w_{,y} + N_{xy} w_{,y} \delta w_{,x} + N_{xy} w_{,x} \delta w_{,y}) dy dx \quad (3)$$

where the sign conventions for N_x , N_y , and N_{xy} are shown in figure 1.

In appendix A, equations (A1) to (A3) are expressed in trigonometric finite-difference form (see fig. 2 for finite-difference station layout) and are substituted into the statement of the principle of virtual work, that is,

$$\delta U = \delta V_N + \delta V_S \quad (4)$$

where δV_S is the virtual work of the discrete springs. (See appendix A, eq. (A11).) Equation (4) yields the governing equations which are of the following form:

$$K_{ij} + S_{ij} + N_x \alpha_{ij} + N_y \psi_{ij} + 2N_{xy} \chi_{ij} = 0 \quad \left(\begin{array}{l} i = 1, \dots, M \\ j = 1, \dots, N \end{array} \right) \quad (5)$$

where K_{ij} , S_{ij} , α_{ij} , ψ_{ij} , and χ_{ij} are defined by equations (A13) to (A17) in appendix A.

The numerical technique of trigonometric finite differences and the numerical extraction of the buckling loads N_x , N_y , and N_{xy} from equation (5) are different from those conventionally used and therefore require further discussion.

Numerical Techniques

Trigonometric finite differences. - Conventionally, the central difference approximation for the derivative of a function $f(x)$ at $x = x_0$ is approximated as

$$\frac{df}{dx}(x_0) \approx \frac{1}{\Delta_x} \left[f\left(x_0 + \frac{\Delta_x}{2}\right) - f\left(x_0 - \frac{\Delta_x}{2}\right) \right] \quad (6)$$

The right-hand side of equation (6) is denoted as the conventional finite-difference approximation for the derivative. In the limit as the finite-difference mesh spacing Δ_x approaches zero, the right-hand side of equation (6) expresses the definition of the derivative. If $f(x)$ is parabolic in the neighborhood of x_0 ,

$$f(x) = \gamma_1 + \gamma_2(x - x_0) + \gamma_3(x - x_0)^2 \quad (7)$$

and it may be readily shown that the approximate expression given by equation (6) becomes an equality. If, however, $f(x)$ is trigonometric about $x = x_0$,

$$f(x) = \gamma_1 + \gamma_2 \sin \frac{\pi(x - x_0)}{\lambda_x} + \gamma_3 \cos \frac{\pi(x - x_0)}{\lambda_x} \quad (8)$$

where λ_x is a wavelength parameter. It may be readily shown that

$$\frac{df}{dx}(x_0) = \frac{1}{\hat{\Delta}_x} \left[f\left(x_0 + \frac{\Delta_x}{2}\right) - f\left(x_0 - \frac{\Delta_x}{2}\right) \right] \quad (9)$$

where

$$\frac{1}{\hat{\Delta}_x} = \frac{\pi}{2\lambda_x \sin\left(\frac{\pi\Delta_x}{2\lambda_x}\right)} \quad (10)$$

The right-hand side of equation (9) is denoted as the trigonometric finite-difference approximation for the derivative. (In a two-dimensional problem a similar set of relationships would be derived for the y-direction, introducing the quantities Δ_y , $\hat{\Delta}_y$, and λ_y .)

The only difference between the right-hand side of equation (9) and that of equation (6) is that in the trigonometric expression $1/\hat{\Delta}_x$ replaces $1/\Delta_x$ of the conventional expression. As λ_x approaches infinity, $\hat{\Delta}_x$ approaches Δ_x and, consequently, the trigonometric difference expression reduces to the conventional expression.

Convergence of trigonometric finite-difference solutions.- Inasmuch as the buckling mode shape is usually trigonometric in nature, the trigonometric finite-difference solution can be made to exhibit a much faster convergence rate than the conventional difference solution by appropriate selection of λ_x and λ_y . This advantage is demonstrated with several isotropic plate examples discussed in appendix B. The convergence rate can also be degraded, however, by an inappropriate choice of λ_x and λ_y . It should be emphasized though, that the selection of λ_x and λ_y does not constrain the buckle mode shape to have wavelengths given by λ_x and λ_y . Rather, the trigonometric solution will always converge to the exact solution if enough degrees of freedom (finite-difference stations) are used.

Selection of trigonometric parameters λ_x and λ_y .- Selecting appropriate values of λ_x and λ_y which improve the convergence rate of solutions is predominantly based upon engineering judgment and experience. One engineering approach which has proven useful is to select λ_x and λ_y based upon the buckle length of infinitely long panels; that is,

$$\frac{\lambda_x}{a} = \frac{b/a}{\beta} \quad (11)$$

$$\frac{\lambda_y}{b} = 1 \quad (12)$$

where β is the wavelength parameter of an infinitely long panel, defined as the ratio of the panel width to the buckle length. The value of β for the combined compression and shear buckling of simply supported and clamped infinite panels may be determined from equations (B2) and (B3) in appendix B. Additional suggestions for the selection of λ_x and λ_y are given in appendix B.

Stability determinant evaluation and eigenvalue extraction.- In this analysis the order of the stability determinant is kept to a manageable size by using the two-dimensional marching procedure outlined in appendix C. This procedure is basically an extension of the one-dimensional procedure used in reference 13. Briefly, the marching procedure successively operates on the equilibrium equations at each finite-difference station to achieve a relatively low-order stability determinant.

In searching for the combined load system which produces buckling, it is convenient to introduce dimensionless stress coefficients, \bar{N}_x , \bar{N}_y , and \bar{N}_{xy} , which may be determined from the dimensional quantities, N_x , N_y , and N_{xy} (fig. 1), by multiplying by the factor $b^2\pi/D_{11}$. It is assumed that \bar{N}_x , \bar{N}_y , and \bar{N}_{xy} are linear functions of an eigenvalue \bar{p} , that is,

$$\left. \begin{aligned} \bar{N}_x &= \bar{t}_x + \bar{p}r_x \\ \bar{N}_y &= \bar{t}_y + \bar{p}r_y \\ \bar{N}_{xy} &= \bar{t}_{xy} + \bar{p}r_{xy} \end{aligned} \right\} \quad (13)$$

This assumption allows some loads to be held constant while others are increased to buckling, or it allows the loads to increase with a fixed proportionality.

To find the lowest value of \bar{p} which makes the stability determinant vanish, a determinant plotting technique is used. In order to increase the speed of the plotting technique, a variable step size is employed. This step size is based upon a numerical parabolic extrapolation of the stability determinant at each step of the determinant plotting procedure.

COMPUTER PROGRAM

A computer program denoted BOP (Buckling of Orthotropic Panels) has been developed for the buckling of flat rectangular orthotropic laminated panels. The program is applicable to panels with compression and/or shear loading, discrete lateral deflection and rotational springs, discrete stiffeners, and general boundary conditions.

The program utilizes trigonometric finite differences to improve the problem convergence and thus requires the selection of λ_x and λ_y . The user has the option of determining and supplying λ_x and λ_y (based upon the discussion in appendix B) or allowing the program to automatically calculate and use values based on equations (11) and (12).

In addition, the user has the option of either (1) supplying the bending stiffnesses of the panel or (2) supplying the elastic moduli, filament orientation, and thickness of each lamina in a laminated panel and allowing the program to calculate the bending stiffnesses. When the second option is chosen, the program prints the flexural stiffness matrix D , defined in reference 11, as well as the laminate Young's moduli, shear modulus, and Poisson's ratios. (The second option may be used independently of the buckling analysis.) A complete description of the program is provided in appendix D.

Results from the computer program have been compared with many classical results for unstiffened isotropic and orthotropic panels under various boundary conditions and with some classical results for stiffened isotropic panels. These comparisons which are discussed in subsequent sections were found to be excellent, thereby indicating the validity of the program.

RESULTS AND DISCUSSION

Shear Buckling of General Orthotropic Panels

From the general fourth-order equation for the shear buckling of orthotropic panels the buckling load coefficient may be expressed as

$$k_S = \frac{b^2 N_{xy}}{\pi^2 \sqrt[4]{D_{11} D_{22}^3}} \quad (14)$$

This coefficient is a function of only two variables

$$\Theta = \frac{\sqrt{D_{11} D_{22}}}{D_3} \quad (15)$$

and

$$B = \frac{b}{a} \sqrt[4]{\frac{D_{11}}{D_{22}}} \quad (16)$$

where $D_3 = D_{12} + 2D_{66}$. (Note that an isotropic panel implies $\Theta = 1$.)

Classically, general shear-buckling results for simply supported finite aspect-ratio panels have been obtained only for values of $\Theta \geq 1$ (see ref. 6). In figure 3 numerical results for $\Theta < 1$ have been presented. Also, for completeness and comparison purposes numerical results for $\Theta \geq 1$ are presented. The good agreement between these curves and those of reference 6 indicates the validity of the numerical results from the computer program. General results for the shear buckling of clamped panels, furthermore, do not appear in the literature for any range of Θ with the exception of $\Theta = 1$ (the isotropic case); consequently, numerical results for clamped panels are presented in figure 4.

Both the results for simply supported and clamped panels indicate that the percentage decline in buckling load from $B = 1$ to $B = 0$ decreases as Θ increases. Also, a comparison of figures 3 and 4 shows that the percentage increase in buckling load of clamped panels over simply supported panels increases with increasing Θ . The abrupt changes in slope appearing in these figures are due to changes in mode shape (from symmetric to antisymmetric modes). As anticipated from isotropic results (ref. 1), these abrupt changes are more predominant in clamped panels than in simply supported panels.

Tables 1 and 2 present the shear-buckling load coefficients used in obtaining the general orthotropic panel results of figures 3 and 4. Additionally, the trigonometric dif-

ference parameters (the mesh-spacing parameters a/Δ_x and b/Δ_y and the wavelength parameters λ_x/a and λ_y/b) used in obtaining the buckling coefficients are presented in tables 1 and 2.

Shear Buckling of a Simply Supported Panel With a Central Stiffener

Figure 5 presents results for the shear buckling of simply supported isotropic panels each of which contains one central flexural stiffener parallel to either the longer or shorter edges of the panel. As anticipated, the use of a central stiffener always provides an increase in the shear-buckling stress coefficient over that of the unstiffened panels ($\frac{EI}{bD} = 0$). The percentage increase over unstiffened panels is greater in square panels than in rectangular panels. In rectangular panels of the same aspect ratio, the percentage increase over unstiffened panels is greater when the stiffeners are parallel to the longer direction than when they are parallel to the shorter direction. The central-stiffener results of figure 5, moreover, are in reasonably good agreement with similar results given in reference 14 for slightly curved panels. This agreement indicates the validity of the computer program for the solution of stiffened panels.

Parametric Studies of Orthotropic Filament Reinforced Panels

Results are presented for the buckling of sandwich panels whose upper and lower skins are of laminated graphite-epoxy construction. Although some of the results in this section could be obtained from general orthotropic curves, such as those of figures 3 and 4, it is of interest to examine the effect of filament orientation upon the buckling load. (The material properties for the graphite-epoxy skins are given in table 3, with their equivalent general orthotropic parameter values Θ and B at various filament orientations.)

In addition to the assumptions listed in the analysis section of this report, it is assumed in this section that

1. The panel is symmetric about the middle surface
2. Each lamina has the same filament orientation θ except for sign
3. The core carries no load and undergoes no transverse shear deformation

As a consequence of these assumptions, it may be shown that the buckling parameters \hat{N}_x , \hat{N}_y , and \hat{N}_{xy} defined as

$$\hat{N}_x = \frac{b^2 N_x}{E_1 t^3 \left[1 - \left(\frac{h}{t} \right)^3 \right]} \quad (17a)$$

$$\hat{N}_y = \frac{b^2 N_y}{E_1 t^3 \left[1 - \left(\frac{h}{t} \right)^3 \right]} \quad (17b)$$

$$\hat{N}_{xy} = \frac{b^2 N_{xy}}{E_1 t^3 \left[1 - \left(\frac{h}{t} \right)^3 \right]} \quad (17c)$$

depend only on the magnitude of θ , the panel aspect ratio, and the boundary conditions. They do not depend on the thickness of each lamina, the number of laminas, or the core thickness. However, in order for assumption 2 of the analysis section to be reasonable – that is, neglect of bending-twisting coupling – it may be necessary that the ratio of core thickness to total thickness h/t be nearly unity and that the amount of material in either cover oriented in the $+\theta$ and $-\theta$ directions be equal.

The variation of the buckling load with filament orientation for panels of various aspect ratios is presented in figure 6 for axial compression and in figure 7 for shear. The figures indicate that the buckling loads are highly dependent upon filament orientation and that optimum orientations (those which yield a maximum buckling load) may be determined for each aspect ratio. Also, the figures indicate that clamping has a greater effect on compressive buckling than on shear buckling.

An indication of the buckling strength of the epoxy panels as compared to equal-weight aluminum panels is provided by a comparison of the discrete buckling loads appearing on the right-hand ordinate of figures 6 and 7 with the curves in the same figures. These comparable values are valid for thin-skinned sandwich panels which have the same core, of thickness h , as the graphite-epoxy panels, but which have aluminum skins. For all the cases considered, a range of filament orientations exists for which the buckling strength of the graphite-epoxy panels exceeds that of the comparable aluminum panel with the same aspect ratio and boundary conditions. In the case of a clamped square panel in shear, the buckling strength of the graphite-epoxy panel exceeds that of the aluminum panel at all filament orientations.

It should be noted that, if the restriction that each lamina have the same filament orientation $\pm\theta$ is removed, isotropic skins can be produced from groups of three or more laminas (for example, 0, +60, and -60) which will have the same weight as the $\pm\theta$ skins but will yield a higher buckling load for each case shown in figures 6 and 7 and for many other shear and compression loadings. However, this is not necessarily true in all cases; for example, in the transverse compression of long panels (a/b approaching zero), an orthotropic panel with filaments running transversely ($\theta = 0^\circ$) provides a higher

buckling load than an equivalent isotropic panel. Furthermore, there are many applications where for various reasons (for example, strength or fabrication criteria) orthotropic panels are preferable to isotropic ones.

In figures 8 to 11 optimum filament orientations are shown for all aspect ratios. The curve of figure 8 was determined from the exact closed-form relationship for the compression of simply supported plates (ref. 6), while the curves of figures 9 to 11 were determined using program BOP. The abrupt changes in the slopes of these curves are caused by changes in the buckling mode shape associated with the optimum filament orientation. Except for figure 8, the location of these abrupt changes has been approximated since it is difficult to determine exactly where they occur.

In the compressive buckling curves (figs. 8 and 9) the optimum filament orientation for small aspect ratio a/b is 0° (parallel to the X-axis or to the direction of compression). This orientation angle rapidly increases at about $a/b = 0.56$ for simply supported panels and at about $a/b = 1.05$ for clamped panels. However, a comparison of the aspect-ratio 1 and 1.1 curves for a clamped panel as shown in figure 6 indicates that the optimum buckling load does not exhibit such a rapid change but decreases slightly as the aspect ratio goes from 1 to 1.1. For higher aspect ratios the optimum orientation oscillates with decreasing excursion about $\pm 45^\circ$ and, in general, a practical filament orientation for $a/b > 1$ is $\theta = \pm 45^\circ$.

In the case of shear buckling (figs. 10 and 11), the symmetry of the problem requires that the deviation of the optimum filament orientation from 45° for a panel of aspect ratio a/b be equal but opposite to that of a panel with aspect ratio b/a . Also, the peaks of figure 7 are quite flat; that is, they have a large radius of curvature associated with them. Consequently, it was difficult to determine precisely the optimum filament orientations in figures 10 and 11. However, it is reasonable to say from figures 10 and 11 that for large aspect ratios $a/b > 2$, $\theta = \pm 60^\circ$ to $\pm 62^\circ$ is a practical filament orientation.

Figures 12 and 13 present interaction curves for the buckling of simply supported and clamped panels in combined axial compression and shear for various filament orientations and aspect ratios. The optimum filament orientations (those that correspond to the highest values of the buckling parameters) change according to aspect ratio a/b and the ratio of N_{xy}/N_x . For simply supported panels (fig. 12), when $a/b = 1$, the optimum orientation for all combinations of N_x and N_{xy} is $\theta = \pm 45^\circ$. When $a/b = 2$ or 5 , the optimum filament orientation for predominantly shear loading is near $\pm 60^\circ$ and for predominantly compressive loading is near $\pm 45^\circ$. For clamped panels (fig. 13) when $a/b = 1$ the optimum orientation changes from $\theta = \pm 45^\circ$ for shear loading to $\theta = 0^\circ$ for compression. When $a/b = 2$ or 5 , the optimum orientation changes from $\theta = \pm 60^\circ$ for pure shear to $\theta = \pm 45^\circ$ for pure compression. This behavior was the same as that exhibited by simply supported panels.

A summary of the data from figures 12 and 13 is shown in figure 14, which indicates the banded region in which all the results lie. For orthotropic panels it was found that the band is bounded from below by the following simple relationship given in reference 15 for isotropic panels:

$$R_x + R_{xy}^2 = 1 \quad (18)$$

where

$$\left. \begin{aligned} R_x &= \frac{N_x}{N_{x_0}} \\ R_{xy} &= \frac{N_{xy}}{N_{xy_0}} \end{aligned} \right\} \quad (19)$$

In equations (19), N_{x_0} and N_{xy_0} are the buckling loads for pure longitudinal compression and pure shear, respectively. Consequently, for the orthotropic cases considered, equation (18) is a reasonable conservative approximation for combined longitudinal compression and shear buckling of composite panels.

Figures 15 and 16 contain, respectively, compression and shear-buckling results for graphite-epoxy sandwich panels with nondeflecting edge supports and rotational edge springs for various filament orientations and aspect ratios. The associated boundary conditions are given by equations (A20) to (A22), and the rotational springs were assumed to be uniformly distributed about the panel edges. When the spring stiffness is zero, all four edges are simply supported and, when infinite, all four edges are clamped.

In general, the figures indicate that the buckling load increases sharply as the spring stiffness parameter bk_R/E_1t^3 increases from zero to one, the buckling loads obtaining at least 80 percent of their clamped value when the spring stiffness parameter is one. With further increase in the spring stiffness the buckling loads slowly approach the clamped value, increasing to within at least 10 percent of the clamped value when the spring stiffness parameter is three. Furthermore, the curves for the $\pm 45^\circ$ filament orientation generally approached the clamped values most rapidly.

CONCLUDING REMARKS.

A computerized analysis has been developed for the combined compression and shear buckling of stiffened orthotropic composite panels on discrete springs. Boundary

conditions are general and include elastic boundary restraints. Buckling solutions are obtained by using a newly developed trigonometric finite-difference procedure which increases the solution convergence rate over conventional finite-difference methods, thus allowing problems to be solved with the same accuracy as with conventional differences but with fewer degrees of freedom. The trigonometric finite-difference procedure introduces two new parameters into the solution. These parameters can be internally selected by the program during problem execution or can be selected by the user. The validity of the program has been substantiated by comparisons with many existing known solutions. A program listing, input description, and sample problem are provided.

Using the program, the classical general shear-buckling results (in terms of universal orthotropic parameters), which are available only for simply supported panels over a limited range of orthotropic properties, have been extended to the complete range of these properties for simply supported panels and clamped panels. Results for the shear buckling of isotropic panels with a central stiffener have also been obtained.

The program has been applied to parametric studies which examine the effect of filament orientation upon the buckling of graphite-epoxy sandwich panels. From these studies optimum filament orientations (those which yield maximum buckling loads) were determined within a class of graphite-epoxy sandwich panels for all aspect ratios. In particular, it was found that for shear buckling of high-aspect-ratio panels (greater than two) reasonable filament orientations are between $\pm 60^\circ$ and $\pm 62^\circ$ while, for axial compression of panels with aspect ratio greater than one, a reasonable filament orientation is $\pm 45^\circ$. In addition, interaction curves were determined for the combined axial compression and shear buckling of panels with varying filament orientations. A parabolic interaction relationship previously developed for isotropic infinite strips in combined axial compression and shear provided a reasonably accurate and conservative estimate for the buckling loads of the orthotropic panels considered herein.

Langley Research Center
National Aeronautics and Space Administration
Hampton, Va. 23665
August 1, 1975

APPENDIX A

DEVELOPMENT OF GOVERNING EQUATIONS

For completeness, equations (1) to (3) of the main text are repeated here:

$$\delta U = \int_0^b \int_0^a (M_x \delta w_{,xx} + M_y \delta w_{,yy} + 2M_{xy} \delta w_{,xy}) dx dy \quad (A1)$$

$$\left. \begin{aligned} M_x &= D_{11}w_{,xx} + D_{12}w_{,yy} \\ M_y &= D_{12}w_{,xx} + D_{22}w_{,yy} \\ M_{xy} &= 2D_{66}w_{,xy} \end{aligned} \right\} \quad (A2)$$

$$\delta V_N = \int_0^a \int_0^b (N_x w_{,x} \delta w_{,x} + N_y w_{,y} \delta w_{,y} + N_{xy} w_{,y} \delta w_{,x} + N_{xy} w_{,x} \delta w_{,y}) dy dx \quad (A3)$$

Then, replacing the derivatives in equations (A2) by trigonometric central differences yields

$$\left. \begin{aligned} (w_{,xx})_{ij} &= \frac{1}{\hat{\Delta}_x} \frac{1}{2} (w_{i+1,j} - 2w_{ij} + w_{i-1,j}) \\ (w_{,yy})_{ij} &= \frac{1}{\hat{\Delta}_y} \frac{1}{2} (w_{i,j+1} - 2w_{ij} + w_{i,j-1}) \\ (w_{,xy})_{ij} &= \frac{1}{\hat{\Delta}_x \hat{\Delta}_y} (w_{i+1,j+1} - w_{i,j+1} - w_{i+1,j} + w_{ij}) \end{aligned} \right\} \quad (A4)$$

where $\hat{\Delta}_x$ and $\hat{\Delta}_y$ are the trigonometric difference coefficients defined by equation (10). The terms $(w_{,xx})_{ij}$ and $(w_{,yy})_{ij}$ are defined at the full stations denoted by the circles in figure 2(b), while $(w_{,xy})_{ij}$ is defined at the half stations denoted by the

APPENDIX A

squares in figure 2(b). Consequently, the indices (i,j) attached to a variable may refer to the variable being evaluated at either full or half stations, depending on the variable.

Introducing equations (A2) and (A4) into equation (A1) and replacing the double integral by a double sum yields

$$\delta U = \Delta_x \Delta_y \sum_{j=1}^N \sum_{i=1}^M \left\{ \xi_{x_i} \xi_{y_j} \left[\frac{1}{\hat{\Delta}_x} M_{x_{ij}} (\delta w_{i+1,j} - 2\delta w_{ij} + \delta w_{i-1,j}) + \frac{1}{\hat{\Delta}_y} M_{y_{ij}} (\delta w_{i,j+1} - 2\delta w_{ij} + \delta w_{i,j-1}) \right] + 2\eta_{x_i} \eta_{y_j} \frac{M_{xy_{ij}}}{\hat{\Delta}_x \hat{\Delta}_y} (\delta w_{i+1,j+1} - \delta w_{i,j+1} - \delta w_{i+1,j} + \delta w_{ij}) \right\} \quad (A5)$$

where N and M are the total number of finite-difference stations in the x- and y-directions, respectively, and ξ_{x_i} , ξ_{y_j} , η_{x_i} , and η_{y_j} have the following definitions:

$$\xi_{x_i} = \begin{cases} 0 & (i < I_1 \text{ or } i > I_3) \\ 1/2 & (i = I_1 \text{ or } i = I_3) \\ 1 & (I_1 < i < I_3) \end{cases} \quad (A6)$$

$$\xi_{y_j} = \begin{cases} 0 & (j < J_4 \text{ or } j > J_2) \\ 1/2 & (j = J_4 \text{ or } j = J_2) \\ 1 & (J_4 < j < J_2) \end{cases} \quad (A7)$$

$$\eta_{x_i} = \begin{cases} 0 & (i < I_1 \text{ or } i \geq I_3) \\ 1 & (I_1 \leq i \leq I_3) \end{cases} \quad (A8)$$

APPENDIX A

$$\eta_{y_j} = \begin{cases} 0 & (j < J_4 \text{ or } j \geq J_2) \\ 1 & (J_4 \leq j < J_2) \end{cases} \quad (A9)$$

In equations (A6) to (A9), I_1 and I_3 are the row designations of boundaries ① and ③, respectively, and J_2 and J_4 are the column designations of boundaries ② and ④, respectively. (See fig. 2(a).)

Replacing the derivatives in equation (A3) by central trigonometric differences and the double integral by a double sum yields

$$\begin{aligned} \delta V_N = -\Delta_x \Delta_y \sum_{i=1}^M \sum_{j=1}^N & \left\{ \xi_{y_j} \eta_{x_i} \frac{N_x}{\Delta_x} (w_{i+1,j} - w_{ij}) (\delta w_{i+1,j} - \delta w_{ij}) + \xi_{x_i} \eta_{y_j} \frac{N_y}{\Delta_y} (w_{i,j+1} \right. \\ & - w_{ij}) (\delta w_{i,j+1} - \delta w_{ij}) + \eta_{x_i} \eta_{y_j} \frac{N_{xy}}{4 \hat{\Delta}_x \hat{\Delta}_y} [(w_{i+1,j} - w_{ij} + w_{i+1,j+1} - w_{i,j+1}) (\delta w_{i,j+1} \\ & - \delta w_{ij} + \delta w_{i+1,j+1} - \delta w_{i+1,j}) + (w_{i,j+1} - w_{ij} + w_{i+1,j+1} - w_{i+1,j}) (\delta w_{i+1,j} - \delta w_{ij} \\ & \left. + \delta w_{i+1,j+1} - \delta w_{i,j+1})] \right\} \quad (A10) \end{aligned}$$

In deriving equation (A10), the first and second terms in the integrand of equation (A3) have been replaced by trigonometric differences evaluated at stations indicated by "x" and "y," respectively, in figure 2(b), while the third and fourth terms have been evaluated at half stations, indicated by squares in figure 2(b), by averaging the derivatives.

The external forces and moments on the panel are those coming from discrete lateral deflection and rotational springs. The virtual work of these forces and moments may be expressed as

$$\begin{aligned} \delta V_S = \sum_{i=1}^M \sum_{j=1}^N k_{\ell_{ij}} w_{ij} \delta w_{ij} + \sum_{i=1}^M \sum_{j=1}^N \frac{k_{x_{ij}}}{\hat{\Delta}_x} (w_{i+1,j} - w_{ij}) (\delta w_{i+1,j} - \delta w_{ij}) \\ + \sum_{i=1}^M \sum_{j=1}^N \frac{k_{y_{ij}}}{\hat{\Delta}_y} (w_{i,j+1} - w_{ij}) (\delta w_{i,j+1} - \delta w_{ij}) \quad (A11) \end{aligned}$$

APPENDIX A

where k_ℓ is the spring stiffness associated with a lateral deflection spring and k_x and k_y are stiffnesses associated with rotational springs which resist moments acting about the Y- and X-axes, respectively. The k_ℓ type springs act at full stations, indicated by circles in figure 2(b), while the k_x and k_y type springs act at positions indicated by "x" and "y," respectively, in figure 2(b).

Substituting equations (A5), (A10), and (A11) into the statement of the principle of virtual work, equation (4) yields

$$\sum_{i=1}^M \sum_{j=1}^N (K_{ij} + S_{ij} + N_x \alpha_{ij} + N_y \psi_{ij} + 2N_{xy} \chi_{ij}) \delta w_{ij} = 0 \quad (A12)$$

where

$$\begin{aligned} K_{ij} = & \xi_{y_j} \frac{1}{\hat{\Delta}_x} \left(\xi_{x_{i+1}} M_{x_{i+1},j} - 2\xi_{x_i} M_{x_{ij}} + \xi_{x_{i-1}} M_{x_{i-1},j} \right) + \xi_{x_i} \frac{1}{\hat{\Delta}_y} \left(\xi_{y_{j+1}} M_{y_{i,j+1}} - 2\xi_{y_j} M_{y_{ij}} \right. \\ & \left. + \xi_{y_{j-1}} M_{y_{i,j-1}} \right) + \frac{1}{\hat{\Delta}_x \hat{\Delta}_y} \left(\eta_{x_{i-1}} \eta_{y_{j-1}} M_{xy_{i-1,j-1}} - \eta_{x_{i-1}} \eta_{y_j} M_{xy_{i-1,j}} \right. \\ & \left. - \eta_{x_i} \eta_{y_{j-1}} M_{xy_{i,j-1}} + \eta_{x_i} \eta_{y_j} M_{xy_{ij}} \right) \end{aligned} \quad (A13)$$

$$\alpha_{ij} = \frac{1}{\hat{\Delta}_x} \left[\xi_{y_j} \eta_{x_i} (w_{i+1,j} - w_{ij}) - \xi_{y_j} \eta_{x_{i-1}} (w_{ij} - w_{i-1,j}) \right] \quad (A14)$$

$$\psi_{ij} = \frac{1}{\hat{\Delta}_y} \left[\xi_{x_i} \eta_{y_j} (w_{i,j+1} - w_{ij}) - \xi_{x_i} \eta_{y_{j-1}} (w_{ij} - w_{i,j-1}) \right] \quad (A15)$$

$$\begin{aligned} \chi_{ij} = & \frac{1}{4\hat{\Delta}_x \hat{\Delta}_y} \left[(w_{i+1,j+1} - w_{ij}) \eta_{x_i} \eta_{y_j} - (w_{i+1,j-1} - w_{ij}) \eta_{x_i} \eta_{y_{j-1}} \right. \\ & \left. - (w_{ij} - w_{i-1,j-1}) \eta_{x_{i-1}} \eta_{y_{j-1}} + (w_{ij} - w_{i-1,j+1}) \eta_{x_{i-1}} \eta_{y_j} \right] \end{aligned} \quad (A16)$$

APPENDIX A

$$S_{ij} = \frac{1}{\Delta_x \Delta_y} k_{\ell ij} w_{ij} + \frac{1}{\Delta_x \Delta_y \hat{\Delta}_x^2} \left[k_{x_{i-1,j}} (w_{ij} - w_{i-1,j}) - k_{x_{ij}} (w_{i+1,j} - w_{ij}) \right] \\ + \frac{1}{\Delta_x \Delta_y \hat{\Delta}_y^2} \left[k_{y_{i,j-1}} (w_{ij} - w_{i,j-1}) - k_{y_{ij}} (w_{i,j+1} - w_{ij}) \right] \quad (A17)$$

From equations (A2) and (A4), the moments are related to the displacements as follows:

$$\left. \begin{aligned} (M_x)_{ij} &= (D_{11})_{ij} (w_{i+1,j} - 2w_{ij} + w_{i-1,j}) \frac{1}{\hat{\Delta}_x^2} + (D_{12})_{ij} (w_{i,j+1} - 2w_{ij} + w_{i,j-1}) \frac{1}{\hat{\Delta}_y^2} \\ (M_y)_{ij} &= (D_{22})_{ij} (w_{i,j+1} - 2w_{ij} + w_{i,j-1}) \frac{1}{\hat{\Delta}_y^2} + (D_{12})_{ij} (w_{i+1,j} - 2w_{ij} + w_{i-1,j}) \frac{1}{\hat{\Delta}_x^2} \\ (M_{xy})_{ij} &= 2(D_{66})_{ij} (w_{i+1,j+1} - w_{i,j+1} - w_{i+1,j} + w_{ij}) \frac{1}{\hat{\Delta}_x \hat{\Delta}_y} \end{aligned} \right\} \quad (A18)$$

where $(M_x)_{ij}$ and $(M_y)_{ij}$ act at the full stations, indicated by circles in figure 2(b), and $(M_{xy})_{ij}$ acts at the half stations, indicated by squares in figure 2(b).

Boundary Conditions

All four boundaries free or spring-supported. - If on the plate boundaries no constraints exist on w or its derivatives normal to the boundary, equation (A12) must be valid for all virtual displacements δw_{ij} , thus yielding equation (5) which is repeated here:

$$K_{ij} + S_{ij} + N_x \alpha_{ij} + N_y \psi_{ij} + 2N_{xy} \chi_{ij} = 0 \quad \begin{matrix} (i = 1, \dots, M) \\ (j = 1, \dots, N) \end{matrix} \quad (A19)$$

Equation (A19) represents equilibrium at each finite-difference station with each equilibrium equation containing an array of 13 values of w as depicted in figure 2(b). In solving these equations by the procedure discussed in appendix C, the terms w_{ij} represent the unknowns and equations (A18) are used to determine the moments appearing in the relationship for K_{ij} , equation (A13).

APPENDIX A

When a difference station lies on the boundary of the plate (that is, $i = I_1$ or $i = I_3$ or $j = J_4$ or $j = J_2$), the corresponding equilibrium equation reduces to the natural boundary condition on the Kirchhoff shear, reference 6. Also, when a difference station lies one finite difference interval off the plate (that is, $i = I_1 - 1$ or $i = I_3 + 1$ or $j = J_4 - 1$ or $j = J_2 + 1$), the corresponding equilibrium equation reduces to the natural boundary condition on the bending moment. Furthermore, when a difference station lies two or more finite-difference intervals off the plate (that is, $i < I_1 - 1$ or $i > I_3 + 1$ or $j < J_4 - 1$ or $j > J_2 + 1$), the corresponding equilibrium equations reduce to the trivial equation $0 = 0$. Consequently, no equilibrium equations exist for these stations.

Edges with nondeflecting lateral supports and rotational springs. - Equation (A19) may be used in approximating the solution of problems with nondeflecting edges; for example, if $w = 0$ on an edge, equation (A19) may be used in conjunction with extremely stiff lateral springs placed along the edge. Alternatively, an edge which is restrained from lateral motion may be handled as a special case, and in so doing the number of computations required for the problem solution is reduced.

The boundary condition for a nondeflecting edge is

$$w = 0 \quad \text{(on the edge)} \quad \text{(A20)}$$

If, in addition, uniformly distributed rotational springs act along boundaries ① and ③ (see fig. 2(a)),

$$M_x = k_R w_{,x} \quad \text{(on the edge)} \quad \text{(A21)}$$

or, if uniformly distributed rotational springs act along boundary ② or ④,

$$M_y = k_R w_{,y} \quad \text{(on the edge)} \quad \text{(A22)}$$

As a result of the foregoing, equation (A20) replaces the boundary condition on the Kirchhoff shear, while the difference form of equation (A21) or (A22) replaces the boundary condition on the edge moment. Furthermore, as an example, equation (A21) on boundary ① becomes

$$(M_x)_{I_1,j} = \frac{k_R (w_{I_1+1,j} - w_{I_1-1,j})}{\hat{\Delta}_x^*} \quad \text{(A23)}$$

APPENDIX A

where

$$\frac{1}{\hat{\Delta}_x^*} = \frac{\pi}{2\lambda_x \sin \frac{\pi \Delta_x}{\lambda_x}} \quad (\text{A24})$$

Substituting for M_x from equations (A18) and employing equation (A23) yields

$$(M_x)_{I_1,j} = \frac{(D_{11})_{I_1,j}}{\hat{\Delta}_x^2} (w_{I_1+1,j} + w_{I_1-1,j}) = \frac{k_R}{\hat{\Delta}_x^*} (w_{I_1+1,j} - w_{I_1-1,j}) \quad (\text{A25})$$

Then

$$w_{I_1-1,j} = \frac{\left[\frac{k_R}{\hat{\Delta}_x^*} - \frac{(D_{11})_{I_1,j}}{\hat{\Delta}_x^2} \right] w_{I_1+1,j}}{\frac{k_R}{\hat{\Delta}_x^*} + \frac{(D_{11})_{I_1,j}}{\hat{\Delta}_x^2}} \quad (\text{A26})$$

Substituting into the first of equation (A25) yields

$$(M_x)_{I_1,j} = \frac{(D_{11})_{I_1,j}}{\hat{\Delta}_x^2} \left[1 + \frac{\frac{k_R}{\hat{\Delta}_x^*} - \frac{(D_{11})_{I_1,j}}{\hat{\Delta}_x^2}}{\frac{k_R}{\hat{\Delta}_x^*} + \frac{(D_{11})_{I_1,j}}{\hat{\Delta}_x^2}} \right] w_{I_1+1,j} \quad (\text{A27})$$

It is evident from an examination of the first of equation (A25) that equation (A23) is satisfied by setting $w_{I_1-1,j} = 0$ and $(D_{11})_{I_1,j} = (D_{11}^*)_{I_1,j}$ where

$$(D_{11}^*)_{I_1,j} = \left[1 + \frac{\frac{k_R}{\hat{\Delta}_x^*} - \frac{(D_{11})_{I_1,j}}{\hat{\Delta}_x^2}}{\frac{k_R}{\hat{\Delta}_x^*} + \frac{(D_{11})_{I_1,j}}{\hat{\Delta}_x^2}} \right] (D_{11})_{I_1,j} \quad (\text{A28})$$

Similar relationships may be developed for boundaries ②, ③, and ④.

APPENDIX A

In summary, for a nondeflecting boundary with uniformly distributed rotational springs, equilibrium on the boundary and one station off the boundary are not used. Instead, in the remaining equilibrium equations, w on the boundary and one station off the boundary are set equal to zero and D_{11} on the boundary is set equal to D_{11}^* if the boundary is number ① or ③, and D_{22} on the boundary is set equal to D_{22}^* if the boundary is number ② or ④.

The limiting cases of simply supported or clamped boundaries are readily provided by letting k_R approach zero or infinity, respectively. Hence, for a simply supported boundary

$$D_{11}^* = 0 \quad \text{if the boundary is ① or ③}$$

$$D_{22}^* = 0 \quad \text{if the boundary is ② or ④}$$

and for a clamped boundary

$$D_{11}^* = 2D_{11} \quad \text{if the boundary is ① or ③}$$

$$D_{22}^* = 2D_{22} \quad \text{if the boundary is ② or ④}$$

Flexural Stiffeners

The effects of flexural stiffeners are accounted for in a manner similar to that used for nondeflecting supports. At each finite-difference station along the stiffener, $(D_{11})_{ij}$ is replaced by $(\bar{D}_{11})_{ij}$ if the stiffener is parallel to the X-axis and $(D_{22})_{ij}$ is replaced by $(\bar{D}_{22})_{ij}$ if the stiffener is parallel to the Y-axis, where

$$\left. \begin{aligned} (\bar{D}_{11})_{ij} &= (D_{11})_{ij} + \frac{EI}{\Delta_y} \\ (\bar{D}_{22})_{ij} &= (D_{22})_{ij} + \frac{EI}{\Delta_x} \end{aligned} \right\} \quad (\text{A29})$$

and EI is the lateral bending stiffness of the stiffener about the neutral plane of the panel.

APPENDIX A

Summary of Finite-Difference Stations at Which Equilibrium Is Enforced

As a result of the foregoing discussions on free or spring-supported edges and non-deflecting edges, the rows i and columns j at which equilibrium is enforced are, respectively,

$$\left. \begin{aligned} M_e &= I_3 - I_1 + 3 - \text{Twice the number of nondeflecting edges parallel to the Y-axis} \\ N_e &= J_2 - J_4 + 3 - \text{Twice the number of nondeflecting edges parallel to the X-axis} \end{aligned} \right\} \text{(A30)}$$

APPENDIX B

TRIGONOMETRIC FINITE DIFFERENCES

Trigonometric finite differences introduce the trigonometric parameters λ_x and λ_y which are not present in conventional finite differences. Consequently, the first purpose of this appendix is to present and demonstrate some effective procedures for selecting values of λ_x and λ_y which results in an improved convergence rate over conventional differences. The second purpose is to point out some of the limitations of trigonometric finite differences.

Selection of λ_x and λ_y

Selection of values of λ_x and λ_y which improve the convergence rate of trigonometric finite-difference solutions over those of conventional finite-difference solutions is predominantly based on engineering considerations and experience. Experience has shown that it is often advantageous to select trigonometric parameters whose ratio is determined on the basis of the infinitely long panel solution as is done in equations (11) and (12), that is,

$$\frac{\lambda_y}{\lambda_x} = \beta \tag{B1}$$

where β is the wavelength parameter of an infinitely long panel, defined as the ratio of the panel width to the buckle length. Imposing equation (B1) on the parameter selection should be reasonable for panels which buckle with more than two half waves along their length.

The value of β may be determined to any degree of accuracy by extending the isotropic results of reference 16. For a panel with its long dimension parallel to the X-axis, first approximations of the buckling eigenvalue \bar{p}_∞ and wavelength parameter β satisfy the following two simultaneous equations for panels whose long sides are simply supported:

$$\left. \begin{aligned} (\bar{t}_{xy} + \bar{p}_\infty r_{xy})^2 - \frac{9}{4} M_1 M_2 &= 0 \\ \frac{\partial}{\partial \beta} (M_1 M_2) &= 0 \end{aligned} \right\} \tag{B2}$$

APPENDIX B

and, for panels whose long sides are clamped, \bar{p}_∞ and β satisfy the two simultaneous equations

$$\left. \begin{aligned} (t_{xy} + \bar{p}_\infty r_{xy})^2 - \frac{15}{32}(2M_0 + M_2)(M_1 + M_3) &= 0 \\ \frac{\partial}{\partial \beta}(M_0 + M_2)(M_1 + M_3) &= 0 \end{aligned} \right\} \quad (B3)$$

where

$$M_n = \frac{\pi}{8\beta} \left[\frac{D_{22}}{D_{11}} n^4 + 2 \frac{D_3}{D_{11}} n^2 \beta^2 + \beta^4 - \beta^2 (\bar{t}_x + \bar{p}_\infty r_x) - n^2 (\bar{t}_y + \bar{p}_\infty r_y) \right] \quad (n = 0, 1, 2, 3)$$

Convergence Behavior

Figures 17(a) to 17(f) illustrate the convergence of trigonometric finite-difference solutions when λ_y/λ_x is fixed on the basis of equation (B1). Results for both simply supported and clamped isotropic panels under either axial compression or shear are shown in these figures. In each case the panel was modeled using an equal number of finite-difference stations in the x- and y-directions. Exact and approximate values for these cases are given in references 1, 6, 16, and 17.

The dashed curve in each of figures 17(a) to 17(f) illustrates the convergence of the conventional difference solution – that is, λ_x and λ_y infinite – while the solid and dash-dot curves illustrate the convergence achieved with some finite values of λ_x . Comparison of the curves indicates that some values of λ_x increase the convergence rate over the conventional rate while other values decrease it. (In those special cases where the buckle shape is exactly a double sine wave, the trigonometric difference solution is exact when λ_x and λ_y are equal to the buckle half wavelength.) Consider though the dash-dot curve of each figure. These curves show the convergence when λ_y is simply taken equal to the panel width and λ_x is taken equal to the buckle length of the infinitely long panel; that is, equations (11) and (12) are applied. Comparison of the dash-dot curves and the dashed curves indicates that equations (11) and (12) provide reasonable values of λ_x and λ_y which improve the solution convergence. As figures 17(a) to 17(f) indicate, however, other values of λ_x/a could be selected which further improve the convergence rate. Such values may be found by making a condensed cross plot of each figure; for example, consider the case of the compression of a square isotropic clamped panel as shown in figure 17(c). For this case, equations (B3) predict $\beta = 1.5$. Then, using program BOP with $\lambda_y/\lambda_x = 1.5$, λ_x/a is varied from 0.25 to 1 for mesh sizes of $a/\Delta_x = b/\Delta_y = 5$ and $a/\Delta_x = b/\Delta_y = 6$; these curves are shown in figure 18. As the

APPENDIX B

mesh spacing is decreased, the curves will approach the exact solution at all values of λ_x/a . However, the two curves cross at $\lambda_x/a = 0.35$ and $\bar{N}_x = 9.75$, which implies that convergence is most rapid at this value of λ_x/a since increasing the mesh size did not change the buckling stress coefficient. It is evident from figure 17(c) that, if such a choice of λ_x were used, convergence would be improved beyond that achieved by selecting λ_x from equation (11).

As further examples, consider the results in table 4 for the shear buckling of the orthotropic panels described in table 3. The values of λ_x and λ_y were determined by making the required cross plots. It is evident by comparing the conventional and trigonometric solutions given in the table that the selected values of λ_x and λ_y provided excellent results.

The additional effort involved in finding better values of λ_x may be justified in problems where convergence would otherwise be extremely slow. It may also be justified in the performance of parameter studies. In such studies some typical problems within the problem class to be studied are chosen; for these, improved values of λ_x are found and then interpolated to yield λ_x for other problems within the study class.

Correction Factors for Equations (11) and (12)

Equations (B2) and (B3) which provide β for equations (11) and (12) do not cover every case; the boundary conditions may not be simply supported or clamped, or it may be inappropriate to use β based on an infinitely long panel. Consequently, equations (11) and (12) must be used with engineering judgment. Some allowance is provided by introducing correction factors C_x and C_{yx} into equations (11) and (12), that is,

$$\frac{\lambda_y}{\lambda_x} = C_{yx}\beta \quad (B4)$$

$$\frac{\lambda_x}{a} = \frac{b}{a} \frac{C_x}{\beta} \quad (B5)$$

A numerical routine which calculates β from equations (B2) or (B3), and then λ_x and λ_y from equations (11) and (12), is used in program BOP. This program is briefly discussed in the main text and is documented in appendix D.

Limitations of Trigonometric Finite Differences

In figure 19 a sketch of the variation with λ_x of the coefficient $1/\hat{\Delta}_x$ as defined by equation (10) is presented. The reader's attention is called to the singularities of

APPENDIX B

$1/\hat{\Delta}_x$ at $\lambda_x = \frac{\Delta_x}{2}, \frac{\Delta_x}{4}, \frac{\Delta_x}{8}$, etc. In order to avoid these singularities and the rapidly varying behavior of $1/\hat{\Delta}_x$ between them, λ_x and similarly λ_y must be chosen such that

$$\left. \begin{array}{l} \lambda_x > \frac{\Delta_x}{2} \\ \lambda_y > \frac{\Delta_y}{2} \end{array} \right\} \quad (B6)$$

Moreover, if uniformly distributed rotational springs are prescribed on the boundaries in the manner presented in equations (A20) to (A24), then to avoid singularities in $\hat{\Delta}_x^*$ and $\hat{\Delta}_y^*$ choose

$$\left. \begin{array}{l} \lambda_x > \Delta_x \\ \lambda_y > \Delta_y \end{array} \right\} \quad (B7)$$

APPENDIX C

STABILITY DETERMINANT EVALUATION

Since the total number of rows and columns at which equilibrium is enforced is M_e and N_e , respectively, a stability determinant of order $M_e N_e \times M_e N_e$ would result. To produce a stability determinant of smaller size, a marching procedure is employed. This procedure, which is described herein, operates on the equilibrium equations to produce, by a process of successive elimination, a determinant of size $2M_e \times 2M_e$.

The marching procedure takes advantage of the fact that each of the difference equations of equilibrium, equations (5), is linear and homogeneous, with each one containing no more than 13 unknown deflections. For a station (i,j) away from the plate edges

$$I_f + 1 < i < I_\ell - 1$$

$$J_f + 1 < j < J_\ell - 1$$

where I_f and I_ℓ are the first and last rows of finite-difference stations at which equilibrium is prescribed, and J_f and J_ℓ are the first and last columns of finite-difference stations at which equilibrium is prescribed, the 13 unknown deflections form the geometric pattern shown in figure 2(b). It is evident from this pattern that the deflections at stations in column $j + 2$ can be determined by using equilibrium at stations in column j if the deflections in columns $j - 2$, $j - 1$, j , and $j + 1$ are known or prescribed. For equilibrium at stations lying near the edges, however, the geometric pattern of figure 2(b) is reduced. Consequently, equilibrium at stations in the first column J_f may be used to determine the deflections at stations in column $J_f + 2$ if the deflections only in columns J_f and $J_f + 1$ are prescribed, since deflections in columns $J_f - 1$ and $J_f - 2$ do not appear in these equilibrium equations.

Having found the deflections in column $J_f + 2$ from prescribed values in column J_f and $J_f + 1$, equilibrium at stations in column $J_f + 1$ can be used to obtain the deflections in column $J_f + 3$; likewise, equilibrium at stations in column $J_f + 2$ can provide deflections in column $J_f + 4$, etc. Thus, a marching routine is developed from column to column which determines the deflections throughout the panel from prescribed values in the first two columns. It should be noted that equilibrium at stations in the last two columns, $J_\ell - 1$ and J_ℓ , is not used at this stage of the marching procedure.

The evaluation of the stability determinant can now be performed numerically for a given value of the eigenvalue by choosing $2M_e$ linearly independent sets of assumed

APPENDIX C

deflections for the first two columns. These assumed sets are taken as

$$\begin{aligned}
 [w^{(1)}] &= \begin{bmatrix} 1 \\ 0 \\ 0 \\ 0 \\ \cdot \\ \cdot \\ \cdot \\ 0 \end{bmatrix} & [w^{(2)}] &= \begin{bmatrix} 0 \\ 1 \\ 0 \\ 0 \\ \cdot \\ \cdot \\ \cdot \\ 0 \end{bmatrix} & [w^{(3)}] &= \begin{bmatrix} 0 \\ 0 \\ 1 \\ 0 \\ \cdot \\ \cdot \\ \cdot \\ 0 \end{bmatrix}, \dots, [w^{(2M_e)}] &= \begin{bmatrix} 0 \\ 0 \\ 0 \\ 0 \\ \cdot \\ \cdot \\ \cdot \\ 1 \end{bmatrix}
 \end{aligned} \tag{C1}$$

where each column contains $2M_e$ values. By marching across the plate with the r th set of these assumed values, deflections throughout the plate $w_{ij}^{(r)}$ are determined. However, the equilibrium equation at stations in the last two columns will not, in general, be satisfied by any of these assumed sets. Therefore, consider the column matrix

$$\{e^{(r)}\} = \begin{bmatrix} e_{I_f, J_{\ell-1}}^{(r)} \\ \cdot \\ \cdot \\ \cdot \\ e_{I_{\ell}, J_{\ell-1}}^{(r)} \\ e_{I_f, J_{\ell}}^{(r)} \\ \cdot \\ \cdot \\ \cdot \\ e_{I_{\ell}, J_{\ell}}^{(r)} \end{bmatrix} \tag{C2}$$

where each element of the matrix represents the value of the left-hand side of an equilibrium equation at a station in columns $J_{\ell} - 1$ or J_{ℓ} for the r th assumed set and would be identically zero if the assumed deflections were exact. The total solution is a linear superposition of all the assumed sets, that is,

$$w_{ij} = \sum_{r=1}^{2M_e} A^{(r)} w_{ij}^{(r)} \quad \begin{pmatrix} I_f \leq i \leq I_{\ell} \\ J_f \leq j \leq J_{\ell} \end{pmatrix} \tag{C3}$$

APPENDIX C

Correspondingly, the total contribution to equilibrium at columns $J_\ell - 1$ and J_ℓ for all assumed sets of deflections is

$$[e] = \sum_{r=1}^{2M_e} A^{(r)} \{e^{(r)}\} \quad (C4)$$

The coefficients $A^{(r)}$ are determined by enforcing equilibrium at stations in the last two columns which leads to

$$[e] = 0 \quad (C5)$$

or

$$\begin{bmatrix} e^{(1)} & e^{(2)} & \dots & e^{(r)} & \dots & e^{(2M_e)} \end{bmatrix} \begin{bmatrix} A^{(1)} \\ A^{(2)} \\ \cdot \\ \cdot \\ \cdot \\ A^{(r)} \\ \cdot \\ \cdot \\ \cdot \\ A^{(2M_e)} \end{bmatrix} = 0 \quad (C6)$$

For a nontrivial solution of equation (C6) the determinant of the coefficients must vanish, resulting in

$$|e| = 0 \quad (C7)$$

and it is clear from equation (C6) that $|e|$ is of order $2M_e \times 2M_e$.

APPENDIX D

COMPUTER PROGRAM

The computer program BOP (Buckling of Orthotropic Panels) was written in FORTRAN IV on a SCOPE 3.1 system modified for Langley Research Center and executes and loads with a field length of 60000 octal locations. The program is applicable to the combined compression and shear of stiffened, variable-thickness, flat rectangular orthotropic panels on discrete springs; boundary conditions are general and include elastic boundary restraints. A description of the input, an example problem showing input and output, and a program listing are provided.

Input Description

For each case the input consists of a single identification card and a Namelist BUCKLE as follows:

ISTIFF, ISTEP, IX, JX, MSHAPE, MA, NOMAT, TH, AT, MATYPE, E1, E2, U1, G12, IBC, AKR, D1, D2, D12, D66, DS1, XA, XB, AKL, AKX, AKY, NUPRIT, EI, IORIENT, LOC, TX, TY, TXY, RX, RY, RXY, P1, DELP, PFIN, TEST, MR, NC, X, Y, DS2, DS12, DS66

Many of the input variables have associated default values as will be indicated in the following descriptions:

Control parameters

ISTIFF = 1 no preprocessing of laminate properties – execute for buckling (only)
 = 2 preprocess and execute for buckling
 = 3 preprocess only – do not execute for buckling

DEFAULT:ISTIFF = 2

ISTEP = 1 program automatically varies the input step size, DELP
 = 2 step size fixed and equal to DELP

DEFAULT:ISTEP = 1

IX = 1 output of intermediate results
 = 2 output of intermediate results suppressed

JX = 1 output of flexural stiffnesses at each finite-difference station
 = 2 output of flexural stiffnesses suppressed

DEFAULT:IX = JX = 2

APPENDIX D

MSHAPE = 1 compute mode shape
 = 2 do not compute mode shape

DEFAULT:MSHAPE = 2

Laminate and lamina properties (Required if ISTIFF = 2 or 3)

MA number of laminas in the laminate

NOMAT number of different materials comprising the laminate

TH a one-dimensional array in which the *i*th element of the array corresponds to the filament orientation (as measured from the X-axis in degrees) in the *i*th lamina

AT a one-dimensional array in which the *i*th element of the array corresponds to the thickness of the *i*th lamina

MATYPE a one-dimensional array in which the *i*th element is the number designation of the material in the *i*th lamina

E1 a one-dimensional array in which the *j*th element of the array corresponds to the Young's modulus parallel to the fibers in the *j*th material

E2 a one-dimensional array specifying the Young's modulus transverse to the fibers

U1 a one-dimensional array specifying Poisson's ratio ν_{12} in each lamina

G12 a one-dimensional array specifying the shear modulus in each material

Boundary conditions

IBC a one-dimensional array of four elements in which the *i*th element refers to the *i*th boundary (see fig. 2(a)); four options are available at each boundary

IBC(I) = 1 nondeflecting lateral support with uniform rotational springs on edge I

 = 2 simple support on edge I

 = 3 clamped on edge I

 = 4 free on edge I

 = 5 other boundary conditions – set by user through appropriate input of D1, D2, D12, and D66

APPENDIX D

AKR a one-dimensional array in which the *i*th element of the array corresponds to the uniformly distributed rotational spring stiffness per unit length of boundary on the *i*th boundary; required if any boundary has $IBC = 1$

Laminate flexural stiffnesses (Required if $ISTIFF = 1$)

D1 a two-dimensional array in which the (*i,j*)th element of the array corresponds to the value of $(D_{11})_{ij}$

D2 similar to D1, but specifying $(D_{22})_{ij}$

D12 similar to D1, but specifying $(D_{12})_{ij}$

D66 similar to D1, but specifying $(D_{66})_{ij}$

DS1 reference value of D_{11}

Plate geometry

XA = a dimension parallel to X-axis (fig. 2(a))

XB = b dimension parallel to Y-axis (fig. 2(a))

Discrete springs

AKL a two-dimensional array in which the (*i,j*)th element corresponds to $(k_{\ell})_{ij}$

AKX similar to AKL but referring to $(k_x)_{ij}$

AKY similar to AKL but referring to $(k_y)_{ij}$

Discrete flexural stiffeners

NUPRIT number of stiffeners

EI a one-dimensional array whose *i*th element specifies the flexural stiffness of the *i*th stiffener about the neutral plane of the panel

IORIENT a one-dimensional array whose *i*th element specifies whether the stiffener is parallel to X- or Y-axis

= 1 stiffener parallel to X-axis

= 2 stiffener parallel to Y-axis

LOC a one-dimensional array whose *i*th element gives the row or column location of the *i*th stiffener

DEFAULT: NUPRIT = 0; EI, IORIENT and LOC need not be input

APPENDIX D

Applied in-plane loads

In-plane loads are assumed to be uniform over the boundary to which they are applied and are increased to buckling according to the relationships prescribed by equations (13); therefore, the user inputs

$$TX = \bar{t}_x$$

$$TY = \bar{t}_y$$

$$TXY = \bar{t}_{xy}$$

$$RX = r_x$$

$$RY = r_y$$

$$RXY = r_{xy}$$

Eigenvalue search parameters

P1 starting value of \bar{p} . If $P1 < 0.$, the program will calculate P1 from equation (B2) or (B3) according to the relation,

$$P1 = \text{ABS}(P1) * \text{PBAR} \quad (D1)$$

where PBAR is \bar{p}_∞ from equation (B2) or (B3).

DEFAULT:P1 = 0.9*PBAR

DELP increment of (\bar{p}); if $P1 < 0.$, DELP = 0.1*PBAR; if ISTEP = 1, DELP is automatically varied during the eigenvalue search

PFIN maximum value of \bar{p} during the eigenvalue search

TEST eigenvalue accuracy

DEFAULT:1. $\times 10^{-3}$

Trigonometric finite-difference data

MR number of rows of finite-difference stations interior to the plate – not including boundaries

NC number of columns of finite-difference stations interior to the plate – not including boundaries

Note: The marching procedure requires $NC \geq 4$

$$X = \lambda_x/a$$

$$Y = \lambda_y/b$$

APPENDIX D

Note: If the user inputs $X \leq 0$, the program automatically calculates a new value of X and Y according to the relationship expressed by equations (B4) and (B5); that is,

$$X = \text{ABS}(X) * X_B / \text{BETA} / X_A \quad (\text{D2})$$

$$Y = \text{ABS}(Y) \quad (\text{D3})$$

where the input magnitudes of X and Y (that is, $\text{ABS}(X)$ and $\text{ABS}(Y)$) replace C_X and C_{YX} in equations (B4) and (B5). Also, in equation (D1), $\text{BETA} = \beta$, and β is calculated from equation (B2) or (B3).

When $\text{ISTIFF} = 1$ and the evaluation of X and Y is chosen, the user must also input

DS2 average or typical value of D_{22}

DS12 average or typical value of D_{12}

DS66 average or typical value of D_{66}

DEFAULT: Calculation of X and Y using equations (D2) and (D3) where $\text{ABS}(X)$ and $\text{ABS}(Y)$ are set equal to unity.

Example Problem

Consider the shear buckling of a 12-inch by 3-inch clamped sandwich panel which has as its lay-up, 45/-45/45/-45/CORE/-45/45/-45/45. The core thickness is 0.0605 inch and each lamina of the skins is graphite-epoxy with a thickness of 0.0055 inch.

Sample Input

```
THIS IS A FREE FIELD IDENTIFICATION CARD
$BUCKLE TX=.0,TY=.0,TXY=.0,RX=.0,RY=.0,RXY=1.,
XA=12,XB=3.,MR=12,NC=6,IBC=4*3,NOMAT=2,E1=2.10E7,1.,E2=2.39E6,1.,
U1=.31,.2,G12=6.5E5,1.,MA=9,MATYPE=4*1,2,4*1,
AT=4*.0055,.0605,4*.0055,TH=45.,-45.,45.,-45.,.0,-45.,45.,-45.,45.
$
```

APPENDIX D

Sample Output

INPUT FOR CASE

THIS IS A FREE FIELD IDENTIFICATION CARD

11111111111111111111***** Y
4 2
4 2
4 2
4 2
4 2
4 2
4 2
33333333333333
*
*
*
*
X

ISTIFF=2 ISTEP=1 IX=2 JX=2 TEST= 1.00000000E-03

XA= 1.20000000E+01 XB= 3.00000000E+00 ASPECT RATIO= 4.00000000E+00

MR=12 NC= 6

TX= 0. TY= 0. TXY= 0.

PI= -9.00000000E-01 DELP= 1.00000000E-01 PFIN= 1.00000000E+02

X= -1.00000000E+00 Y= 1.00000000E+00

RX= 0. RY= 0. RXY= 1.00000000E+00

APPENDIX D

LAMINATED PLATE PROPERTIES

MATERIAL KIND	E1	E2	U1	GXY
1	2.10000000E+07	2.39000000E+06	3.10000000E-01	6.50000000E+05
2	1.00000000E+00	1.00000000E+00	2.00000000E-01	1.00000000E+00

LAYER NO.	MAT. KIND	THICK	THETA
1	1	5.50000000E-03	4.50000000E+01
2	1	5.50000000E-03	-4.50000000E+01
3	1	5.50000000E-03	4.50000000E+01
4	1	5.50000000E-03	-4.50000000E+01
5	2	6.05000000E-02	0.
6	1	5.50000000E-03	-4.50000000E+01
7	1	5.50000000E-03	4.50000000E+01
8	1	5.50000000E-03	-4.50000000E+01
9	1	5.50000000E-03	4.50000000E+01

CAUTION -- COUPLING BETWEEN EXTENSION AND BENDING MAY BE SIGNIFICANT
 IF THE FOLLOWING FOUR VALUES ARE NOT ALL EQUAL.
 IF THIS IS THE CASE, THE RESULTS SHOULD BE USED WITH DISCRETION

4.7677528E-17 7.15163293E-17 8.80102296E-17 5.97234077E-17

A MATRIX

3.05215229E+05	2.48015179E+05	0.
2.48015179E+05	3.05215229E+05	0.
0.	0.	2.43655139E+05

B MATRIX

1.45519152E-11	2.18278728E-11	8.00355338E-11
2.18278728E-11	2.18278728E-11	7.27595761E-11
7.27595761E-11	7.27595761E-11	1.45519152E-11

APPENDIX D

D MATRIX

5.31653046E+02	4.32016589E+02	4.69571561E+01
4.32016589E+02	5.31653046E+02	4.69571561E+01
4.69571561E+01	4.69571561E+01	4.24421785E+02

OVERALL LAMINATE PROPERTIES

EX= 9.92156003E+05 EY= 9.92156003E+05 GXY= 2.33162813E+06
NUXY= 8.12591100E-01 NUXX= 8.12591100E-01

P= 1.30776204E+01 B= 9.57954000E-01 F= -1.83044904E-08G= 3.83577069E-03

PROGRAM HAS COMPUTED AND USED X= 2.60972865E-01
AND Y= 1.00000000E+00 BASED ON THE INFINITE PLATE WAVE LENGTH

BASED ON AN INFINITELY LONG PLATE THE BUCKLING STRESS COEFFICIENTS ARE
NXBAR= 0.
NYBAR= 0.
NXYBAR= 1.30776204E+01
AND THE STRAINS ARE
STRNX= 0.
STRNY= 0.
STRNXY= 3.12923870E-02

PROGRAM WILL NOW CONTINUE WITH FINITE ASPECT RATIO SOLUTION

BOUNDARY CONDITIONS

BOUNDARY NO. 1 IS CLAMPED

BOUNDARY NO. 2 IS CLAMPED

BOUNDARY NO. 3 IS CLAMPED

APPENDIX D

BOUNDARY NO. 4 IS CLAMPED

NXBAR	NYBAR	NXYBAR	DETERMINANT
0.	0.	1.17698583E+01	6.54187653E+12
0.	0.	1.19006345E+01	2.18161022E+12
0.	0.	1.20314107E+01	2.37244168E+11
0.	0.	1.20473676E+01	1.33435159E+11
0.	0.	1.20687996E+01	3.35545245E+10
0.	0.	1.20761369E+01	9.37018457E+09
0.	0.	1.20793082E+01	0.

BUCKLING LOADS PER UNIT OF LENGTH ALONG BOUNDARY EDGE

NX= 0. NY= 0. NXY= 7.04251216E+03

[XB**2)*NX/(PI**2)/(T**3) = 0.
 [XB**2)*NY/(PI**2)/(T**3) = 0.
 [XB**2)*NXY/(PI**2)/(T**3) = 5.62757767E+06

[XB**2)*EPSILONX/(T**2) = -0.
 [XB**2)*EPSILONY/(T**2) = -0.
 [XB**2)*EPSILONXY/(T**2) = -1.19105540E+01

APPENDIX D

PROGRAM BOP(INPUT=201,OUTPUT=201,TAPE5=INPUT,TAPE6=OUTPUT,	100000
1TAPE7=201)	200000
C	300000
C NASA - LANGLEY RESEARCH CENTER - PROGRAM	400000
C	500000
C THE PROGRAM FINDS THE BUCKLING LOADS (COMPRESSIVE OR SHEAR) OF ORTHOTROPIC	600000
C PANELS WHOSE BOUNDARY CONDITIONS ON EACH EDGE MAY BE EITHER SIMPLY	700000
C SUPPORTED, CLAMPED OR ELASTICALLY CONSTRAINED BY ROTATIONAL SPRINGS.	800000
C THE ORTHOTROPIC ELASTIC PROPERTIES OF THE PANEL MAY BE EITHER DIRECTLY	900000
C SUPPLIED BY THE USER OR MAY BE INTERNALLY PREPROCESSED BY THE PROGRAM	1000000
C FOR LAMINATED PANELS.	1100000
C	1200000
C LAMINATE DEFINITIONS	1300000
C *****	1400000
C	1500000
C MA=NUMBER OF LAMINAS IN THE LAMINATE	1600000
C NOMAT=NUMBER OF DIFFERENT TYPES OF MATERIAL	1700000
C TH=FIBER ORIENTATION (IN DEGREES) MEASURED FROM X AXIS	1800000
C MATYPE=TYPE OF MATERIAL IN EACH LAMINA	1900000
C	2000000
C BOUNDARY CONDITIONS	2100000
C *****	2200000
C	2300000
C IBC=1, ROTATIONAL SPRING SUPPORT	2400000
C IBC=2, SIMPLE SUPPORT	2500000
C IBC=3, CLAMPED SUPPORT	2500001
C IBC=4, FREE BOUNDARY	2600000
C IBC=5, BOUNDARY CONDITION ENTERED THRU D MATRICES	2700000
C AKR=ROTATIONAL SPRING STIFFNESS PER UNIT LENGTH OF BOUNDARY	2800000
C	2900000
C CONTROL OPTIONS	3000000
C *****	3100000
C	3200000
C ISLIFE=1, DO NOT PREPROCESS, BUT EXECUTE FOR BUCKLING	3300000
C ISLIFE=2, PREPROCESS AND EXECUTE FOR BUCKLING (DEFAULT)	3400000
C ISLIFE=3, PREPROCESS ONLY, DO NOT EXECUTE FOR BUCKLING	3500000
C MSHAPE=1, EXECUTE FOR BUCKLING AND EXECUTE MODE SHAPE OPTION	3600000
C MSHAPE=2, DO NOT EXECUTE MODE SHAPE OPTION	3700000
C MSHAPE=3, DO NOT EXECUTE FOR BUCKLING, BUT DO EXECUTE MODE SHAPE OPTION.	3800000
C ISTEP=1, PROGRAM AUTOMATICALLY VARIES THE INITIAL STEP SIZE,DELP. (DEFAULT	3900000
C ISTEP=2, STEP SIZE FIXED AND EQUAL TO DELP	4000000
C	4100000

APPENDIX D

			4200000
			4300000
			4400000
000003	DIMENSION A(26,56),W(32,32),CASE(8),PP(200),DEI(200)		4500000
000003	DIMENSION D1(32,32),D2(32,32),D12(32,32),D66(32,32),IBC(4),AKS(4)		4600000
	1,TH(100),AI(100),MATYPE(100),EI(10),E2(10),UI(10),GI2(10)		4700000
	2,EI(5),IORIENT(5),LOC(5),B(56,1),IPIVCI(56)		4800001
	* ,AKR(4),K(56)		4900000
000003	EQUIVALENCE (AKS,AKS)		5000000
			5100000
			5200000
000003	COMMON/LAYER/NOMAT,EI,E2,UI,GI2,MA,MATYPE,AT,TH		5300000
000003	COMMON/SIZE/LBPOS1,JBPOS2,JBPOS3,JBPOS4,MRJOT,NCJOT,ZIX(32),		5400000
	1Z1Y(32),ETAX(32),ETAY(32)		5500000
000003	COMMON/SPRING/AKL(32,32),AKX(32,32),AKY(32,32)		5600000
000003	COMMON/XY/TX,TY,IXY,RX,RY,KXY,PI,ADB,DS1,DS2,DS12,DS66,		5700000
	1IBC2,AKS2,X3,EX,EY,EXY,GXY,IT		5800000
000003	NAMELIST/BUCKLE/ISTIFF,IX,JX,IXY,IXY,RX,RY,IXY,		5900000
	1 XA,X3,MR,NC,X,Y,TEST,		6000001
	2 AKK,IBC,D1,D2,D12,D66,PI,DELP,PFIN,		6100000
	3 NOMAT,EI,E2,UI,GI2,MA,MATYPE,AT,TH		6200000
	4,NUPRIT,EI,IORIENT,LOC,MSHAPE,ISTEP		6300000
	5,AKL,AKX,AKY,DS1,DS2,DS12		6400000
000003	ABSCISA(X3,X2,X1,Y3,Y2,Y1)=X3+((Y1*Y3-Y2*Y3)*(X3-X1)/(Y1*00000026		6600000
	1Y2*(X1-X2)+Y1*Y3*(X3-X1)+Y2*Y3*(X2-X3))	00000027	6700000
			6800000
			7000000
			7100000
000032	SET DEFAULTS		7200000
	NUPRIT=0		7300000
000033	X=-1.		7400000
000035	Y=1.		7500000
000036	MSHAPE=2		7600000
000037	ISTIFF=2		7700000
000040	IX=JX=2		7800000
000042	ISTEP=1		7900001
000043	AKS(2)=0		8000000
000044	PI=-.9		8100000
000046	PFIN=100.		8200000
000047	INCX=0		8300000
000050	ICNT=1		8300001
000051	DELP=.1		8300002
000052	P=1.		8400000
000053	TEST=1,E=3		
000055	DO 9 I=1,32		

APPENDIX D

000056	DO 9 J=1,32		85000000
000057	9 AKI(I,J)=AKX(I,J)=AKY(I,J)=.0		86000000
	C	END OF DEFAULT LIST	87000000
	C		88000000
000070	1 IELCNT .GT. 1JGO TO 2		89000000
000074	7 READ(5,5001) CASE		90000000
000102	IE(EOF,5) 4,5		91000000
000105	4 PRINT 8997		92000000
000111	STOP		93000000
000113	5 PRINT 5032		94000001
000117	WRITE(6,5000) CASE		94000002
000122	WRITE(7,5000) CASE		95000000
000133	PRINT 5025		96000000
000137	READ BUCKLE		97000000
000142	WRITE(7,8998) MR,NC,X,Y		98000000
000156	8998 FORMAT(5X,*MP=*,I2,* NC=*,I2,* X=*,F16.8,* Y=*,F10.8/)		99000000
000156	ADB=X/X3		100000000
000160	WRITE(7,3939) TH(1),ADB		10100000
000170	8999 FORMAT(/,5X,*TH(1)=*,E16.8,5X,*ASPECT RATIO=*,E16.8/)		10200000
000170	ADB2=ADB*ADB		10300000
000172	EL=MR+1		10400000
000174	B=NC+1		10500000
000176	PLS=PI		10600000
000200	DELPS=DELP		10700000
000201	PEINS=PEIN		10800000
000203	XSS=X		10900000
000204	PEIN1 5021,ISTIFF,ISTEP,IX,JX,TEST		11000001
000222	IE(ISTIFF .EQ. 3 .OR. ISTEP .EQ. 3)GO TO 98		11100000
000231	PRINT 5022,XA,X6,ADB,MR,NC		11200000
000246	PRINT 5023,IX,IY,IXY,PI,DELP,PEIN,X,Y,RX,RY,RXY		11300000
000300	GO TO 97		11400000
000301	98 PRINT 5038		11500000
000302	97 CONTINUE		11600000
000305	CALL PREP(D1,D2,D12,D66,DS1,DS2,DS12,DS66,IX,JX,MR,NC,IT,EX,EY,EXY,GXY		11700000
	1,GXY,I3C,ISTIFF)		11800000
000330	MB1=MBOT		11900000
000332	NC1=NCICI		12000000
000333	105 CONTINUE		12100000
000334	PI=3.14159265359		12200000
000335	PI2=PI*PI		12300000
000336	IBC2=IBC(2)		12400000
000337	AKS2=AKS(2)		12500000
000341	IE(INCX .EQ. 3)GO TO 249		12600000

APPENDIX D

```

000342      2 X=XSTARI+(ICNT-1)*XDELIA      12700000
000350      IF(X .GT. XSTOP)GO TO 7      12800000
000353      IF(ICNT .EQ. 1)CALL AUTOXY(XZ,YZ,BETA,INCX)      12900000
000357      Y=AD9*X*BETA      13000000
000362      ICNT=ICNT+1      13100000
000363      PRINT 3996,MR,NC,X,Y      13200000
000377      WRITE(7,E958) MR,NC,X,Y      13300000
000413      GO TO 165      13400000
000414      249 IF(X .LF. 0. .GR. PI .LT. 0.)CALL AUTOXY(X,Y,BETA,INCX,P)      13500001
000427      168 CONTINUE      13600000
000427      PRINT 501C      13700000
000433      S2X=SIN(.5*PI/X/EL)      13800000
000441      SX=SIN(PI/X/EL)      13900000
000446      S2Y=SIN(.5*PI/Y/b)      14000000
000454      SY=SIN(PI/Y/H)      14100000
000461      IF(NUPRIT .EQ. 0)GO TO 113      14400000
000462      PRINT 5027      14500000
000465      DO 112 I=1,NUPRIT      14600000
000467      EH=EI(I)      14700000
000471      IF(IGRIENT(I) .EQ. 2)GO TO 114      14800000
000473      EPS=X/EL      14900000
000475      EI(I)=EH/EPS/DS1      15000000
000500      R=L.+EI(I)      15100000
000502      CALL SET(D1,I,IBPOS1,IBPOS3,LOC(I),R)      15200000
000506      GO TO 112      15300000
000507      114 EPS=X/b      15400000
000511      EI(I)=EH/EPS/DS1      15500000
000515      R=DS2+EI(I)      15600000
000517      CALL SET(D2,2,IBPOS4,IBPOS2,LOC(I),R)      15700000
000523      112 PRINT 5026,I,IGRIENT(I),LOC(I),EH,EI(I)      15800000
000544      113 CONTINUE      15900000
000544      CALL BC(X,Y,EL,0,AKS,DS1,DS2,DS12,D1,D2,D12,D66,MR,NC,IBC,
* XA,XB)
000565      IF(JX .EQ. 2)GO TO 125      16000000
000567      PRINT 5016      16100000
000573      PRINT 5015, ((D1(I,J),J=1,NCL),I=1,MR1)      16200000
000612      PRINT 5017      16300000
000616      PRINT 5015, ((D2(I,J),J=1,NCL),I=1,MR1)      16400000
000635      PRINT 5018      16500000
000641      PRINT 5015, ((D12(I,J),J=1,NCL),I=1,MR1)      16600000
000660      PRINT 5019      16700000
000664      PRINT 5015, ((D66(I,J),J=1,NCL),I=1,MR1)      16800000
000703      125 CONTINUE      16900000

```

APPENDIX D

```

000703      IF(LSTIFF.EQ.3)GO TO 84      17.000000
C
C      BEGIN BUCKLING ANALYSIS      17190000
C      17200000
C      17300000
C      17400000
000705      IF(X.GE.100.OR.Y.GE.100)GO TO 122      17500000
C      EDL=EHATX/EHATY*ADB      17600000
C      SX=SIN(.5*PI/EL/X)      17700000
C      XSX=2.*X*SX/PI      17800000
C      EDL=X/Y*ADB*SX/SIN(.5*PI/B/Y)      17900000
C      EDL1=2.*X/Y*ADB*SX/SIN(PI/B/Y)      18000000
C      EDE=2.*SX/SIN(PI/EL/X)      18100000
C      GO TO 123      18200000
C      122 EDE=1.      18300000
C      XSX=1./EL      18400000
C      EDL=EDL1+ADB*B/EL      18500000
C      123 MR2=2*(MR1-4)      18600000
C      PIEL=PI**2      18700000
C      TXSS=TX*PIEL      18800000
C      TYSS=TY*PIEL      18900000
C      TXYSS=TX*PIEL      19000000
C      IF(MSHAPE.EQ.3)GO TO 84      19100000
C      120 P1=PI*S*PIEL      19200000
C      01003 DELP=DELP*S*PIEL      19300000
C      01005 PEIN=PEIN*S*PIEL      19300001
C      01006 IF(P1.GT.0)GO TO 129      19300002
C      01011 P1=ABS(P1)*P      19300003
C      01012 DELP=.01*P*PIEL      19300004
C      01015 129 CONTINUE      19400000
C      01015 PIR=P1      19500000
C      01017 PRINT 61      19600000
C      01022 7700 L=0      19700000
C      01023 LC=1      00000108
C      01024 7702 CONTINUE      19800000
C      01024 P1=PIB*ADB2      19900000
C      01026 TXS=TXSS*ADR2+RX*PI      20000000
C      01032 TYS=TYSS*ADB2+RY*PI      20100000
C      01035 TXYSS=TXSS*ADB2+RXY*PI      20200000
C      01041 77 CALL ARRAY(D1,D2,D12,D66,EDL,W,A,TXS,TYS,TXYSS,MR,NC,XSX,EDL1,EDE,      20300000
C      1,2,IBC)      20400000
C      01062 4002 L=L+1      20500000
C      01064 CALL DEUPPS(A,MR2,CDEF,56)      20600000
C      01067 DET(L)=CDEF      20700000
C      01071 PP(L)=PIB/PIEL      20800000

```


APPENDIX D

001073	IXS=IXS/PIEL/ADB2	20900000
001076	IYS=IYS/PIEL/ADB2	21000000
001077	IXYS=IXYS/PIEL/ADB2	21100000
001101	80 PRINT 6,IXS,IYS,IXYS,DET(L)	21200000
001115	IF(L,1,3)GO TO 90	21300000
001120	AD1=DET(L)*DET(L-1)	21400000
001122	A02=DET(L)*DET(L-2)	21500000
001124	IF (ABS(DELP) .LT. PP(L)*TEST*PIEL)GO TO 155	21600000
001131	IF(L,STEP, EQ, 2)GO TO 154	21700000
001133	IF(LC, EQ, 2)GO TO 155	21800000
001135	DELP=DET(L)*DELP/(DET(L-1)-DET(L))	21900000
001141	IF (DELP .LT. 0. .AND. LC .GT. 5)GO TO 155	22000000
001152	IF (DELP .GT. LC, *DELPS*PIEL)DELP=LC.*DELPS*PIEL	22100000
001157	IF (ABS((PP(L-1)-PP(L))/PP(L)),GT. .01 .AND. LC .EQ. 1)GO TO 154	22200000
001174	IF (LC .GE. 15)GO TO 156	22300000
001176	DEL1=(PP(L)-PP(L-1))*PIEL	22400000
001202	DEL2=(PP(L-1)-PP(L-2))*PIEL	22500000
001204	DEL1P2=DEL1+DEL2	22600000
001206	FD=(DET(L)-DET(L-1))/(PP(L)-PP(L-1))/PIEL	22700000
001213	FDD=(DEL1*DET(L-2)-DEL1P2*DET(L-1)+DEL2*DET(L))/(.5*DEL1*DEL2 1 *DEL1P2)	22800000
001225	DELP=-DET(L)/FD - FDD*(DET(L)**2)/(8.*FD**3)	22900000
001235	IF (ABS(DELP) .LT. PP(L)*1.5-6)GO TO 155	23000000
001241	LC=LC+1	23100000
001243	GO TO 154	23200000
001243	156 DELP=.03*PP(L)*PIEL	23300000
001246	LC=LC+1	23400000
001250	154 IF(L,GT, 100)GO TO 1	23500000
001254	IF (AD1 .GE. 0. .AND. AD2 .GE. 0)GO TO 90	23600000
001263	155 CONTINUE	23700000
001263	CISSA=ABSCISA(PP(L), PP(L-1), PP(L-2), DET(L), DET(L-1), DET(L-2))	23800000
001270	P=CISSA	23900000
001271	DD=0.	24000000
001272	IXS=IXSS/PIEL+RX*P	24100000
001275	IYS=IYSS/PIEL+RY*P	24200000
001300	IXYS=IXYSS/PIEL+RXY*P	24300000
001304	PRINT 6,IXS,IYS,IXYS,DD	24400000
001317	WRITE(7,6)IXS,IYS,IXYS,DD	24500000
001333	WRITE(7,6) P,DD	24600000
001343	IXS=IXS*PI*PI*DS1/(XB*XB)	24700000
001347	IYS=IYS*PI*PI*DS1/(XB*XB)	24800000
001351	IXYS=IXYS*PI*PI*DS1/(XB*XB)	24900000
001353	PRINT 5,14,IXS,IYS,IXYS	25000000
		25100000

APPENDIX D

001365	WEIIE(7,5,14)IXS,IYS,IXYS	25200000
C		25300000
C	COMPUTATION OF USEFUL BUCKLING PARAMETERS	25400000
C		25500000
001377	IF(LISTIFF .NE. 2)GO TO 130	25600000
001401	FA=XB*XB/PI2/(II**3)	25700000
001403	IXI=IXS*FA	25800000
001406	IYI=IYS*FA	25900000
001410	IXYT=IXYS*FA	26000000
001411	PRINT 5030, IXI, IYI, IXYT	26100000
001423	FA=XB*XB/(II**3)	26200000
001426	EXT=FA*(1./EX)*(IXS-EXY/EY*YXS)	26300000
001434	EYT=FA*(1./EY)*(IYS-EXY/EX*IXS)	26400000
001442	EXYT=.5*FA*TXYS/GXY	26500000
001446	EXT=-EXT	26600000
001447	EYT=-EYT	26700000
001450	EXYT=-EXYT	26800000
001451	PRINT 5031, EXT, EYT, EXYT	26900000
001462	PRINT 5032	27000000
001469	130 IF(MSHAPE .EQ. 1)GO TO 87	27100000
001470	GO TO 85	27200000
001471	90 IF(PIB .GT. PFIN)GO TO 85	27300000
001475	PIB=PIB+DELPI	27400000
001476	GO TO 7702	27500000
001477	85 PI=PI5	27600000
001501	DELPI=DELPS	27700000
001502	PEINE=PEINS	27800000
001504	X=XSS	27900000
001505	GO TO 1	28000000
C		28100000
C	COMPUTE MODE SHAPES	28200000
C		28300000
001506	84 P=P1	28400000
001510	IF(MSHAPE .EQ. 2)GO TO 1	28500000
001512	87 IXS=(IXSS+EX*PIEL*P)*ADB2	28600000
001517	IYS=(IYSS+EY*PIEL*P)*ADB2	28700000
001524	TXYS=(TXYS+EXY*P*PIEL)*ADB2	28800000
001530	CALL ARRAY(D1,D2,D12,D66,FDL,W,A,IXS,IYS,TXYS,MR,NC,XSX,EDL1,EDE, 1,2,I6C,AKL,LOCX,LOCY,NK)	28900000
001554	D0 I15 I=1,MR2	29000000
001556	115 B(I,I)=-A(I,MR2)	29100000
001565	MR2MI=MR2-1	29200000
001567	CALL GELIM(56,MR2MI,A,1,B,IPIVOT,0,WK,IERR)	29300000
		29400001

APPENDIX D

```

001577      B(MR2,1)=1.
001601      DO 116 I=1,MR
001603      W(I+2,3)=B(I)
001605      116 W(I+2,4)=B(I+MR)
001611      CALL ARRAY(D1,D2,D12,D66,EDL,W,A,IXS,IYS,IXYS,MR,NC,XXS,EDL1,EDE,
           I 1,IBC)
001631      PRINT 5028
001635      WM=0.
001636      DO 170 I=3,MRP2
001640      DO 170 J=3,NCP2
001641      W1=A35(W(I,J))
001645      170 WM=AMAX1(W1,WM)
001654      WMI=1./WM
001656      DO 171 I=2,MRP3
001657      DO 172 J=2,NCP3
001660      172 W(I,J)=W(I,J)*WMI
001666      PRINT 5029, (W(I,J),J=2,NCP3)
001702      171 PRINT 5033
001711      GO TO 85
001711      O FORMAT(2X,E16.8,3X,E16.8,4X,E16.8,10X,E16.8)
001711      61 FURNAT(///,9X,*NXBAR*,15X,*NYBAR*,13X,*NXYBAR*,17X,*DETERMINANT*//)
001711      5000 FURNAT(///,15H INPUT FOR CASE///,1X8A10///)
001711      5001 FURNAT(8A10)
001711      5002 FURNAT(1X8A10)
001711      5010 FURNAT(//,20X,19HBOUNDARY CONDITIONS )
001711      511 FURNAT(/,5X,*BOUNDARY NC. *,11,* HAS A ROTATIONAL SPRING SUPPORT 0
           IF MAGNITUDE *,F16.8//)
001711      512 FURNAT(/,13X,*BOUNDARY NO. *,11,* IS SIMPLY SUPPORTED*,/)
001711      5013 FURNAT(/,15X,*BOUNDARY NO. *,11,* IS CLAMPED*,/)
001711      514 FURNAT(//,15X,*BUCKLING LOADS PER UNIT OF LENGTH ALONG BOUNDARY ED
           16E*,/,5X,*NX=*,E16.8,5X,*NY=*,E16.8,5X,*NXY=*,E16.8//)
001711      5015 FURNAT(/,(3E20.8))
001711      5016 FURNAT(//,30X,*D1*)
001711      5017 FURNAT(//,30X,*D2*)
001711      5013 FURNAT(//,30X,*D12*)
001711      5019 FURNAT(//,30X,*D66*)
001711      5121 FURNAT(5X,*I STIFF=*,11,3X,*I STEP=*,11,10X,*IX=*,11,3X,*JX=*,11,
           * 9X,*TEST=*,F16.8//)
001711      5022 FURNAT(5X,*XA=*,E16.8,5X,*XB=*,E16.8,5X,*ASPECT RATIO=*,E16.8//
           1,15X,*MR=*,12,5X,*NC=*,12//)
001711      5123 FURNAT(5X,*IX=*,E16.8,5X,*IY=*,E16.8,7X,*IXY=*,E16.8//
           1,5X,*PI=*,E16.8,5X,*DELP=*,E16.8,5X,*PFIN=*,E16.8//
           * ,5X,*X=*,E16.8,5X,*Y=*,E16.8//,5X,*RX=*,E16.8,5X,*RY=*,E16.8,7X,

```

APPENDIX D

```

3*ERY=* ,E16.8//)
001711 5024 FORMAT(/,1X,100(1H*))
001711 5025 FORMAT(/,30X,12(1H1),5(1H*),1X,1HY,/,5(30X,1H4,10X,1H2,/,),30X,
1 12(1H3),/,3(30X,1H*,/,),/,3CX,1HX,///)
001711 5026 FORMAT(1X,12,3X,11,3X,12,4X,E16.8,2X,E16.8)
001711 5027 FOPMAT(/,99X,*STIFFENER DATA*,/,*NO.*,2X,*LORIENT*,2X,*LOC*,10X,
1 *EI*,12X,*EI/FPS/D1*,/)
001711 5028 FOPMAT(/,5,2X,*MODE SHAPE*,/)
001711 5029 FOPMAT(1X,5(E15.7,1X))
001711 5030 FOPMAT(/,2X,23H(XB**2)*IX/(PI**2)/(T**3) = ,E16.8/,
1 X,20H(XD**2)*NY/(PI**2)/(T**3) = ,E16.8/,
2 X,29H(XE**2)*NX/(PI**2)/(T**3) = ,E16.8//)
001711 5031 FOPMAT(/,2X,26H(XB**2)*EPSILONX/(T**2) = ,E16.8/,
1 X,26H(XB**2)*EPSILONY/(T**2) = ,E16.8/,
2 X,27H(XB**2)*EPSILONXY/(T**2) = ,E16.8//)
001711 5032 FOPMAT(1H1)
001711 5033 FOPMAT(///)
001711 5035 FOPMAT(/,2X,*WARNING, A BUCKLING VALUE MAY HAVE BEEN SKIPPED*,/)
001711 5038 FOPMAT(/,10X,*ISTEP=3 OR LSTIFF=3 - PREPROCESS ONLY*,//)
001711 8997 FOPMAT(//*
* )
001711 00000032 35800000
* )
001711 35920000
END

```

APPENDIX D

	SUBROUTINE ARRAY(D1,D2,D12,D66,EDL,W,A,TX,TY,IXY,MR,NC,XXS,EDL1,	36000000
	1 EDE,MS,IPC)	36100000
000024	DIMENSION IBC(4)	36200000
000024	DIMENSION D1(32,32),D2(32,32),D12(32,32),D66(32,32)	36300000
000024	DIMENSION W(32,32),A(56,56)	36400000
000024	COMMON/SIZE/IBPOS1,IBPOS2,IBPOS3,IBPOS4,MRTOT,NCIOT,ZIX(32),	36500000
	IZIY(32),ETAX(32),ETAY(32)	36600000
000024	COMMON/SPRING/AKL(32,32),AKX(32,32),AKY(32,32)	36700000
000024	WXX(K,L)=W(K+1,L)-2.*W(K,L)+W(K-1,L)	36800000
000042	WYY(K,L)=(W(K,L+1)-2.*W(K,L)+W(K,L-1))*EDLS	36900000
000057	WXY(K,L)=(W(K+1,L+1)-W(K+1,L)-W(K,L+1)+W(K,L))*EDL	37000000
000075	WX(K,L)=ZIY(L)*ETAX(K)*W(K+1,L)-W(K,L)	37100000
000112	WY(K,L)=ZIY(L)*ETAX(K-1)*W(K,L+1)-W(K,L))*EDLS	37200000
000127	WXY2(K,L)=(W(K+1,L+1)-W(K,L))*ETAX(K)*ETAY(L)-W(K+1,L-1)-W(K,L))	37300000
	1*ETAX(K)*ETAY(L-1) -(W(K,L)-W(K-1,L-1))*ETAX(K-1)*ETAY(L-1)	37400000
	2 +(W(K,L)-W(K-1,L+1))*ETAX(K-1)*ETAY(L)+TY*(WY(K,L)-WY(K,L-1))	37500000
000173	1W(K,L)=(TX*(WX(K,L)-WX(K-1,L)) + TY*(WY(K,L)-WY(K,L-1))	37600000
	1 +2.*TX*WXY2(K,L))*XSX**2	37700000
	2 +(AKL(K,L)*W(K,L))*XSX**2+AKX(K-1,L)*W(K,L)-W(K-1,L))	37800000
	3 -AKX(K,L)*W(K+1,L)-W(K,L)) +(AKY(K,L-1)*W(K,L)-W(K,L-1))	37900000
	4-AKY(K,L)*W(K,L+1)-W(K,L))*EDLS*EDL	38000000
000304	XM(K,L)=D1(K,L)*WXX(K,L)+D12(K,L)*WYY(K,L)	38100000
000327	YM(K,L)=D2(K,L)*WYY(K,L)+D12(K,L)*WXX(K,L)	38200000
000352	XYM(K,L)=2.*D66(K,L)*WXY(K,L)	38300000
000366	XXM(K,L)=XM(K+1,L)-2.*XM(K,L)+XM(K-1,L)	38400000
000413	YYM(K,L)=(YM(K,L+1)-2.*YM(K,L)+YM(K,L-1))*EDLS	38500000
000441	XYXYM(K,L)=(XYM(K,L)-XYM(K,L-1)-XYM(K-1,L)+XYM(K-1,L-1))*EDL	38600000
000474	EKE(K,L)=XXM(K,L)+2.*XYXYM(K,L)+YYM(K,L)+TW(K,L)	38700000
000525	EDLP=EDL*EDE	38800000
000530	EDLS=EDL**2	38900000
000531	IRUM=MRTOT-2	39000000
000533	ICOL=NCIOT-4	39100000
000535	IF(MS.EQ.1)GO TO 35	39200000
000537	NNC=ICOL+1	39300000
000540	NCC=ICOL+2	39400000
000542	DO 10 J=1,NCIOT	39500000
000543	DO 10 I=1,MRTOT	39600000
000544	W(L,J)=0.0	39700000
000550	10 CONTINUE	39800000
000555	MMN=0	39900000
000556	DO 40 N=3,4	40000000
000557	DO 40 M=3,IP05	40100000

APPENDIX D

```

000560 MN=0 402000000
000561 MN=N*IN+1 403000000
000563 DO 39 I=3,IRDW 404000000
000564 39 W(I,3)=W(I,4)=0 405000000
000572 A(M,N)=L,C 406000000
407000000
C 408000000
C 409000000
C 410000000
000576 35 DO 36 J=3,ICD1 411000000
000600 DO 36 I=3,IRDW 412000000
000601 YBZ=-XXW(I,J)-2.*XXXYM(I,J)-TW(I,J) 413000000
000621 YMM=WCM/EDLS+2.*YM(I,J)-YM(I,J-1) 414000000
000636 YK=(YMM-D12(I,J+1)*WXX(I,J+1))/D2(I,J+1) 415000000
000653 IF(I.EQ._IBPOS1_.OR._I.EQ._IBPOS3) YK=YMM/D2(I,J+1) 416000000
000665 W(I,J+2)=YK/EDLS+2.*W(I,J+1)-W(I,J) 417000000
000676 30 CONTINUE 418000000
000703 1 FORMAT(/,2(IX,7F18.8//) 419000000
000703 IF(MS.EQ._1)RETURN 420000000
000706 DO 20 J=NC,NCC 421000000
000710 DO 20 I=3,IRDW 422000000
000711 MN=MN+1 423000000
000713 NUM=NC/2 424000000
000715 CF=10.*NUM 425000000
000720 A(MN,MN)=EKE(I,J)/CF 426000000
000732 20 CONTINUE 427000000
000737 40 CONTINUE 428000000
000743 2 FORMAT(/,4(IX,5F20.8//) 429000000
000743 RETURN 430000000
000744 END

```

APPENDIX D

```

43100000
43200000
43300000
43400000
43500000
43600000
43700000
43800000
43900000
44000000
44100000
44200000
44300000
44400000
44500000
44600000
44700000
44800000
44900000
45000000
45100000
45200000
45300000
45400000
45500000
45600000
45700000
45800000
45900000
46000000
46100000
46200000
46300000
46400000
46500000
46600000
46700000
46800000
46900000
47000000
47100000
47200000

SUBROUTINE DFUPPS(A,N,DET,MAX)
DIMENSION A(MAX,N)
DET=1.
NN = N-1
C PIVOT SEARCH
DO 560 I=1,NN
  CAVM = 0.
  JJ = I
  DO 105 J=I+1,N
    SWAP = A(J,I)
    CAVA=ABS(SWAP)
    IF(CAVM.GE.CAVA) GO TO 105
  IRJW = J
  CAVM = CAVA
  105 CONTINUE
  IF(CAVM.EQ.0.) GO TO 720
  C ROW INTERCHANGE
  IF(IRJW.EQ.I) GO TO 203
  DET = -DET
  DO 200 I=I+1,N
    SWAP = A(IRJW,I)
    A(IRJW,I) = A(I,I)
    A(I,I) = SWAP
  200 CONTINUE
  203 SWAP = A(I,I)
  DET = DET*SWAP
C NORMALIZE PIVOT ROW
K = I+1
DO 350 I=K,N
  350 A(I,I) = A(I,I)/SWAP
C ELIMINATION
DO 550 I=K,N
  SWAP = A(I,I)

```

APPENDIX D

```

000105      DC 500 I=K,N          47300000
000107      A(I,I,I) = A(I,I,I)-A(I,I,I)*SWAP 47400000
000121      500 CONTINUE          47500000
000124      550 CONTINUE          47600000
000126      560 CONTINUE          47700000
000131      GO TO 730            47800000
000131      720 DET=2.           47900000
000132      GO TO 750            48000000
000132      730 DET = DET*A(N,N) 48100000
000136      750 RETURN           48200000
000137      END                  48300000

```


APPENDIX D

	SUBROUTINE BC(X,Y,EL,B,AKS,DSL,DS2,DS12,DL,D2,DI2,D66,MR,NC,IBC,	48400000
	I XA,XB)	48500000
		48600000
C		48700000
C	COMPUTES VALUES OF PLATE STIFFNESSES SUCH THAT THE APPROPRIATE	48800000
C	BOUNDARY CONDITIONS ARE SET	48900000
C		49000000
C	OPTIONS	49100000
C	IBC=1 ROTATIONAL SPRING SUPPORT	49200000
C	IBC=2 SIMPLE SUPPORT	49300000
C	IBC=3 CLAMPED SUPPORT	49400000
C	IBC=4 FREE BOUNDARY	49500000
C	IBC=5, BOUNDARY CONDITIONS NOT SET BY THIS SUBROUTINE	49600000
C		49700000
000024	DIMENSION AKS(4),IBC(4),DI(32,32),D2(32,32),DI2(32,32),D66(32,32)	49800000
000024	COMMON/SIZE/IBPOS1,IBPOS2,IBPCS3,IBPOS4,MR10I,NC10I,ZIX(32),	49900000
	I,LY(32),ETAX(32),ETAY(32)	50000000
000024	PI=3.14159265359	50100000
000025	SX=SIN(PI/X/EL)	50200000
000034	SY=SIN(PI/Y/B)	50300000
000044	S2X=SIN(.5*PI/X/EL)	50400000
000055	S2Y=SIN(.5*PI/Y/B)	50500000
000066	IBP3M1=IBPOS3-1	50600000
000070	IBP2M1=IBPOS2-1	50700000
000072	IBP4P1=IBPOS4+1	50800000
000073	IBP2M1=IBPOS2-1	50900000
000074	DO 150 M=1,4	51000000
000076	L=IBC(M)	51100000
000101	GO TO(151,152,153,154,150)L	51200000
000112	151 PRINT 5011,M,AKS(M)	51300000
000126	IF(M.EQ.2.OR.M.EQ.4)GO TO 160	51400000
000141	GAMMAX=AKS(M)*XA/DSL	51500000
000144	FHATX=4.*X*S2X**2/PI/SX	51600000
000150	CX=(1.-.5*GAMMAX*EHATX)/(1.+5*GAMMAX*EHATX)	51700000
000160	IF(M.EQ.3)GO TO 170	51800000
000162	181 K=DSL*(1.-CX)/DSL	51900000
000165	CALL SET(DI,2,IBPOS4,IBPOS2,IBPOS1,R)	52000000
000172	GO TO 150	52100000
000176	170 K=DSL*(1.-CX)/DSL	52200000
000201	CALL SET(DI,2,IBPOS4,IBPCS2,IBPOS3,R)	52300000
000206	GO TO 150	52400000
000212	160 GAMMAY=AKS(M)*Y/B/DS2	52500000
000216	FHATY=4.*Y*S2Y**2/PI/SY	

APPENDIX D

000223	CY=(1.-.5*GAMMAY*EHATY)/(1.+5*GAMMAY*EHATY)	52600000
000233	IF(M.EG.4)GC IO 180	52700000
000235	183 R=DS2*(1.-CY)/DS1	52800000
000241	CALL SFI(D2,I,IBPOS1,IBPOS3,IBPOS2,R)	52900000
000245	GO TO 150	53000000
000251	180 R=DS2*(1.-CY)/DS1	53100000
000255	CALL SFI(D2,I,IBPOS1,IBPOS3,IBPOS4,R)	53200000
000261	GO TO 150	53300000
000265	152 PRINT 5012,M	53400000
000273	CX=CY=1.	53500000
000276	GO TO(181,183,170,180)M	53600000
000311	153 PRINT 5013,M	53700000
000317	CX=CY=-1.	53800000
000322	GO TO(181,183,170,180)M	53900000
000335	154 PRINT 5014,M	54000000
000343	GO TO (201,202,203,204)M	54100000
000357	201 DO 221 J=IBPOS4,IBPOS2	54200000
000361	D2(1,IBPOS1,J)=.5*D2(1,IBPOS1,J)/(1.-D12(1,IBPOS1,J)/D1(1,IBPOS1,J))	54300000
	1 *D12(1,IBPOS1,J)/D1(1,IBPOS1,J))	54400000
000377	D1(1,IBPOS1,J)=0	54500000
000403	221 D12(1,IBPOS1,J)=0	54600000
000407	GO TO 150	54700000
000410	202 DO 223 I=IBPOS1,IBPOS3	54800000
000412	D1(I,IBPOS2)=.5*D1(I,IBPOS2)	54900000
000416	D2(I,IBPOS2)=.5*D2(I,IBPOS2)	55000000
000421	223 D12(I,IBPOS2)=D12(I,IBPOS2)*.5	55100000
000427	GO TO 150	55200000
000427	203 DO 225 J=IBP4P1,IBP2M1	55300000
000431	D2(1,IBPOS3,J)=.5*D2(1,IBPOS3,J)*(1.-D12(1,IBPOS3,J)/D2(1,IBPOS3,J))	55400000
	1 *D12(1,IBPOS3,J)/D1(1,IBPOS3,J))	55500000
000447	D1(1,IBPOS3,J)=0	55600000
000452	225 D12(1,IBPOS3,J)=0	55700000
000456	GO TO 150	55800000
000457	204 DO 227 I=IBPOS1,IBPOS3	55900000
000461	D1(I,IBPOS4)=.5*D1(I,IBPOS4)	56000000
000465	D2(I,IBPOS4)=.5*D2(I,IBPOS4)	56100000
000470	227 D12(I,IBPOS4)=.5*D12(I,IBPOS4)	56200000
000475	150 CONTINUE	56300000
000477	DO 260 I=1,MRTOT	56400000
000501	ZIX(I)=ETAX(I)=1.	56500000
000505	260 IF(1.I,IBPOS1.OR.1.GI,IBPOS3)ZIX(I)=ETAX(I)=.0	56600000
000525	ZIX(1,IBPOS1)=.5	56700000
000527	ZIX(1,IBPOS3)=.5	56800000

APPENDIX D

000530	ETAX(IBPOS3)=.0	569000000
000531	DO 261 J=1,NCIQT	570000000
000533	ZIY(J)=ETAY(J)=1.	571000000
000537	261 IF(J.LT.IBPOS4 .OR. J.GT.IBPOS2)ZIY(J)=ETAY(J)=.0	572000000
000557	ZIY(IBPOS4)=.5	573000000
000561	ZIY(IBPOS2)=.5	574000000
000562	ETAY(IBPOS2)=.0	575000000
000563	5011 FORMAT(/,13X,*BOUNDARY NU. *11,* HAS A ROTATIONAL SPRING SUPPORT 0	576000000
	IF MAGNITUDE #,F16.8/)	577000000
000563	5012 FORMAT(/,13X,*BOUNDARY NU. *11,* IS SIMPLY SUPPORTED*,/)	578000000
000563	5013 FORMAT(/,13X,*BOUNDARY NU. *11,* IS CLAMPED*,/)	579000000
000563	5014 FORMAT(/,13X,*BOUNDARY NU. *11,* IS FREE*,/)	580000000
000563	RETURN	581000000
000564	END	582000000

APPENDIX D

	SUBROUTINE PREP(D1,D2,D12,D12,D66,DSL,DS2,DS12,DS66,IX,JX,MR,NC,II,EX, LEY,EXY,GXY,IBC,ISL,IFF)	58300000
		58400000
		58500000
C	THIS SUBROUTINE PREPROCESSES THE ORTHOTROPIC PROPERTIES OF A LAMINATE	58600000
C		58700000
000026	DIMENSION Q(10,4),E1(10),E2(10),U1(10),G12(10),DD(3,3),IBC(4), IAT(100),IF(100),MATYPE(100),D1(32,32),D2(32,32),D12(32,32), D66(32,32)	58800000
000026	COMMON/LAYER/NUMAT,E1,E2,U1,G12,MA,MATYPE,AI,IH	59100000
000026	COMMON/SIZE/IBPOS1,IBPOS2,IBPOS3,IBPOS4,MRIOT,NCIOT,ZIX(32), IZIY(32),ETAX(32),ETAY(32)	59200000
000026	IBPOS1=2+IBC(IJ)/4	59300000
000031	IBPOS2=NC+3+IBC(4)/4*2	59400000
000040	IBPOS3=IBPOS1+MR+1	59500000
000043	IBPOS4=2+IBC(4)/4*2	59600000
000051	MRIOT=MR+4+IBC(IJ)/4 +IBC(3)/4	59700000
000055	NCIOT=NC+4+IBC(2)/4*2+IBC(4)/4*2	59800000
000067	FCRMAT(//,1015//)	59900000
000067	IF(ISTIFF.EQ.1)GO TO 160	60200000
000072	DO 165 I=1,MRIOT	60300000
000073	DO 165 J=1,NCIOT	60400000
000074	165 D1(I,J)=D2(I,J)=D12(I,J)=D66(I,J)=.0	60500000
000115	TT=0.	60600000
000116	100 PRINT 5003	60700000
000122	PRINT 5006	60800000
000126	DO 110 K=1,NOMAT	60900000
000133	PRINT 5007,K,E1(K),E2(K),U1(K),G12(K)	61000000
000150	ANVXY=U1(K)	61100000
000152	ANVYX=ANVXY*E2(K)/E1(K)	61200000
000155	ANU=1./(1.-ANVXY*ANVYX)	61300000
000160	Q(K,1)=E1(K)*ANU	61400000
000163	Q(K,2)=E2(K)*ANU	61500000
000165	Q(K,3)=ANVXY*E2(K)*ANU	61600000
000170	110 Q(K,4)=G12(K)	61700000
000200	PRINT 5008	61800000
000203	DO 115 J=1,MA	61900000
000210	PRINT 5009,J,MATYPE(J),AT(J),TH(J)	62000000
000223	115 TT=TT+AT(J)	62100000
000234	ZI=.5*TT	62200000
000236	CALL EVAL(AT,TH,MATYPE,ZI,MA,Q,DD,IX,JX,EX,EY,EXY,GXY)	62300000
000255	DSL=DD(1,1)	62400000
000262	DS2=DD(2,2)	62500000
		62600000

APPENDIX D

000263	DS12=DD(I,2)	62700000
000264	DS66=LD(3,3)	62800000
000266	DO 14C KR=IBPCS1,IBPCS3	62900000
000270	DO 14G KC=IBPCS4,IBPCS2	63000000
000272	D1(KR,KC)=DD(I,1)/DS1	63100000
000276	D2(KG,KC)=DD(2,2)/DS1	63200000
000301	140 D12(NB,KC)=DD(I,2)/DS1	63300000
000310	IB2M1=IBPCS2-I	63400000
000312	IB3M1=IBPCS3-I	63500000
000313	DO 15C KR=IBPCS1,IB3M1	63600000
000315	DO 15G KC=IBPCS4,IB2M1	63700000
000317	150 D66(KP,KC)=DD(3,3)/DS1	63800000
000330	RETURN	63900000
000331	160 DS1J=1./DS1	64000000
000333	DO 17C I=IBPCS1,IBPCS3	64100000
000335	DO 17G J=IBPCS4,IBPCS2	64200000
000337	D1(I,J)=D1(I,J)*DS1J	64300000
000343	D2(I,J)=D2(I,J)*DS1J	64400000
000346	D12(I,J)=D12(I,J)*DS1J	64500000
000350	170 D66(I,J)=D66(I,J)*DS1J	64600000
000357	IB1M1=IBPCS1-I	64700000
000361	IB2P1=IBPCS2+I	64800000
000363	IB3P1=IBPCS3+I	64900000
000364	IB4M1=IBPCS4-I	65000000
000365	DO 180 I=1,IB1M1	65100000
000367	DO 180 J=1,NC101	65200000
000370	D1(I,J)=D12(I,J)=D2(I,J)=D66(I,J)=.0	65300000
000405	180 CONTINUE	65400000
000411	DO 181 I=1,IB3P1,MRI01	65500000
000413	DO 181 J=1,NC101	65600000
000414	D1(I,J)=D12(I,J)=D2(I,J)=D66(I,J)=.0	65700000
000431	181 CONTINUE	65800000
000435	DO 182 J=1,IB4M1	65900000
000437	DO 182 I=IBPCS1,IBPCS3	66000000
000441	D1(I,J)=D12(I,J)=D2(I,J)=D66(I,J)=.0	66100000
000456	182 CONTINUE	66200000
000463	DO 183 J=1,IB2P1,NC101	66300000
000465	DO 183 I=IBPCS1,IBPCS3	66400000
000467	D1(I,J)=D12(I,J)=D2(I,J)=D66(I,J)=.0	66500000
000504	183 CONTINUE	66600000
000511	5003 FORMAT(//,30X,26HMINIMATED PLATE PROPERTIES)	66700000
000511	5004 FORMAT(//,20X,35HMID-PLANE USED AS REFERENCE SURFACE)	66800000
000511	5005 FORMAT(//,20X,5HZREF=,F16.8)	66900000

APPENDIX D

000511	5006 FURMAT(//,1X,13HMATERIAL KIND,8X,3H E1,15X,3H E2,13X,5H U1 ,12X, 13HGXY)	670000000
		671000000
000511	5007 FURMAT(7X,12,7X,E16.8,3(1X,E16.8))	672000000
000511	5008 FURMAT(//,1X,9HLAYER NU.,3X,9HMAT. KIND,6X,5HTHICK,12X,5HIHEIA)	673000000
000511	5009 FURMAT(5X,12,9X,12,5X,E16.8,1X,E16.8)	674000000
000511	REIUPN	675000000
000512	END	676000000

APPENDIX D

000020	SUBROUTINE EVAL(I,TH,IL,ZL,NL,Q,DD,IX,JX,EX,EY,EXY,GXY)	67700000
000020	DIMENSION I(100),IH(100),IL(100),IL(100),DD(3,3),Q(10,4),AA(3,3),BB(3,3),	67800000
	ZOB(3,3)	67900000
000020	O3=1./3.	68000000
000022	TI=0.	68100000
000023	DO 6 IV=1,3	68200000
000024	DO 6 JV=1,3	68300000
000025	AA(IV,JV)=1.	68400000
000030	BB(IV,JV)=Q.	68500000
000032	6 DD(IV,JV)=Q.	68600000
000040	DO 20 J=1,NL	68700000
000042	K=IL(J)	68800000
000044	THEIA=TH(J)*3.14159265359/180.	68900000
000047	CALL TRANS(Q,THEIA,QB,K,IX,JX)	69000000
000054	HJ=ZL-TI	69100000
000062	HJPI=HJ-T(J)	69200000
000065	HSQ=.5*(HJ**2-HJPI**2)	69300000
000070	TI=TI+I(J)	69400000
000073	DO 20 IV=1,3	69500000
000074	DO 20 JV=1,3	69600000
000075	AA(IV,JV)=AA(IV,JV)+QB(IV,JV)*I(J)	69700000
000104	BB(IV,JV)=BB(IV,JV)+QB(IV,JV)*HSQ	69800000
000111	20 CONTINUE	69900000
000120	ZREF1=BB(1,1)/AA(1,1)	70000000
000122	ZREF2=BB(2,2)/AA(2,2)	70100000
000124	ZREF12=BB(1,2)/AA(1,2)	70200000
000126	ZREF3=BB(3,3)/AA(3,3)	70300000
000130	PRINT 9	70400000
000133	PRINT 8, ZREF11,ZREF22,ZREF12,ZREF33	70500000
000147	PRINT 9	70600000
000153	ZI=ZL-ZREF11	70700000
000161	TI=.0	70800000
000161	DO 30 J=1,NL	70900000
000163	K=IL(J)	71000000
000165	THEIA=TH(J)*3.14159265359/180.	71100000
000170	CALL TRANS(Q,THEIA,QB,K,IX,JX)	71200000
000175	HJ=ZL-TI	71300000
000203	HJPI=HJ-T(J)	71400000
000206	HCOBE=O3*(HJ**3-HJPI**3)	71500000
000212	TI=TI+I(J)	71600000
000215	DO 30 IV=1,3	71700000
000216	DO 30 JV=1,3	71800000

APPENDIX D

```

000217 3. DD(IV,JV)=DD(IV,JV)+GB(IV,JV)*HCUBE 719000000
000236 PRINT 3 720000000
000241 PRINT 2,((AA(IV,JV),IV=1,3),JV=1,3) 721000000
000257 PRINT 4 722000000
000263 PRINT 2,((BB(IV,JV),IV=1,3),JV=1,3) 723000000
000301 PRINT 5 724000000
000305 PRINT 2,((DD(IV,JV),IV=1,3),JV=1,3) 725000000
000324 ANUXY=AA(1,2)/AA(2,2) 726000000
000326 ANUYX=AA(1,2)/AA(1,1) 727000000
000333 EX=AA(1,1)*(1.-ANUXY*ANUYX)/IT 728000000
000335 FY=AA(2,2)*(1.-ANUYX*ANUXY)/IT 729000000
000342 EXY=ANUXY*EY 730000000
000344 GXY=AA(3,3)/IT 731000000
000346 PRINT 7,EX,EY,GXY,ANUXY,ANUYX 732000000
000364 2 FORMAT(//,5(IX,E16.8,2X,E16.8,2X,E16.8//)) 733000000
000364 3 FORMAT(//,25X,SHA MATRIX) 734000000
000364 4 FORMAT(//,25X,BHB MATRIX) 735000000
000364 5 FORMAT(//,25X,SHD MATRIX) 736000000
000364 7 FORMAT(//,15X,*OVERALL LAMINATE PROPERTIES*,//,* EX=*,E16.8, 737000000
1 * EY=*,E16.8,* GXY=*,E16.8,/* NUXY=*,E16.8,* NUYX=*,E16.8//) 738000000
000364 3 FORMAT(//,5X,*CAUTION -- COUPLING BETWEEN EXTENSION AND BENDING MA 739000000
IY BE SIGNIFICANT*,//,5X,*IF THE FOLLOWING FOUR VALUES ARE NOT ALL E
2QUAL*,//,5X,*IF THIS IS THE CASE, THE RESULTS SHOULD BE USED WITH
3DESCRITION*,//,4(2X,E16.8),/) 741000000
000364 9 FORMAT(IX,76(1H*),/) 742000000
000364 RETURN 743000000
000365 END 744000000
745000000

```


APPENDIX D

```

SUBROUTINE TRANS(Q,THETA,QB,K,IX,JX)
74600000
DIMENSION T(3,3),TI(3,3),QS(3,3),SI(3,3),QB(3,3),Q(10,4)
74700000
000011 SN=SIN(THETA)
74800000
000011 CS=COS(THETA)
74900000
000024 T(1,1)=TI(1,1),T(2,2)=TI(2,2),CS**2
75000000
000036 T(1,2)=TI(1,2),T(2,1)=TI(2,1),SN**2
75100000
000050 T(1,3)=TI(2,3)=2.*CS*SN
75200000
000055 T(3,1)=TI(3,2)=-SN*CS
75300000
000061 T(2,3)=TI(1,3)=-T(1,3)
75400000
000065 T(3,2)=TI(3,1)=-T(3,1)
75500000
000071 T(3,3)=TI(3,3)=CS*CS-SN*SN
75600000
000076 QS(1,1)=Q(K,1)
75700000
000100 QS(2,2)=Q(K,2)
75800000
000102 QS(1,2)=QS(2,1)=Q(K,3)
75900000
000106 QS(3,3)=2.*Q(K,4)
76000000
000111 QS(1,3)=QS(3,1)=QS(2,3)=QS(3,2)=0.
76100000
000122 IF(IX.EQ.1)PRINT 1,((QS(I,J),J=1,3),I=1,3)
76200000
000145 IF(IX.EQ.1)WRITE(7,1)((QS(I,J),J=1,3),I=1,3)
76300000
000170 DO 5 IM=1,3
76400000
000172 DO 5 IS=1,3
76500000
000173 5 SI(IM,IS)=QB(IM,IS)=0.
76600000
000204 DO 10 IM=1,3
76700000
000205 DO 10 IS=1,3
76800000
000206 DO 10 IR=1,3
76900000
000207 10 ST(IM,IS)=SI(IM,IS) + QS(IM,IR)*T(IR,IS)
77000000
000230 DO 20 IR=1,3
77100000
000231 DO 20 IS=1,3
77200000
000232 DO 20 IM=1,3
77300000
000233 20 QB(IR,IS)=QB(IR,IS)+TI(IR,IM)*ST(IM,IS)
77400000
000254 DO 30 IM=1,3
77500000
000255 30 QB(IM,3)=.5*QB(IM,3)
77600000
000262 IF(IX.EQ.1)PRINT 1,((TI(I,J),J=1,3),I=1,3),I=1,3)
77700000
000317 IF(IX.EQ.1)PRINT 1,((QB(I,J),J=1,3),I=1,3)
77800000
000346 IF(IX.EQ.1)WRITE(7,1)((QB(I,J),J=1,3),I=1,3)
77900000
000375 1 FORMAT(3I3X,E16.8)
78000000
000375 RETURN
78100000
000376 END
78200000

```

APPENDIX D

000010	SUBROUTINE AUTOXY(X,Y,B,INCX,P)	783000001
000010	COMMON/XY/IX,IY,IXY,RX,RY,RXY,PI,AUB,DSL,DS2S,DSL2,DS66,	784000000
000010	LU,C2,AKS2,XB,EX,EY,FXY,GXY,IT	785000000
000010	PRINT 53	785000001
000013	D12S=(DSL2+2.*DS66)/DSL	786000000
000017	DS2=DS2S/DSL	787000000
000020	LC=1	788000000
000021	P=.1	789000000
000026	B=1.	790000000
000027	DP=DB=1.	791000000
000031	PID8=PI/8.	792000000
	C	793000000
	C SIMPLE SUPPORTS, IK=1	794000000
	C CLAMPED SUPPORTS, IK=2	795000000
	C	796000000
000032	IF(LU,C2,LU,3,OK,AKS2*XB/DS2,GI,100,JK=2	797000000
000047	1 CX=IX+P*RX	798000000
000052	CY=IY+P*RY	799000000
000055	CXY=IXY+P*RXY	800000000
000060	AM1=PID8*(DS2+2.*D12S*B*B+B**4-B*B*CX-CY)	801000000
000072	AM1B=PID8*(4.*D12S*B*4.*B*B*B-2.*CX*B)	802000000
000102	AM1B3=PID8*(12.*B*B-2.*CX+4.*D12S)	803000000
000110	AM1P=PID8*(-B*B*RX-RY)	804000000
000113	AM1BP=-PI*.25*RX*B	805000000
000117	AM2=PID8*(16.*DS2+8.*D12S*B*B+B**4-B*B*CX-4.*CY)	806000000
000132	AM2B=PID8*(16.*D12S*B+4.*B**3-2.*CX*B)	807000000
000142	AM2B3=PID8*(12.*B*B*16.*D12S-2.*CX)	808000000
000150	AM2P=PID8*(-B*B*RX-4.*RY)	809000000
000154	AM2BP=-PI*.25*RX*B	810000000
000160	IF(IK,EW,2)GO TO 20	811000000
000162	F=(CXY*3)**2-2.*25*AM1*AM2	812000000
000167	G=2.*CXY*CXY*B-2.*25*(AM1B*AM2+AM2B*AM1)	813000000
000175	F3=G	814000000
000177	FP=2.*CXY*RXY*B*B-2.*25*(AM1P*AM2+AM2P*AM1)	815000000
000207	GH=2.*CXY*CXY-2.*25*(AM1BP*AM2+AM2BP*AM1+2.*AM1B*AM2B)	816000000
000221	GP=-2.*25*(AM1BP*AM2+AM2BP*AM1+AM1B*AM2P+AM2B*AM1P)+4.*CXY*B*RY	817000000
000235	GO TO 25	818000000
000235	2 AM2=PID8*(B**4-B*B*CX)	819000000
000241	AM2B=PID8*(4.*B**3-2.*CX*B)	820000000
000246	AM2B3=PID8*(12.*B*B*16.*D12S-2.*CX)	821000000
000252	AM2P=-PID8*B*RX	822000000
000255	AM2BP=-.25*PI*RX*B	823000000

APPENDIX D

```

000260 AM3=PID8*(81.*DS2+18.*D12S*B*B+B**4-B*B*CX-9.*CY) 82400000
000273 AM3B=PID8*(36.*D12S*B+B+4.*B**3-2.*B*CX) 82500000
000303 AM3BB=PID8*(12.*B*B+36.*D12S-2.*CX) 82600000
000311 AM3P=PID8*(-B*B*RX-9.*RY) 82700000
000316 AM3BP=-.25*PI*RX*B 82800000
000321 F=(CX*B)**2-(.21972656)*(2.*AM0+AM2)*(AM1+AM3) 82900000
000333 G=2.*CX*CY*B-(.21972656)*(2.*AM0B+AM2B)*(AM1+AM3) 83000000
1+(2.*AM0+AM2)*(AM1B+AM3B) 83100000
000352 FB=G 83200000
000354 FP=2.*CX*RY*B*B-(.21972656)*((2.*AM0P+AM2P)*(AM1+AM3) 83300000
1+(2.*AM0+AM2)*(AM1P+AM3P)) 83400000
000374 GB=-(.21972656)*((2.*AM0BB+AM2BB)*(AM1+AM3)+2.*CX*CY 83500000
1+(2.*AM0+AM2)*(AM1BB+AM3BB)+2.*(2.*AM0B+AM2B)*(AM1B+AM3B)) 83600000
000420 GP=-(.21972656)*((2.*AM0BP+AM2BP)*(AM1+AM3)+(2.*AM0+AM2) 83700000
1*(AM1BP+AM3BP)+2.*AM0B+AM2B)*(AM1P+AM3P)+(2.*AM0P+AM2P)*(AM1B 83800000
2+AM3B))+4.*CX*B*RY 83900000
000455 25 IF(ABS(DP).LT.1.E-5 .AND. ABS(DB).LT.1.E-5)GO TO 10 84000000
000467 AJACOB1=FP*GB-FB*GP 84100000
000472 DP=(-F*GB+G*FB)/AJACOB1 84200000
000476 DB=(-F*G+F*GP)/AJACOB1 84300000
000502 P=P+DP 84400000
000503 B=B+DB 84500000
000505 LC=LC+1 84600000
000506 IF(LC.GT.50)RETURN 84700000
000512 GO TO 1 84800000
000513 10 PRINT 101,P,B,F,G 84900000
000527 WRITE(7,101) P,B,F,G 85000000
000546 101 FORMAT( 5X,*P=*,E16.8,2X,*B=*,E16.8,2X,*F=*,E16.8,*G=*,E16.8) 85100000
000546 IF(INCX.F0.1)RETURN 85200000
000554 IF(X.GT.0)GO TO 60 85200001
000557 X=1./E/ADB*ABS(X) 85300000
000562 Y=ABS(Y) 85400000
000563 PRINT 51,X,Y 85500001
000573 WRITE(7,51) X,Y 85500002
000606 60 COEF=PI*PI*DS1/(XB*XB) 85500003
000611 ANX=CX*COEF 85600000
000613 ANY=CY*COEF 85700000
000615 ANXY=CXY*COEF 85800000
000616 SIRNX=(ANX/EX-EXY*ANY/EY)/TT 85900000
000624 SIRNY=(ANY/EY-EXY*ANX/EX)/TT 86000000
000630 SIRNXY=ANXY/GXY/TT 86100000
000632 WRITE(7,52) CX,CY,CXY,SIRNX,SIRNY,SIRNXY 86400000
000652 PRINT 52,CX,CY,CXY,SIRNX,SIRNY,SIRNXY 86500000

```

APPENDIX D

000011	SUBROUTINE SET(S,N,LL,LU,IF,R)	87900000
000011	DIMENSION S(32,32)	88000000
000011	IF(N.EQ.2)GO TO 10	88100000
000013	DO 20 IR=1,LU	88200000
000014	20 S(IR,IF)=R	88300000
000022	RETURN	88400000
000023	10 DO 30 IC=1,LU	88500000
000025	30 S(IC,IC)=R	88600000
000033	RETURN	88700000
000034	END	88800000

REFERENCES

1. Gerard, George; and Becker, Herbert: Handbook of Structural Stability. Part I – Buckling of Flat Plates. NACA TN 3781, 1957.
2. Becker, Herbert: Handbook of Structural Stability. Part II – Buckling of Composite Elements. NACA TN 3782, 1957.
3. Johns, D. J.: Shear Buckling of Isotropic and Orthotropic Plates – A Review. R. & M. No. 3677, British A.R.C., 1971.
4. Lekhnitskii, S. G. (S. W. Tsai and T. Cheron, transl.): Anisotropic Plates. Gordon and Breach Sci. Publ., c.1968.
5. Ashton, J. E.; and Whitney, J. M.: Theory of Laminated Plates. Progress in Materials Science Series, Volume IV, Technomic Pub. Co., Inc., c.1970.
6. Timoshenko, Stephen P.; and Gere, James M.: Theory of Elastic Stability. Second ed. McGraw-Hill Book Co., Inc., c.1961.
7. Almroth, B. O.; Brogan, F. A.; Meller, E.; and Petersen, H. T.: User's Manual for STAGS. LMSC-D358197, Lockheed Missiles & Space Co., Jan. 1974.
8. McCormick, Caleb W., ed.: The NASTRAN User's Manual (Level 15). NASA SP-222(01), 1972.
9. Reed, D. L.: Laminated Sandwich Panel Analysis. FZM-5590, Convair Aerospace Div., General Dynamics, Oct. 1, 1971.
10. Fung, Y. C.: Foundations of Solid Mechanics. Prentice-Hall, Inc., c.1965.
11. Ashton, J. E.; Halpin, J. C.; and Petit, P. H.: Primer on Composite Materials: Analysis. Technomic Pub. Co., Inc., c.1969.
12. Libove, Charles; and Batdorf, S. B.: A General Small-Deflection Theory for Flat Sandwich Plates. NACA Rep. 899, 1948. (Supersedes NACA TN 1526.)
13. Housner, J. M.; and Stein, Manuel: Flutter Analysis of Swept-Wing Subsonic Aircraft With Parameter Studies of Composite Wings. NASA TN D-7539, 1974.
14. Stein, Manuel; and Yaeger, David J.: Critical Shear Stress of a Curved Rectangular Panel With a Central Stiffener. NACA TN 1972, 1949.
15. Stowell, Elbridge Z.; and Schwartz, Edward B.: Critical Stress for an Infinitely Long Flat Plate With Elastically Restrained Edges Under Combined Shear and Direct Stress. NACA WR L-340, 1943. (Formerly NACA ARR 3K13.)

16. Batdorf, S. B.; Schildcrout, Murry; and Stein, Manuel: Critical Combinations of Shear and Longitudinal Direct Stress for Long Plates With Transverse Curvature. NACA TN 1347, 1947.
17. Budiansky, Bernard; and Hu, Pai C.: The Lagrangian Multiplier Method of Finding Upper and Lower Limits to Critical Stresses of Clamped Plates. NACA Rep. 848, 1946. (Supersedes NACA TN 1103.)

TABLE 1. - SHEAR-BUCKLING LOAD COEFFICIENTS FOR RECTANGULAR ORTHOTROPIC PANELS
 WITH ALL EDGES SIMPLY SUPPORTED AND THE TRIGONOMETRIC DIFFERENCE
 PARAMETERS ON WHICH THEY ARE BASED

Stiffness parameter, $\Theta = \frac{\sqrt{D_{11}D_{22}}}{D_3}$	Aspect-ratio parameter, $B = \frac{b^4\sqrt{D_{11}}}{a\sqrt{D_{22}}}$	No. of mesh points in x- and y-directions		Wavelength ratios used in trigonometric differences		Shear-buckling load coefficient, $k_S = \frac{b^2 N_{xy}}{\pi^2 \sqrt{D_{11}D_{22}^3}}$
		a/ Δ_x	b/ Δ_y	λ_x/a	λ_y/b	
0.2 ↓	1.0	9	9	0.56	0.56	26.28
	.8	9	9	.56	.60	21.43
	.6	9	9	.56	.80	17.33
	.5	9	9	.50	.90	15.36
	.4	11	11	.50	1.00	13.77
	.2	13	13	.35	1.00	11.55
	a_0	---	---	---	---	10.87
.4 ↓	1.0	9	9	.56	.56	15.78
	.8	9	9	.56	.60	12.98
	.6	9	9	.56	.80	10.86
	.5	9	9	.50	.90	9.93
	.4	11	11	.50	1.00	9.29
	.2	15	8	.30	1.00	8.21
	a_0	---	---	---	---	7.72
.6 ↓	1.0	9	9	.56	.56	12.21
	.8	9	9	.56	.60	10.11
	.6	9	9	.56	.80	8.67
	.5	9	9	.50	.90	8.09
	.4	11	11	.50	1.00	7.73
	.2	15	8	.25	1.00	6.71
	a_0	---	---	---	---	6.53
.8 ↓	1.0	9	9	.56	.56	10.40
	.8	9	9	.56	.60	8.66
	.6	9	9	.56	.80	7.57
	.5	9	9	.50	.90	7.10
	.4	11	11	.50	1.00	6.80
	.2	15	8	.25	1.00	6.02
	a_0	---	---	---	---	5.79
1 ↓	1.0	9	9	.56	.56	9.31
	.8	9	9	.56	.60	7.68
	.6	9	9	.56	.80	6.91
	.4	11	11	.50	1.00	6.22
	.2	15	8	.23	1.00	5.49
	a_0	---	---	---	---	5.33

^aFor $B = 0$, k_S was calculated by using equations (B2).

TABLE 1.- SHEAR-BUCKLING LOAD COEFFICIENTS FOR RECTANGULAR ORTHOTROPIC PANELS
WITH ALL EDGES SIMPLY SUPPORTED AND THE TRIGONOMETRIC DIFFERENCE
PARAMETERS ON WHICH THEY ARE BASED - Concluded

Stiffness parameter, $\Theta = \frac{\sqrt{D_{11}D_{22}}}{D_3}$	Aspect-ratio parameter, $B = \frac{b\sqrt{D_{11}}}{a\sqrt{D_{22}}}$	No. of mesh points in x- and y-directions		Wavelength ratios used in trigonometric differences		Shear-buckling load coefficient, $k_S = \frac{b^2 N_{xy}}{\pi^2 \sqrt{D_{11}D_{22}^3}}$	
		a/ Δ_x	b/ Δ_y	λ_x/a	λ_y/b		
1.25 ↓	1.0	9	9	0.56	0.56	8.43	
	.8	9	9	.56	.60	7.08	
	.6	9	9	.56	.80	6.38	
	.4	11	11	.50	1.00	5.75	
	.2	15	8	.22	1.00	5.09	
	.1	25	9	.13	1.00	5.05	
	a_0	---	---	---	---	4.96	
	1.667 ↓	1.0	9	9	.56	.56	7.54
		.8	9	9	.56	.60	6.37
		.6	9	9	.56	.80	5.85
.4		11	11	.50	1.00	5.26	
.2		15	8	.22	1.00	4.72	
.1		22	8	.13	1.00	4.68	
a_0		---	---	---	---	4.60	
2.5 ↓		1.0	9	9	.56	.56	6.65
		.8	9	9	.56	.60	5.66
		.6	9	9	.56	.80	5.32
	.4	11	11	.50	1.00	4.77	
	.2	15	8	.22	1.00	4.32	
	.1	22	8	.13	1.00	4.33	
	a_0	---	---	---	---	4.17	
	5 ↓	1.0	9	9	.56	.56	5.74
		.8	9	9	.56	.60	4.94
		.6	9	9	.56	.80	4.78
.4		11	11	.50	1.00	4.27	
.2		15	8	.22	1.00	3.90	
.1		22	8	.13	1.00	3.86	
a_0		---	---	---	---	3.75	
∞ ↓		1.0	9	9	.56	.56	4.83
		.8	9	9	.56	.60	4.22
		.6	9	9	.56	.80	4.25
	.4	11	11	.50	1.00	3.76	
	.2	15	8	.22	1.00	3.47	
	a_0	---	---	---	---	3.30	

^a For $B = 0$, k_S was calculated by using equations (B2).

TABLE 2. - SHEAR-BUCKLING LOAD COEFFICIENTS FOR RECTANGULAR ORTHOTROPIC PANELS
 WITH ALL EDGES CLAMPED AND THE TRIGONOMETRIC DIFFERENCE
 PARAMETERS ON WHICH THEY ARE BASED

Stiffness parameter, $\Theta = \frac{\sqrt{D_{11}D_{22}}}{D_3}$	Aspect-ratio parameter, $B = \frac{b}{a}\sqrt{\frac{D_{11}}{D_{22}}}$	No. of mesh points in x- and y-directions		Wavelength ratios used in trigonometric differences		Shear-buckling load coefficient, $k_s = \frac{b^2 N_{xy}}{\pi^2 \sqrt{D_{11}D_{22}^3}}$
		a/ Δ_x	b/ Δ_y	λ_x/a	λ_y/b	
0.2 ↓	1.0	9	9	1.00	1.0	32.56
	.8	9	9	.80	1.0	26.31
	.6	9	9	.60	1.0	22.21
	.4	11	11	.40	1.0	18.91
	.2	17	9	.31	1.0	17.34
	.1	25	9	.15	1.0	17.31
	a_0	---	---	---	---	---
.4 ↓	1.0	9	9	1.10	1.1	21.63
	.8	9	9	.90	1.0	17.92
	.6	9	9	.60	1.0	15.43
	.4	11	11	.40	1.0	13.62
	.2	17	9	.25	1.0	12.64
	.1	25	9	.13	1.0	12.89
	a_0	---	---	---	---	---
.6 ↓	1.0	9	9	1.10	1.1	17.86
	.8	9	9	.90	1.0	14.89
	.6	9	9	.60	1.0	13.06
	.4	11	11	.40	1.0	11.60
	.2	15	8	.22	1.0	10.64
	.1	25	9	.13	1.0	10.95
	a_0	---	---	---	---	---
.8 ↓	1.0	9	9	1.10	1.1	15.94
	.8	9	9	.90	1.0	13.34
	.6	9	9	.60	1.0	11.84
	.4	11	11	.40	1.0	10.55
	.2	17	9	.24	1.0	9.99
	.1	25	9	.13	1.0	10.16
	a_0	---	---	---	---	---
1 ↓	1.0	9	9	1.20	1.2	14.81
	.8	9	9	1.00	1.0	12.44
	.6	9	9	.60	1.0	11.08
	.4	11	11	.40	1.0	9.89
	.2	17	9	.22	1.0	9.27
	.1	25	9	.12	1.0	9.11
	a_0	---	---	---	---	---

^a For $B = 0$, k_s was calculated by using equations (B3).

TABLE 2. - SHEAR-BUCKLING LOAD COEFFICIENTS FOR RECTANGULAR ORTHOTROPIC PANELS
 WITH ALL EDGES CLAMPED AND THE TRIGONOMETRIC DIFFERENCE
 PARAMETERS ON WHICH THEY ARE BASED - Concluded

Stiffness parameter, $\Theta = \frac{\sqrt{D_{11}D_{22}}}{D_3}$	Aspect-ratio parameter, $B = \frac{b^4\sqrt{D_{11}}}{a\sqrt{D_{22}}}$	No. of mesh points in x- and y-directions		Wavelength ratios used in trigonometric differences		Shear-buckling load coefficient, $k_s = \frac{b^2 N_{xy}}{\pi^2 \sqrt{D_{11}D_{22}^3}}$
		a/ Δ_x	b/ Δ_y	λ_x/a	λ_y/b	
1.25 ↓	1.0	9	9	1.20	1.2	13.87
	.8	9	9	1.00	1.0	11.68
	.6	9	9	.60	1.0	10.46
	.4	9	9	.40	1.0	9.39
	.2	15	8	.22	1.0	8.80
	.1	22	8	.12	1.0	8.98
	a_0	---	---	---	---	8.45
1.667 ↓	1.0	9	9	1.20	1.2	12.91
	.8	9	9	1.00	1.0	10.90
	.6	9	9	.60	1.0	9.80
	.4	9	9	.40	1.0	8.86
	.2	15	8	.22	1.0	8.34
	.1	22	8	.12	1.0	8.58
	a_0	---	---	---	---	7.93
2.5 ↓	1.0	9	9	1.20	1.2	11.93
	.8	9	9	1.00	1.0	10.11
	.6	9	9	.60	1.0	9.07
	.4	9	9	.40	1.0	8.31
	.2	15	8	.22	1.0	7.84
	.1	25	9	.12	1.0	8.12
	a_0	---	---	---	---	7.32
5 ↓	1.0	9	9	1.20	1.2	10.94
	.8	9	9	1.00	1.0	9.31
	.6	9	9	.60	1.0	8.33
	.4	9	9	.40	1.0	7.74
	.2	15	8	.22	1.0	7.33
	.1	25	9	.12	1.0	7.66
	a_0	---	---	---	---	6.72
∞ ↓	1.0	9	9	1.20	1.2	9.92
	.8	9	9	1.00	1.0	8.48
	.6	9	9	.60	1.0	7.57
	.4	11	11	.40	1.0	6.97
	.2	15	8	.22	1.0	6.79
	.1	25	9	.12	1.0	7.17
	a_0	---	---	---	---	6.11

^a For $B = 0$, k_s was calculated by using equations (B3).

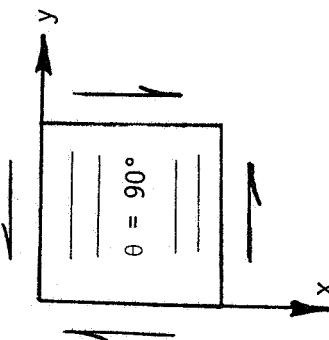
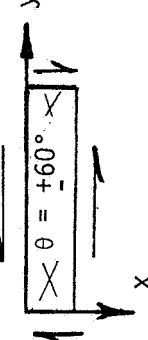
TABLE 3.- MATERIAL PROPERTIES OF GRAPHITE-EPOXY SKINS
 WITH THEIR EQUIVALENT ORTHOTROPIC PARAMETERS
 AT VARIOUS FILAMENT ORIENTATIONS

$$\left[E_1 = 145 \text{ GN/m}^2 (21 \times 10^6 \text{ psi}); E_2/E_1 = 0.1138; \right.$$

$$\left. G_{12}/E_1 = 0.03095; \nu_{12} = 0.31 \right]$$

Filament orientation, $\pm\theta$, deg	$\Theta = \frac{\sqrt{D_{11}D_{22}}}{D_3}$	$\frac{a}{b} B = \sqrt{\frac{4D_{11}}{D_{22}}}$
0	3.50	1.722
30	.511	1.389
45	.415	1.000
60	.511	.720
90	3.50	.581

TABLE 4. - COMPARISON OF CONVENTIONAL AND TRIGONOMETRIC FINITE DIFFERENCES
FOR ORTHOTROPIC PANELS

Problem description	Degrees of freedom		\bar{N}_{xy}		λ_x/a	λ_y/λ_x
	M_e	N_e	Conventional	Trigonometric		
Shear buckling of a clamped, square, graphite-epoxy panel 	4	4	56.03	----	---	---
	6	6	48.43	42.84	0.55	1
	8	8	45.65	----	---	---
	12	12	43.79	----	---	---
	20	20	42.90	----	---	---
Shear buckling of a simply supported 5 x 1 graphite-epoxy panel 	20	10	20.40	19.17	0.21	1
	29	13	19.70	----	---	---
	40	15	19.39	----	---	---
	50	20	19.22	----	---	---

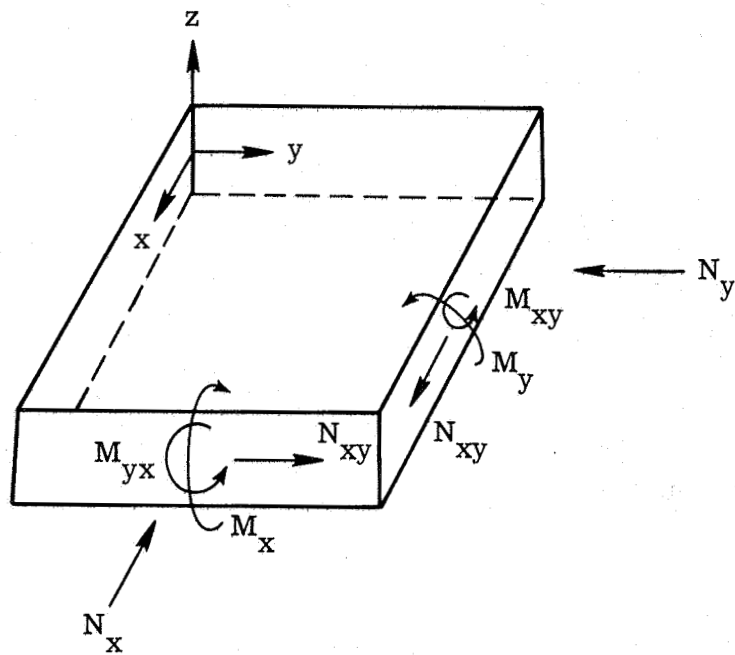
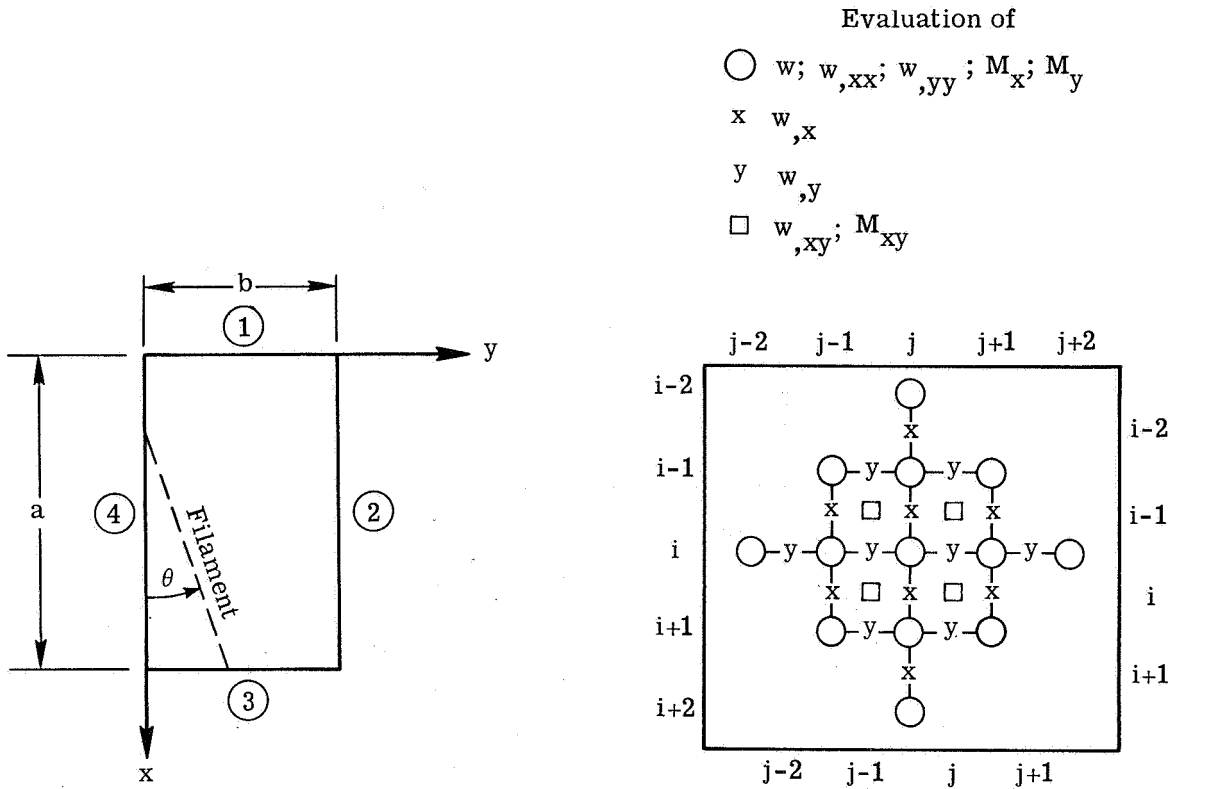
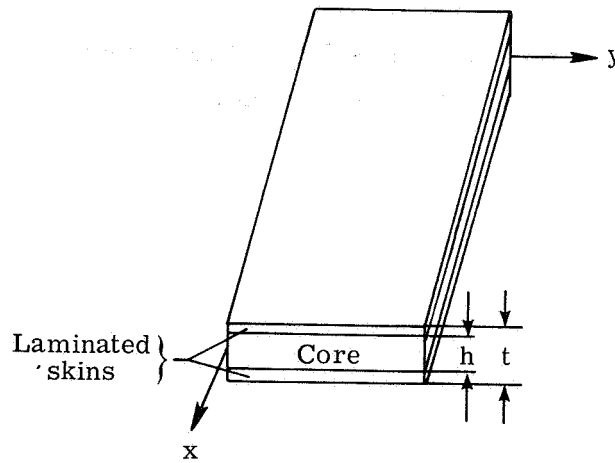


Figure 1. - Stress resultants acting upon an element of the plate.



(a) Panel geometry and boundary designation.

(b) Finite-difference station layout and designation.



(c) Sandwich panel.

Figure 2. - Geometrical and numerical configurations.

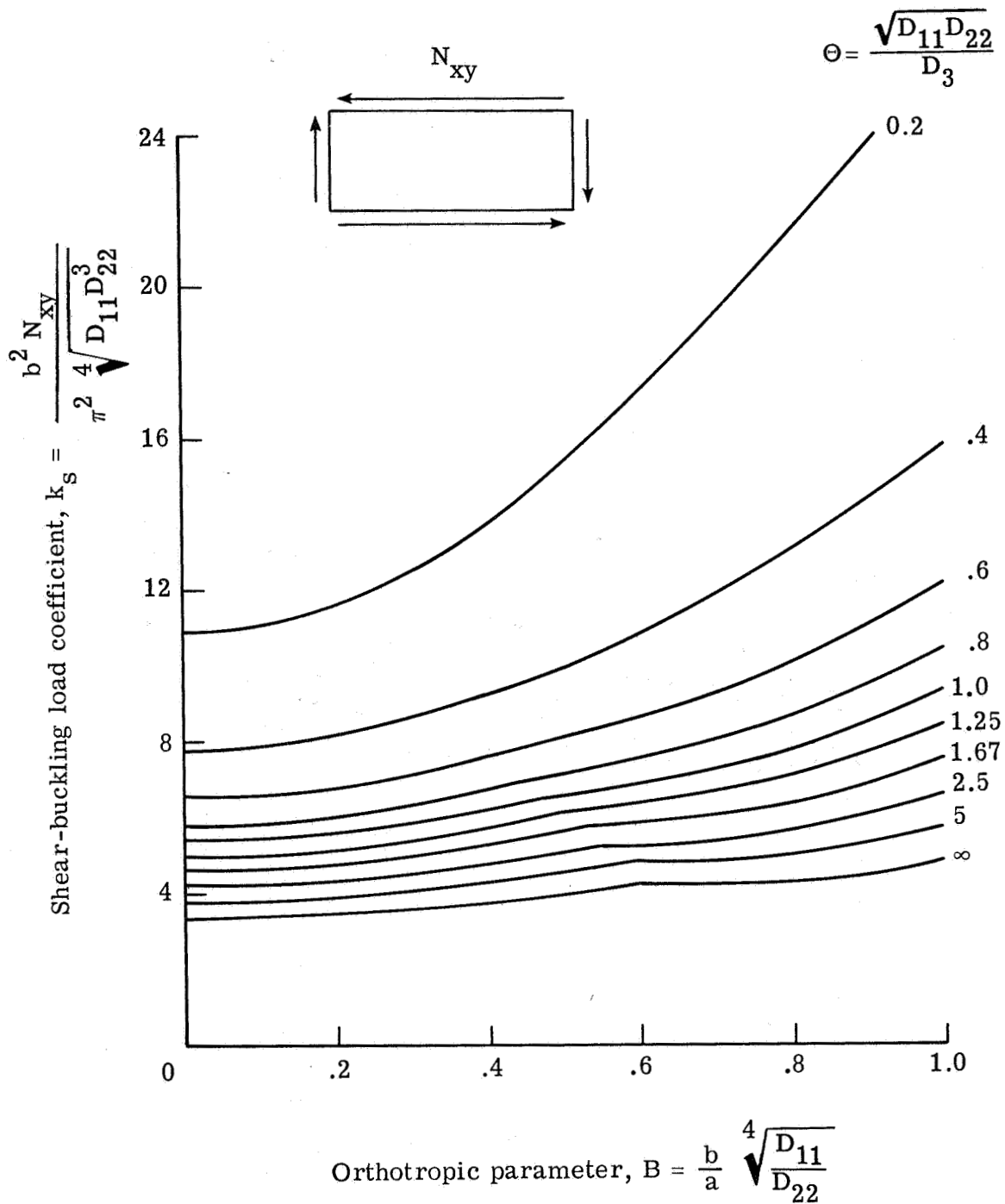


Figure 3.- Shear-buckling load coefficients for rectangular orthotropic plates with all edges simply supported.

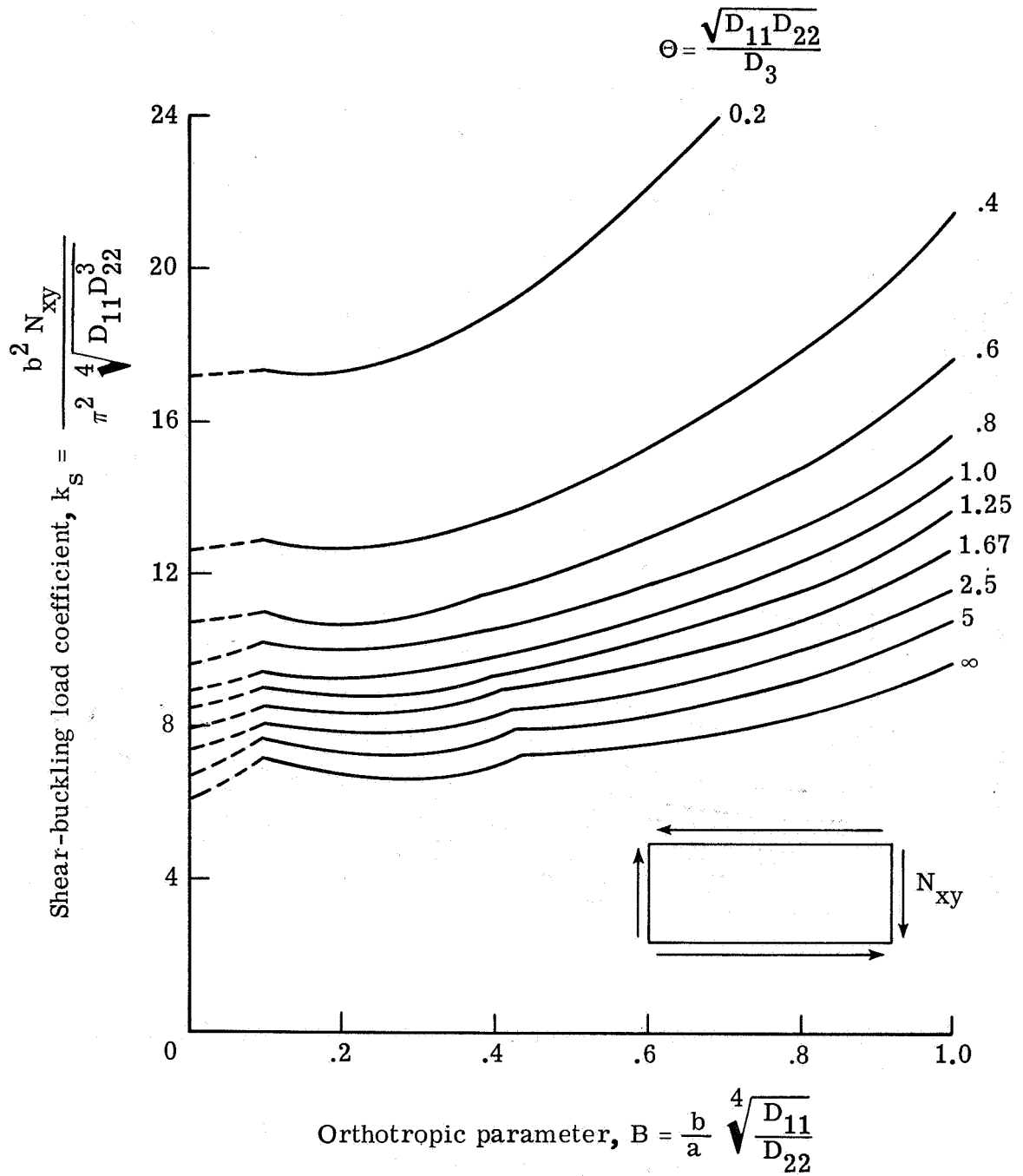


Figure 4.- Shear-buckling load coefficients for rectangular orthotropic plates with all edges clamped.

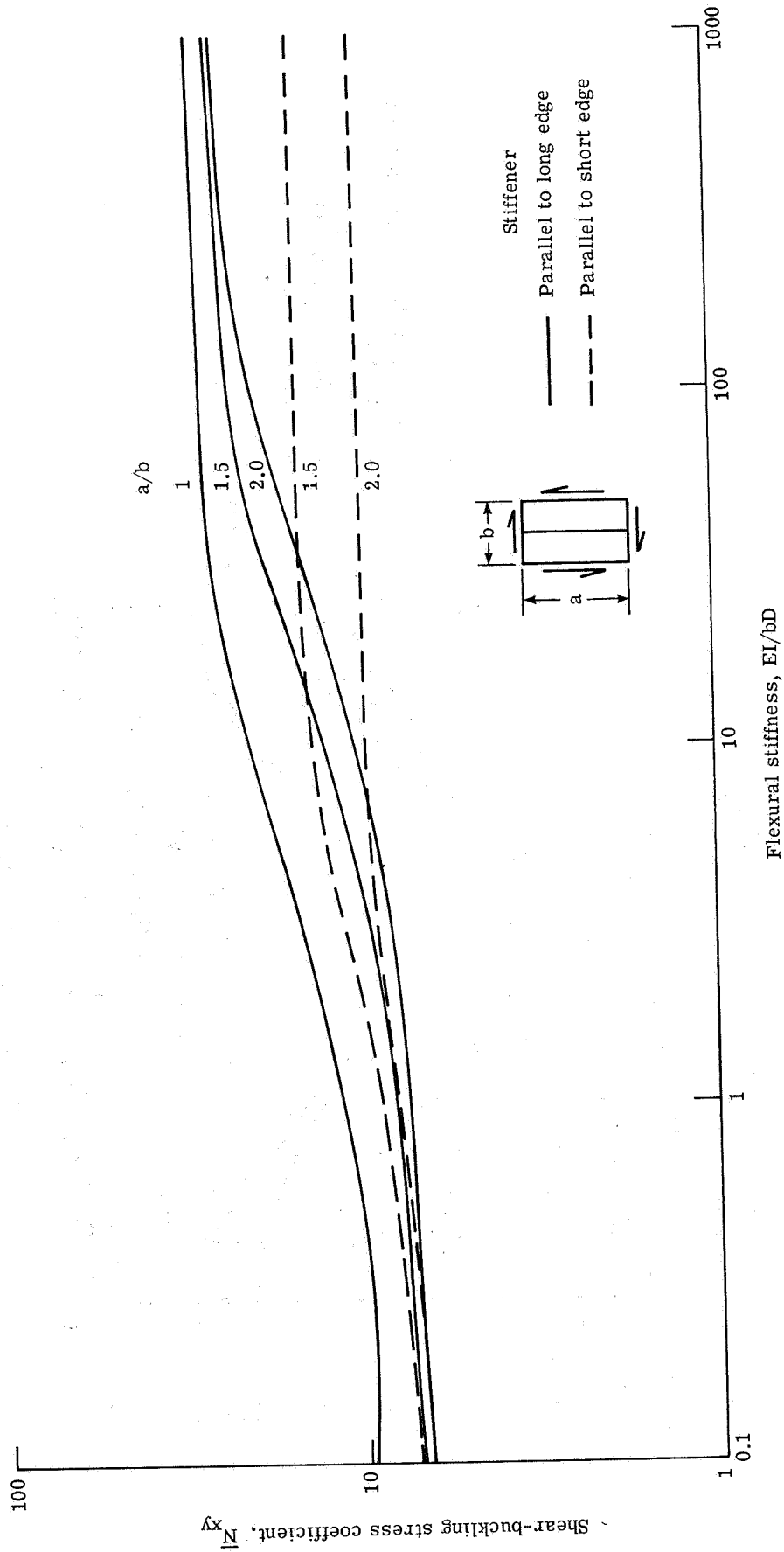
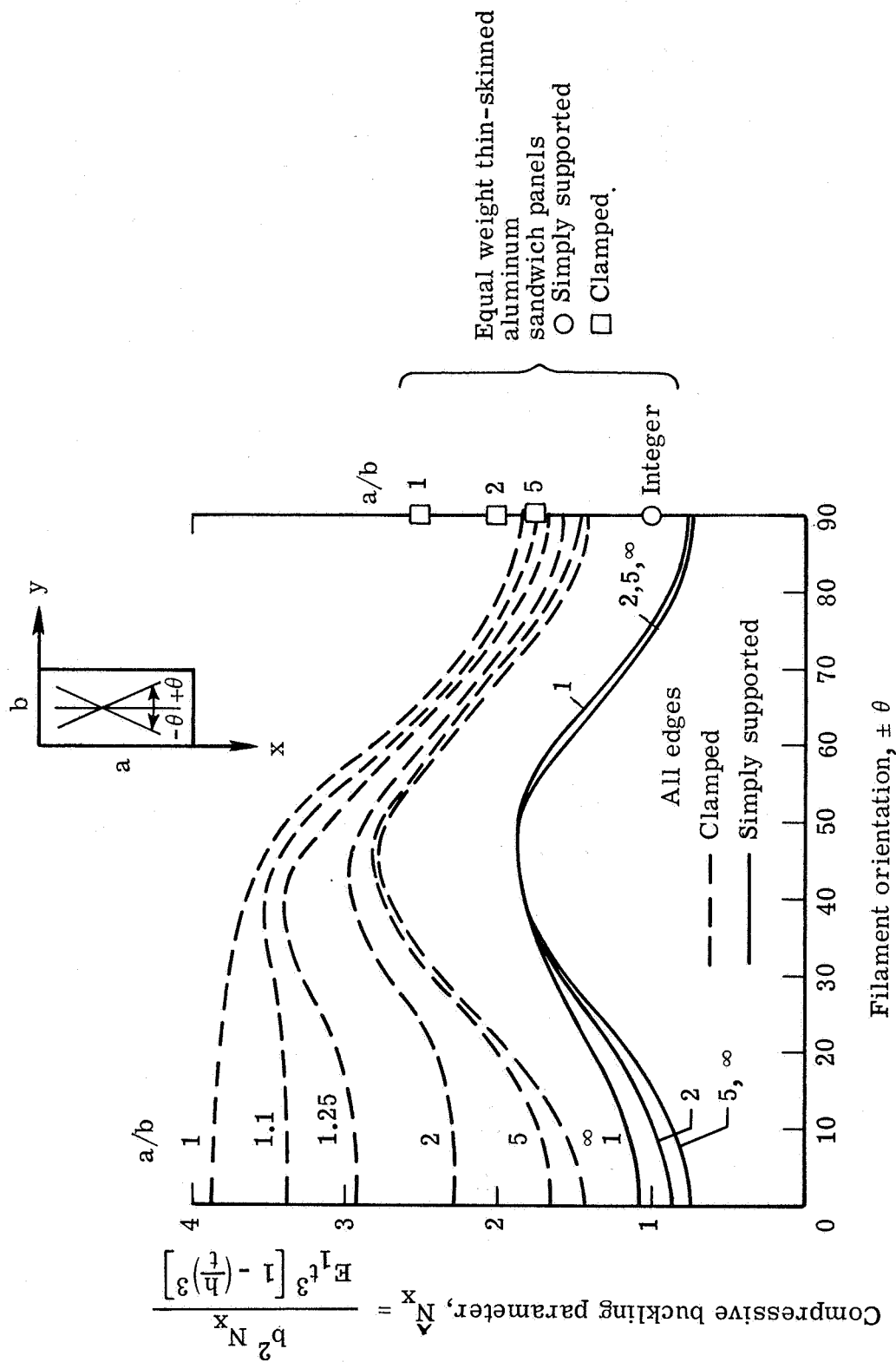


Figure 5. - Shear buckling of simply supported isotropic panels each with a central stiffener.



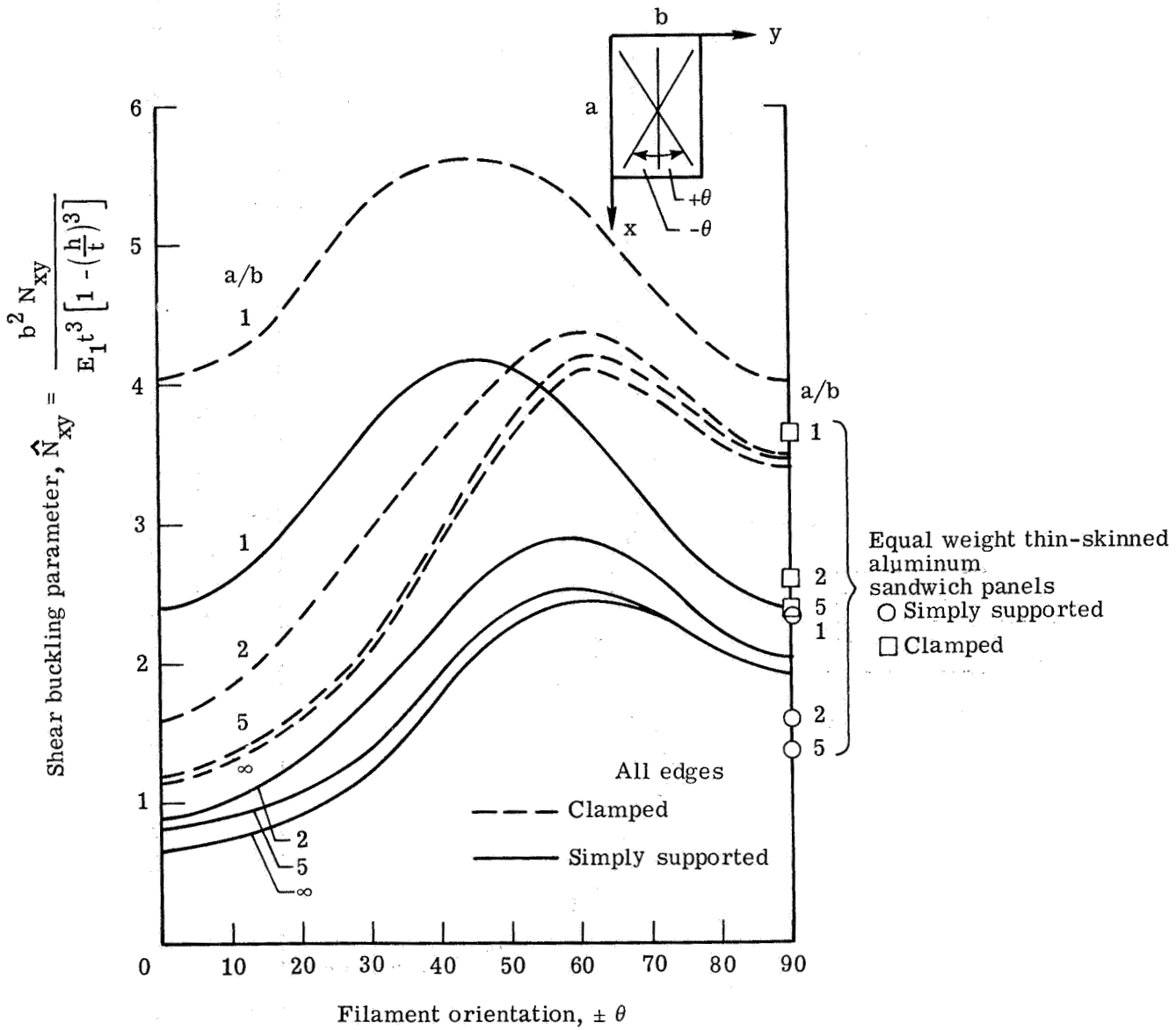


Figure 7.- Variation of shear buckling load with filament orientation for panels of various aspect ratios.

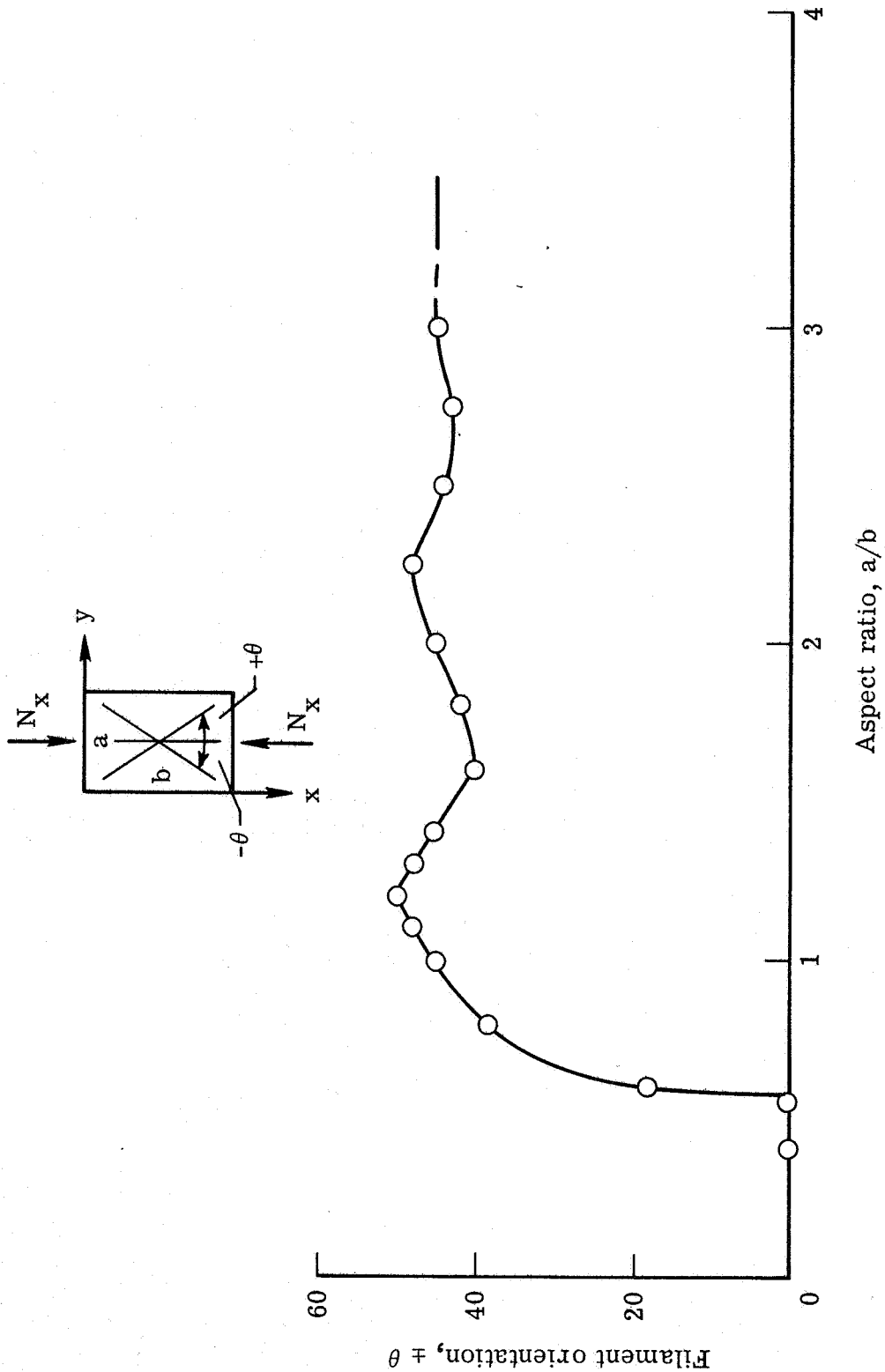


Figure 8. - Optimum filament orientation for the compressive buckling of a simply supported panel.

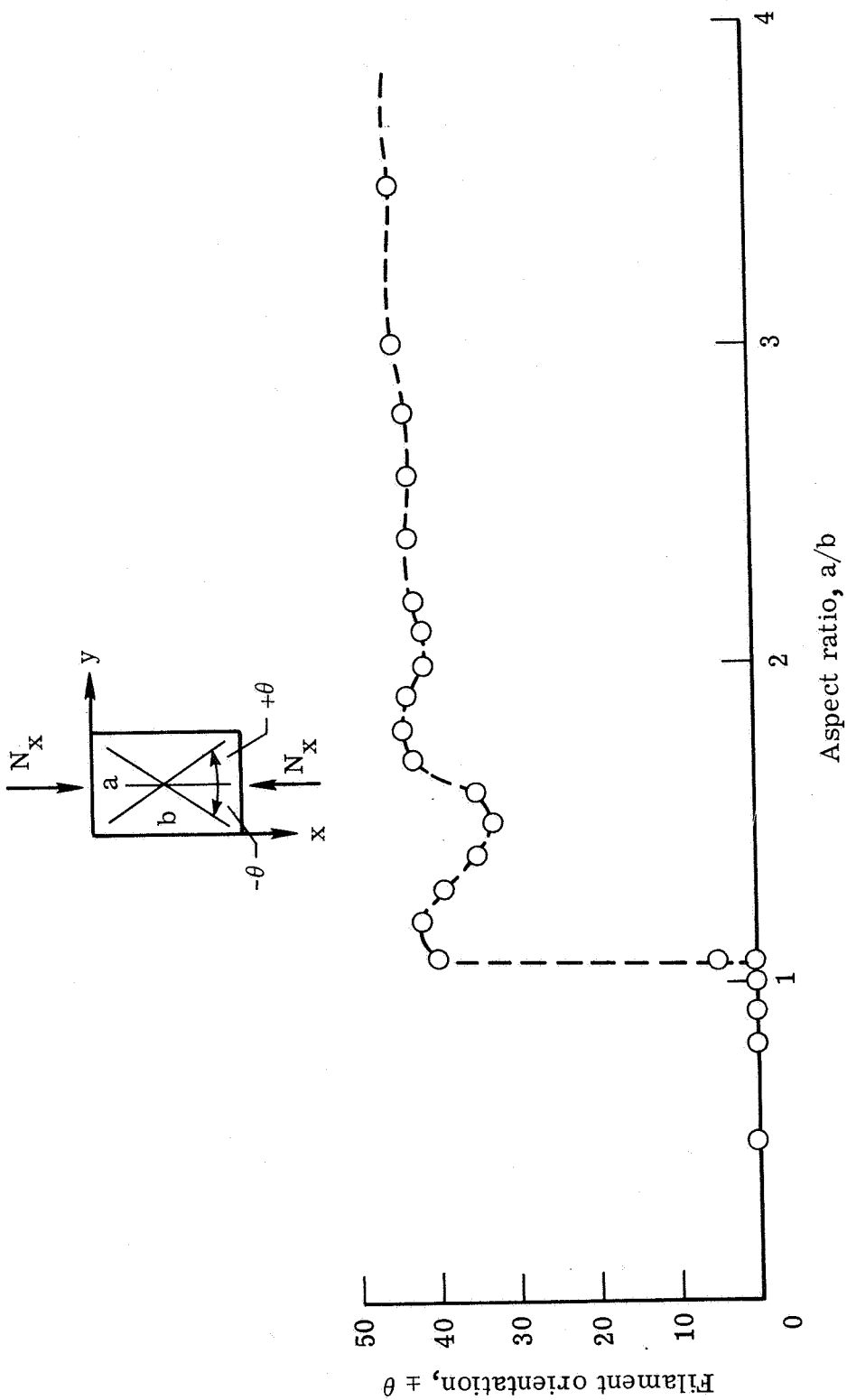


Figure 9. - Optimum filament orientation for the compressive buckling of a clamped panel.

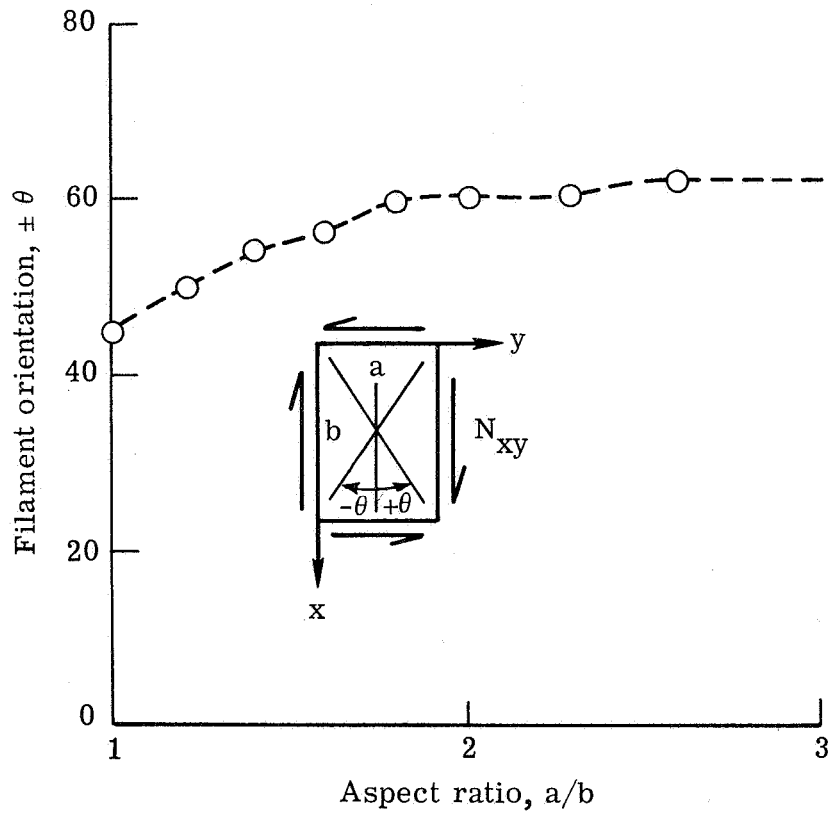


Figure 10.- Optimum filament orientation for the shear buckling of a simply supported panel.

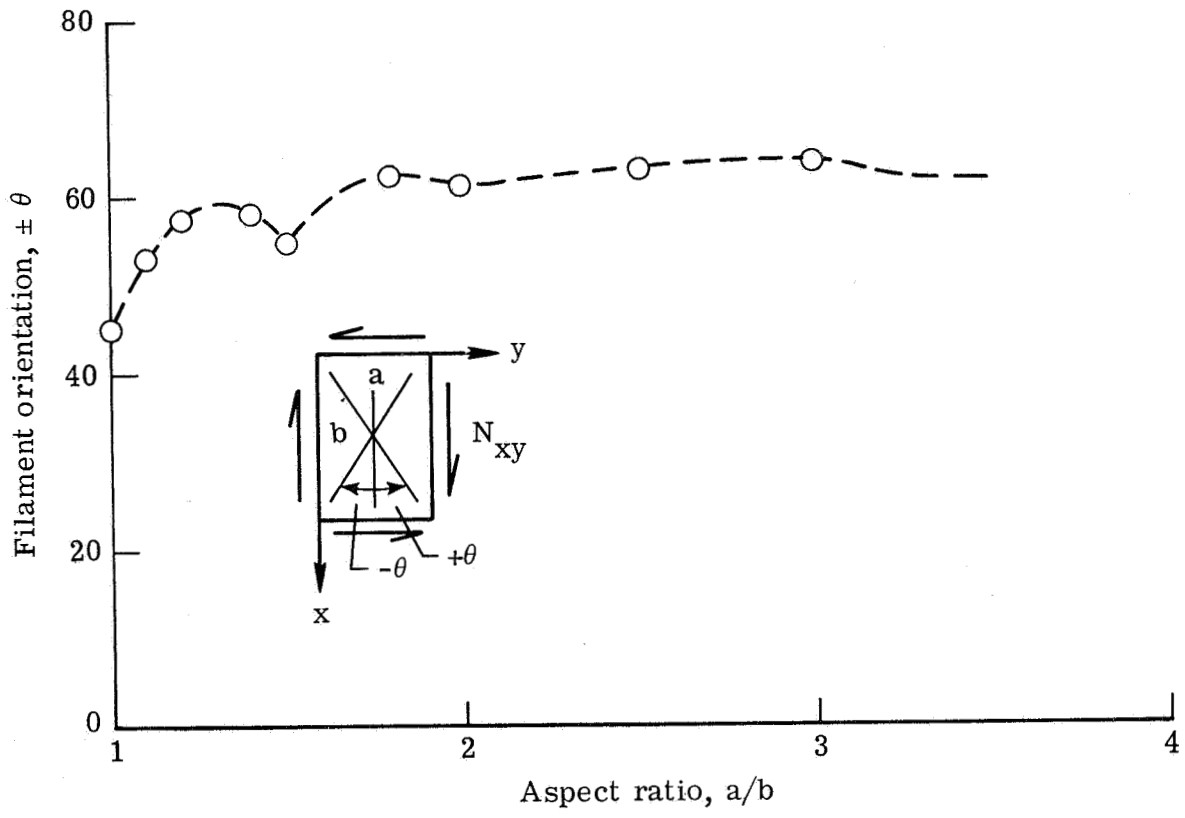


Figure 11.- Optimum filament orientation for the shear buckling of a clamped panel.

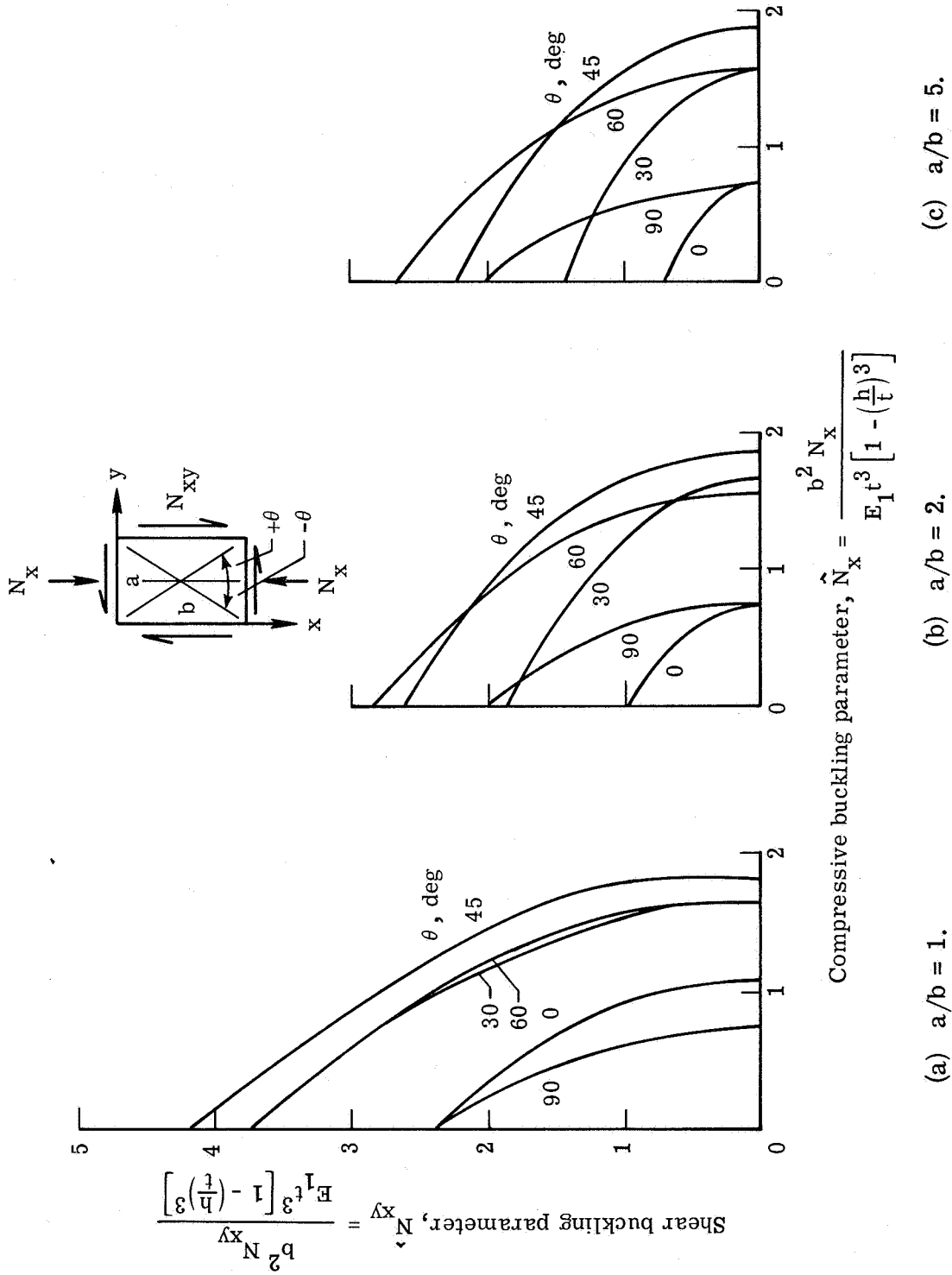
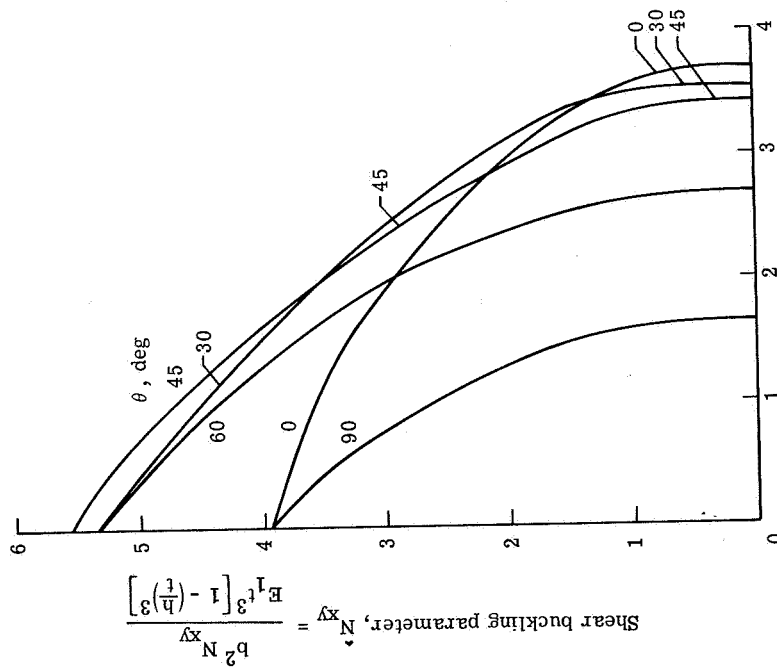
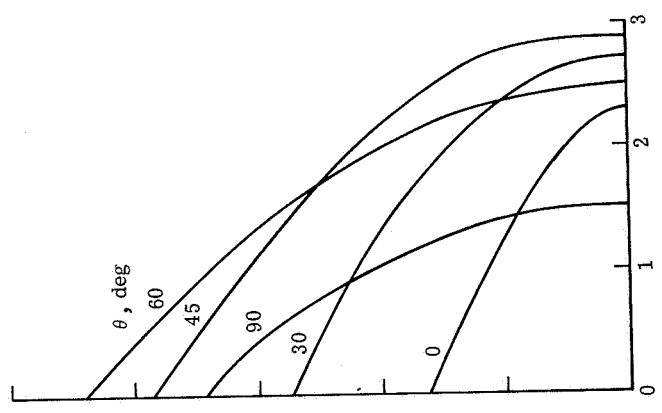


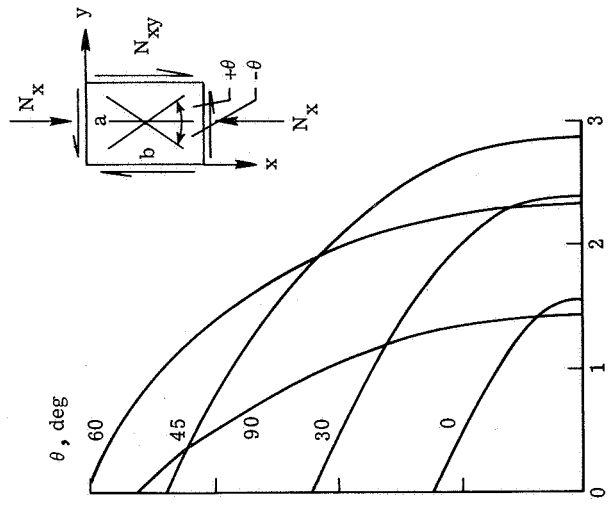
Figure 12.- Combined axial compression and shear of simply supported panels.



(a) $a/b = 1$.



(b) $a/b = 2$.



(c) $a/b = 5$.

Figure 13. - Combined axial compression and shear of clamped panels.

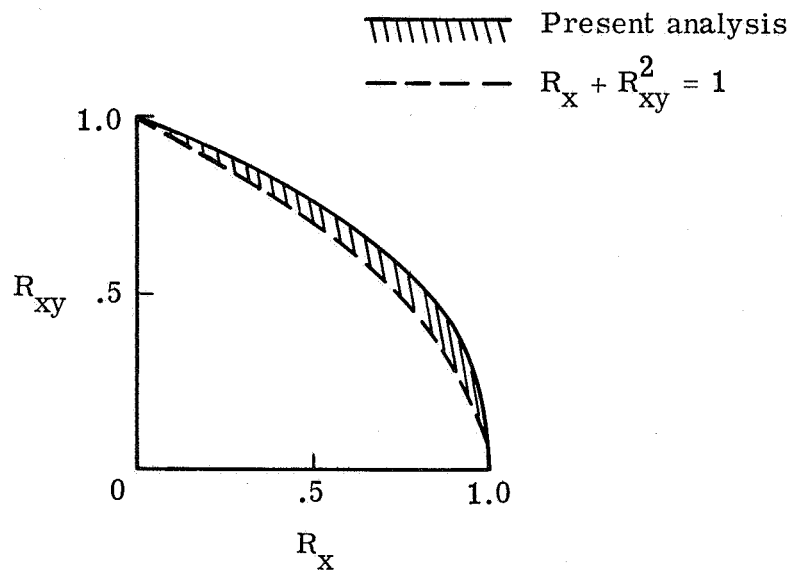


Figure 14.- Summary of combined axial compression and shear-buckling results for simply supported and clamped panels.

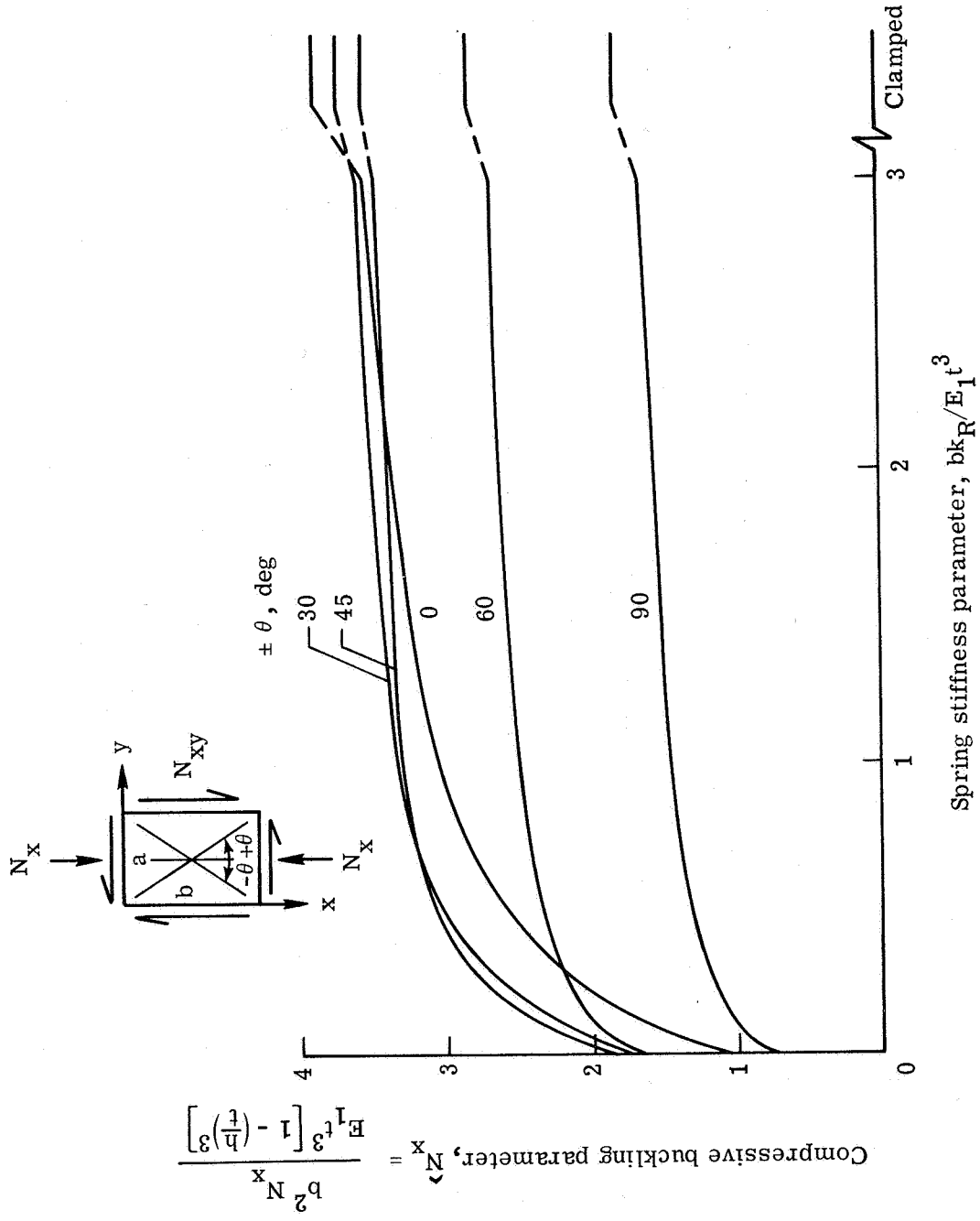
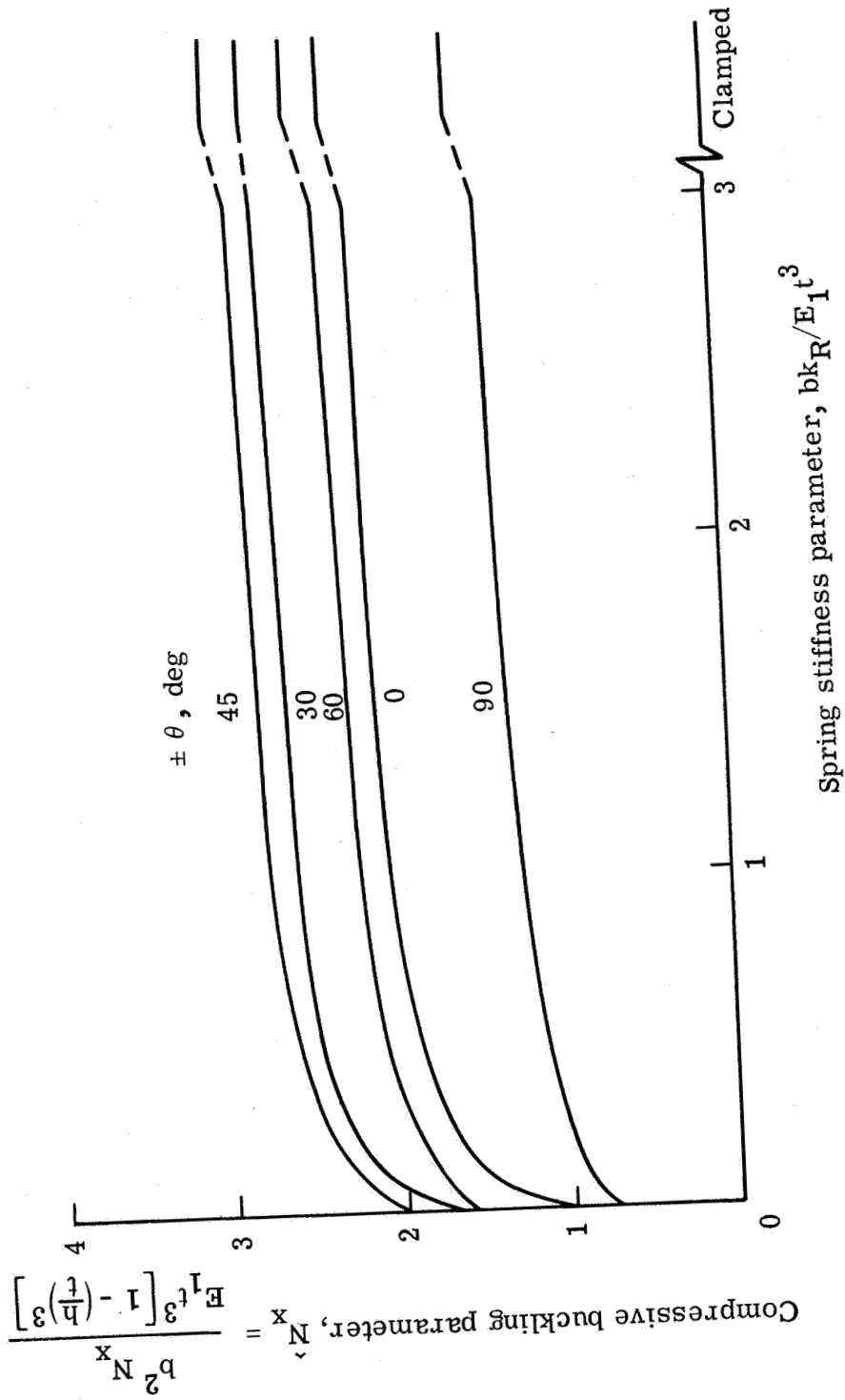
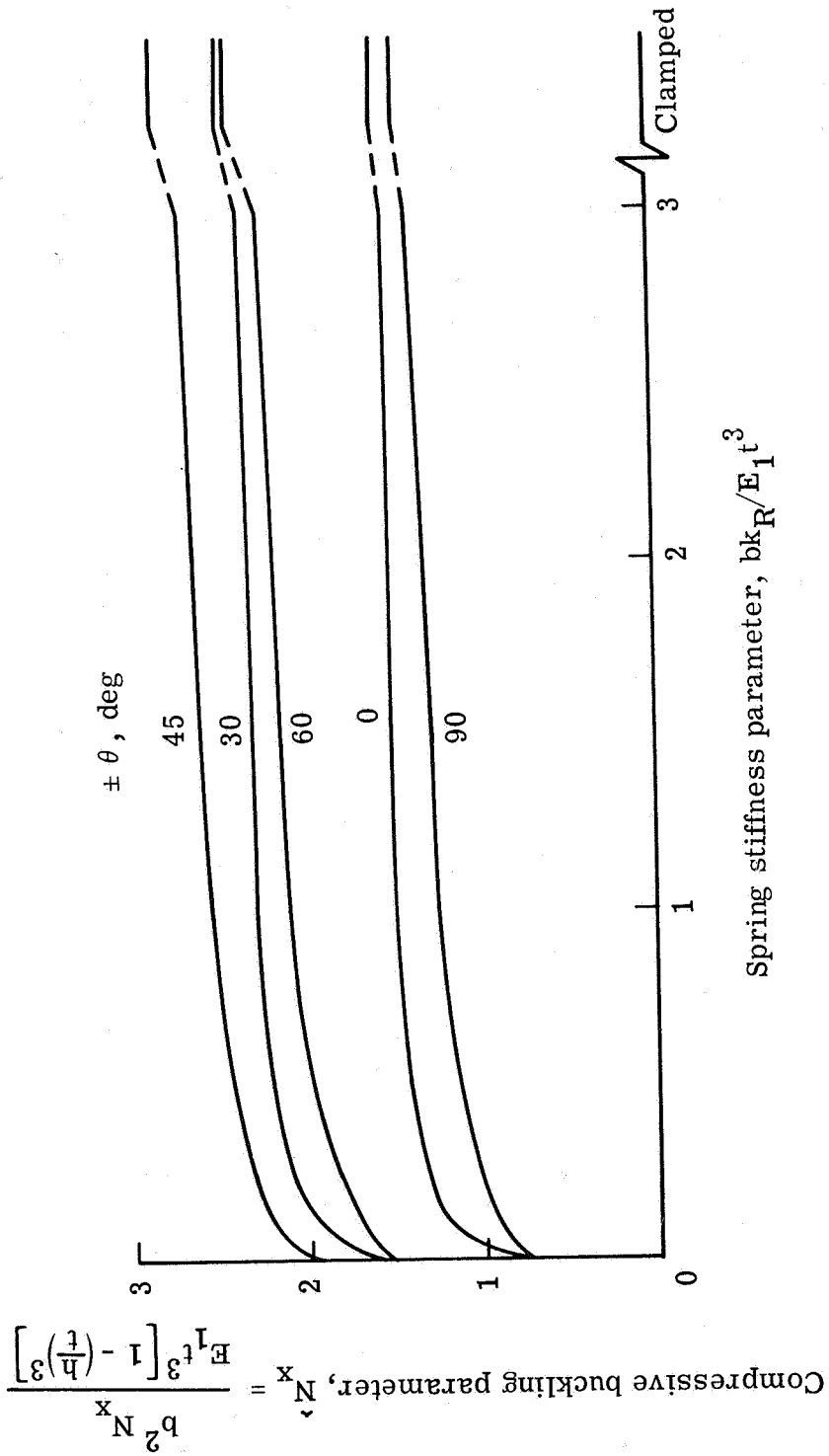


Figure 15.- Variation of compressive buckling parameter with rotational edge spring stiffness.



(b) $a/b = 2$.

Figure 15.- Continued.



(c) $a/b = 5$.

Figure 15.- Concluded.

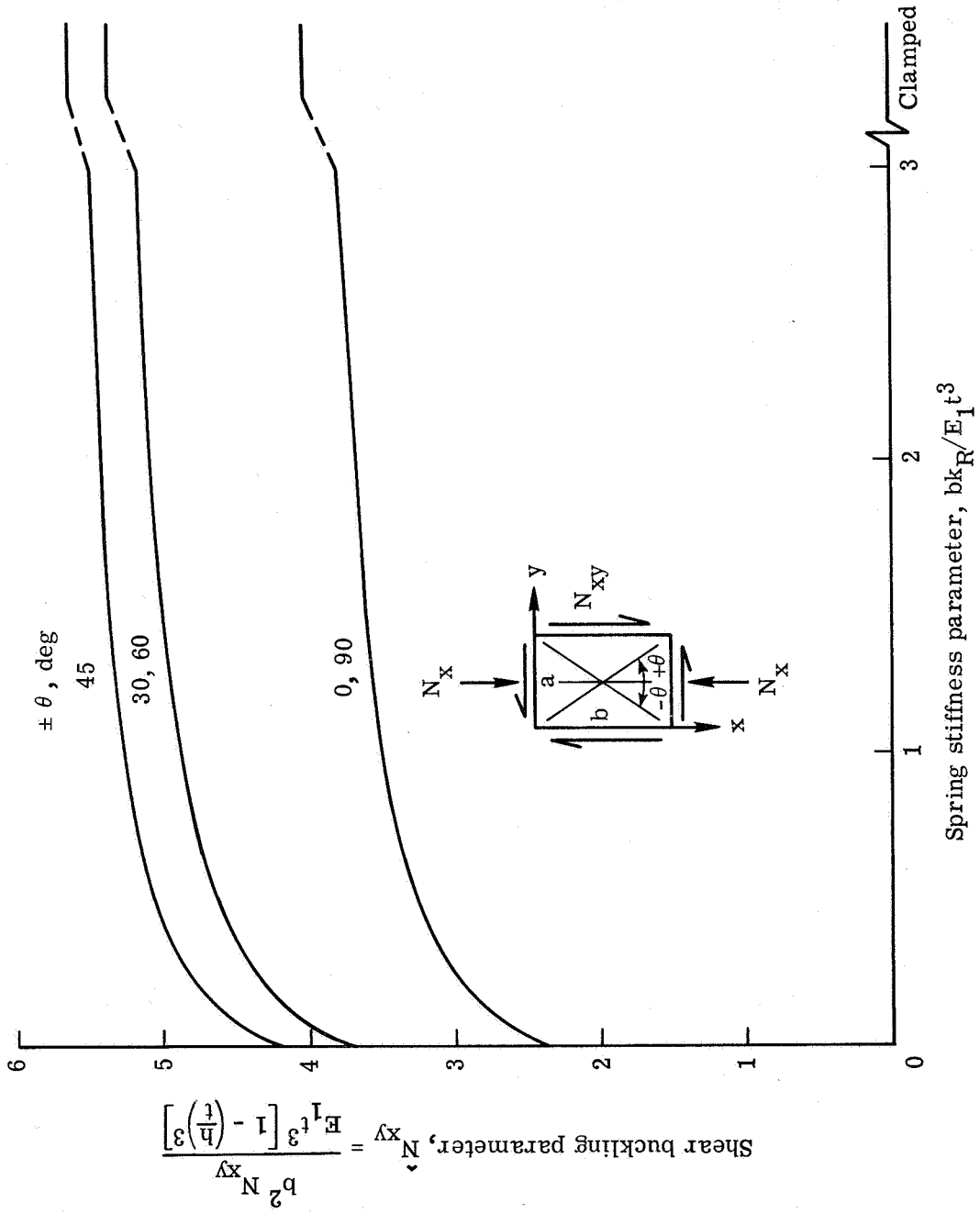
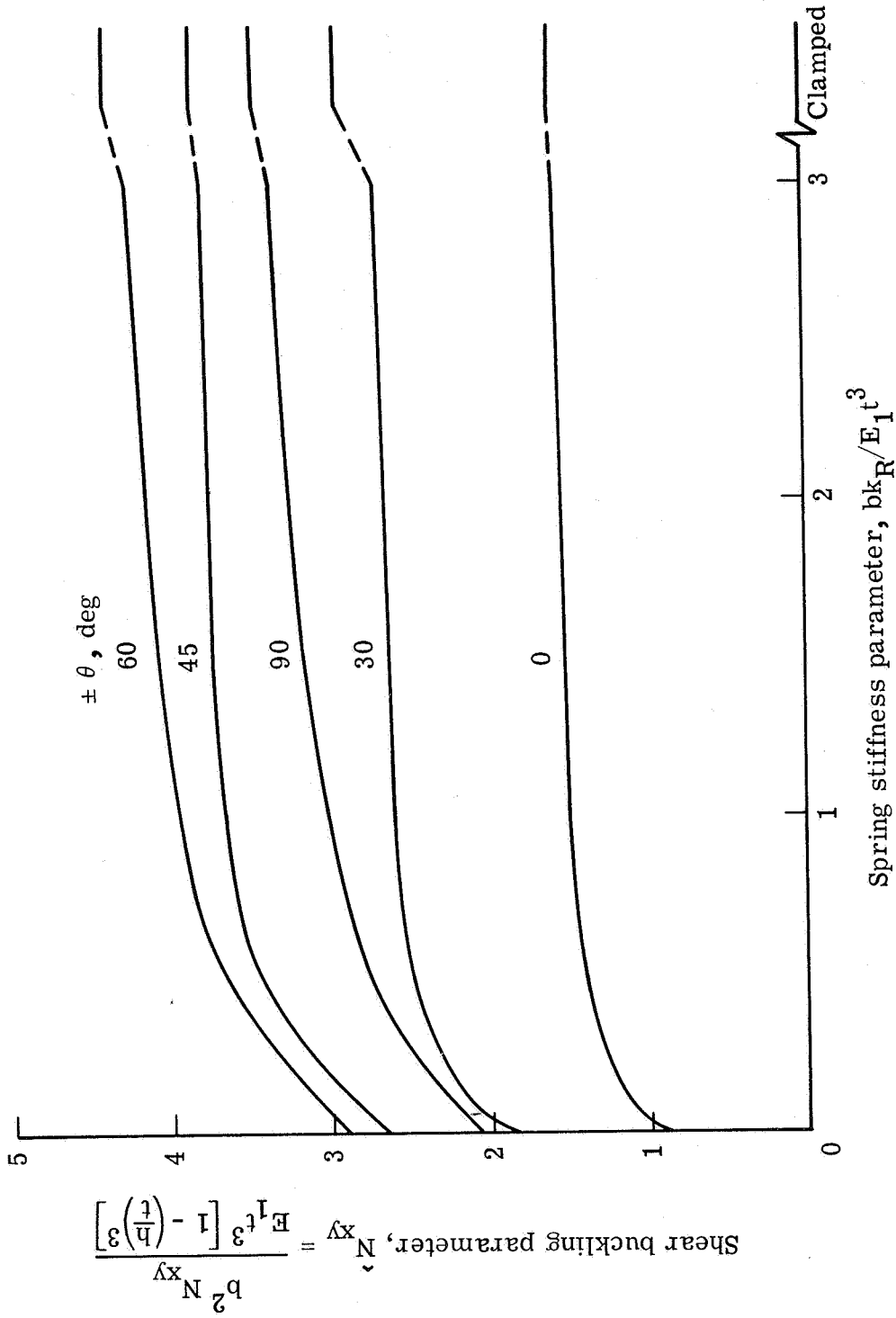
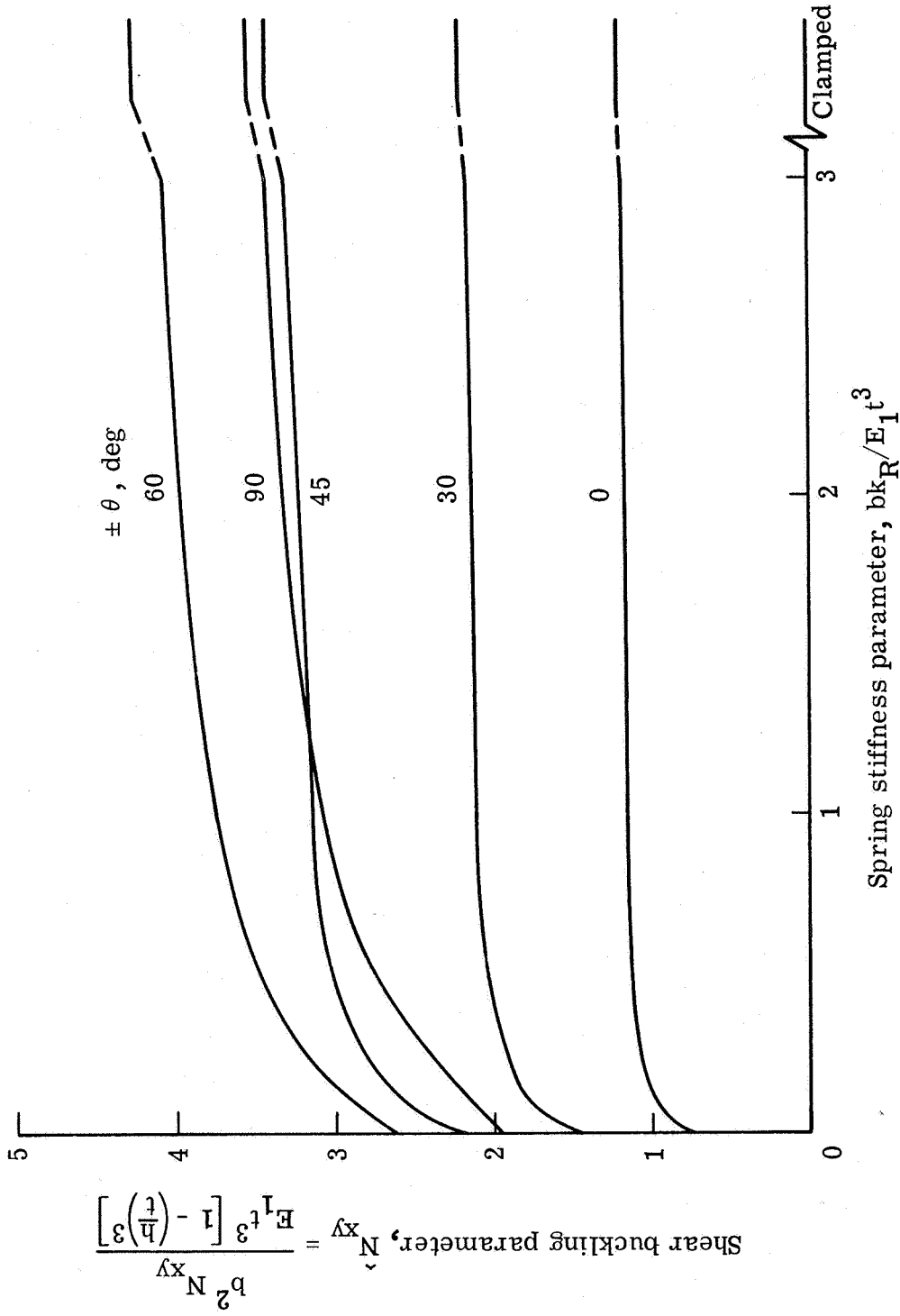


Figure 16.- Variation of shear buckling parameter with rotational edge spring stiffness.



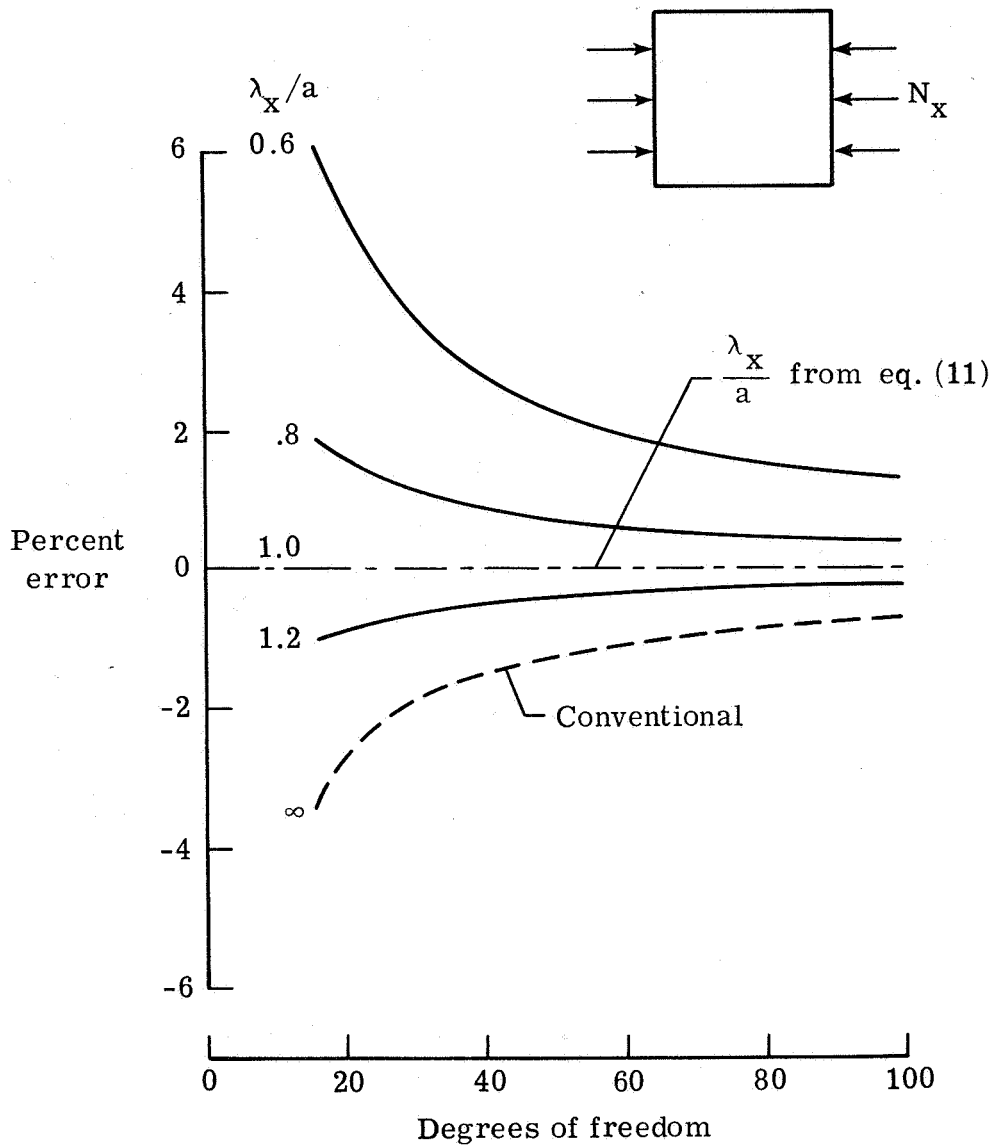
(b) $a/b = 2$.

Figure 16.- Continued.



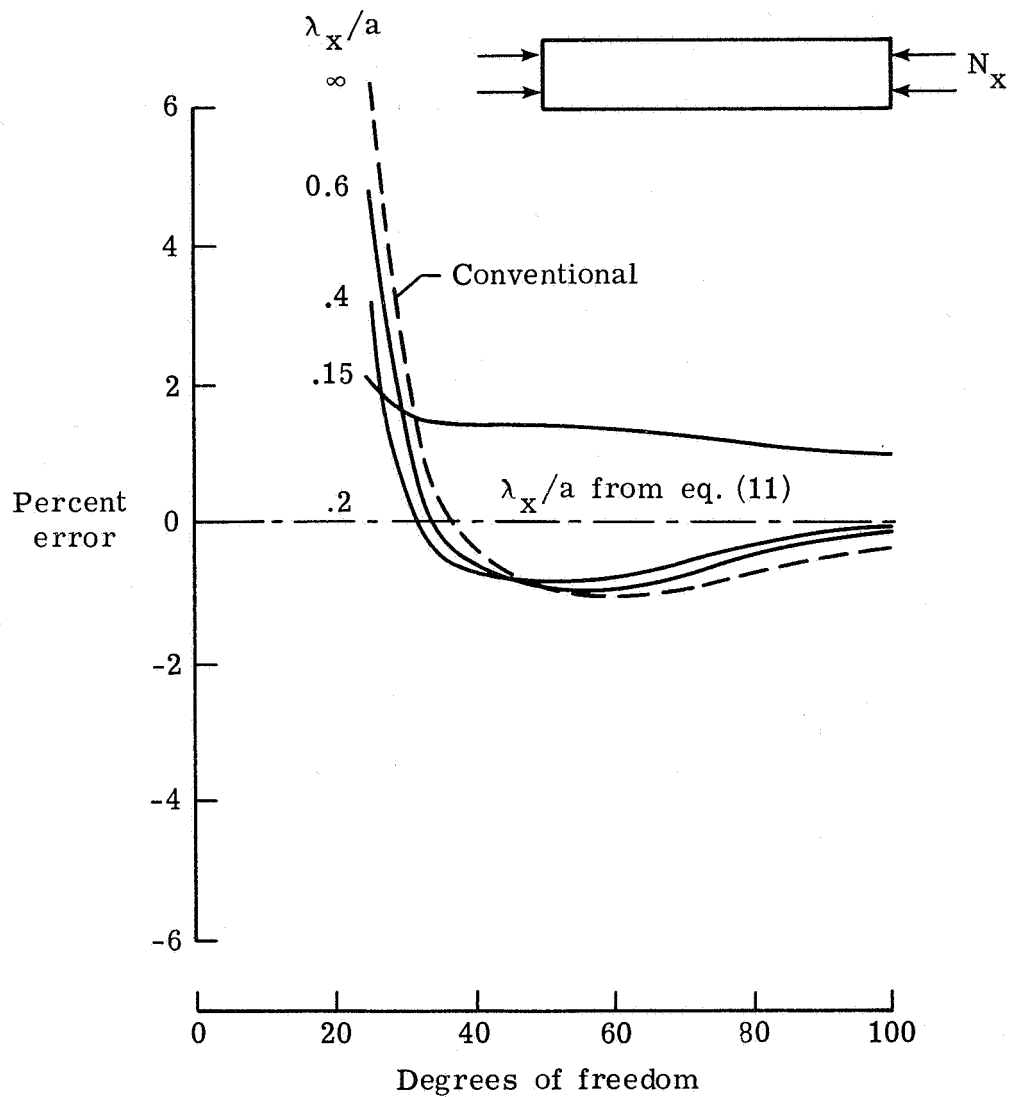
(c) $a/b = 5$.

Figure 16.- Concluded.



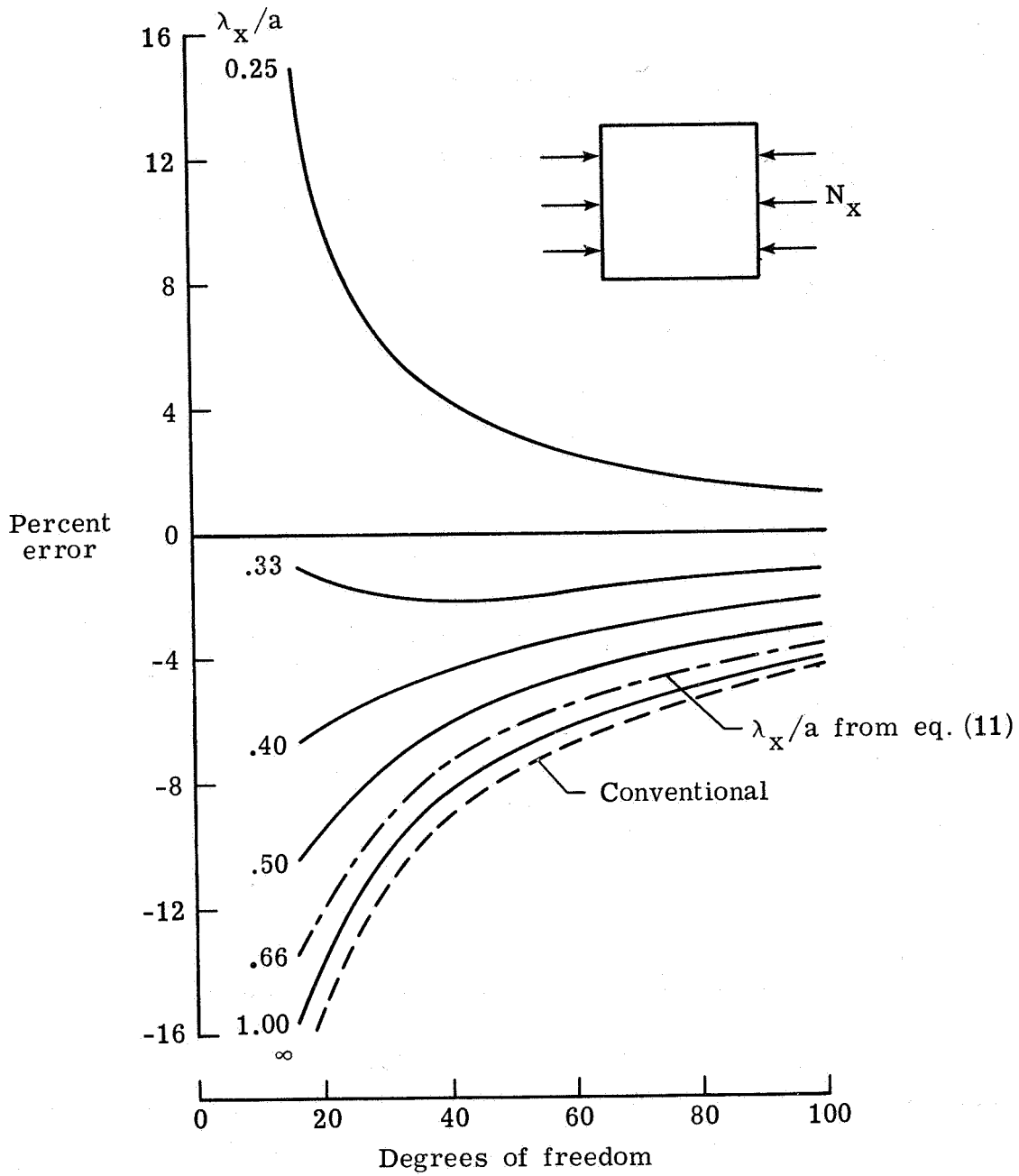
(a) Convergence for the compressive buckling of simply supported isotropic square panels. $\lambda_y/\lambda_x = \beta = 1$. From reference 6, $\bar{N}_x = 4.0$.

Figure 17.- Convergence characteristics of trigonometric finite differences.



(b) Convergence for the compressive buckling of 5×1 simply supported isotropic panels.
 $\lambda_y/\lambda_x = \beta = 5$. From reference 6, $\bar{N}_x = 4.0$.

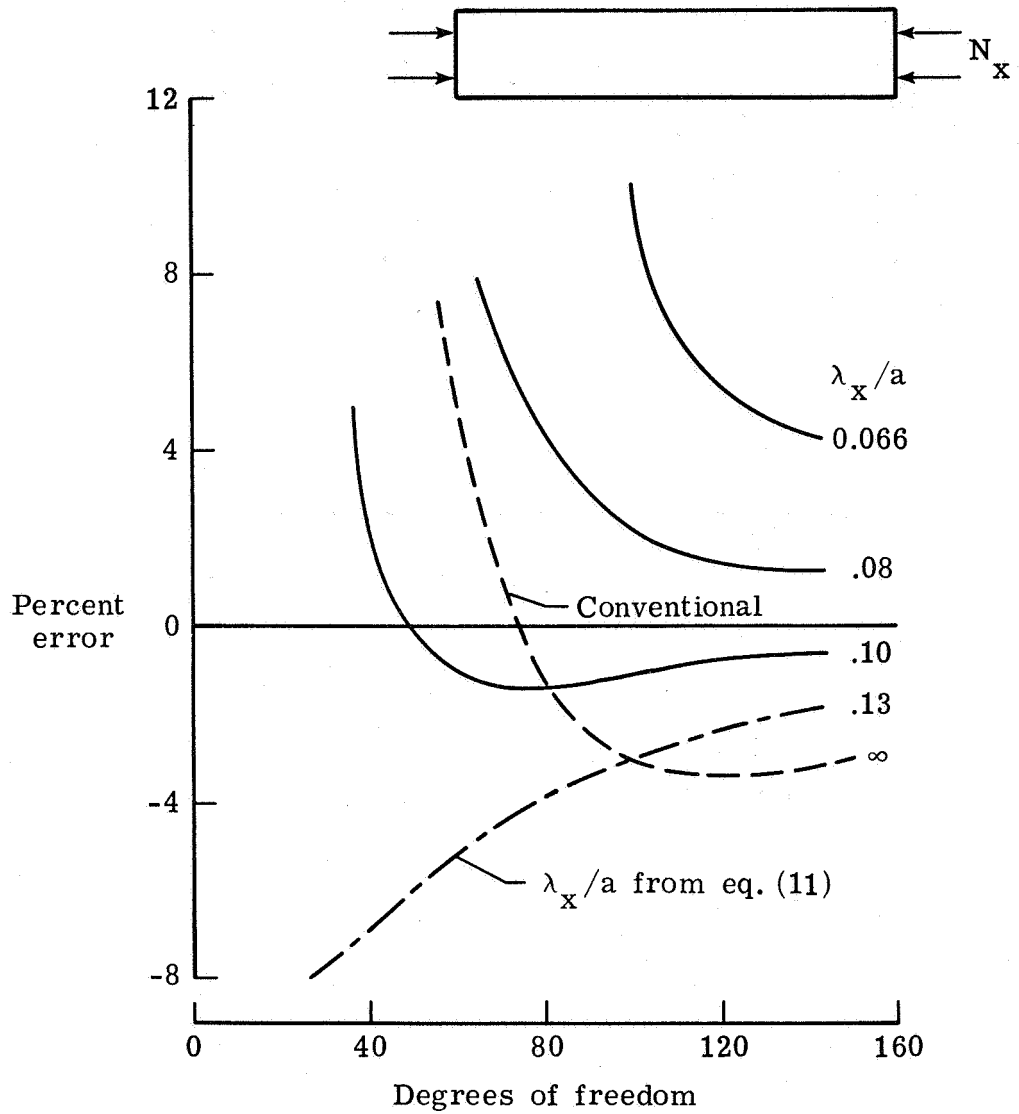
Figure 17.- Continued.



(c) Convergence for the compressive buckling of clamped square isotropic panels.

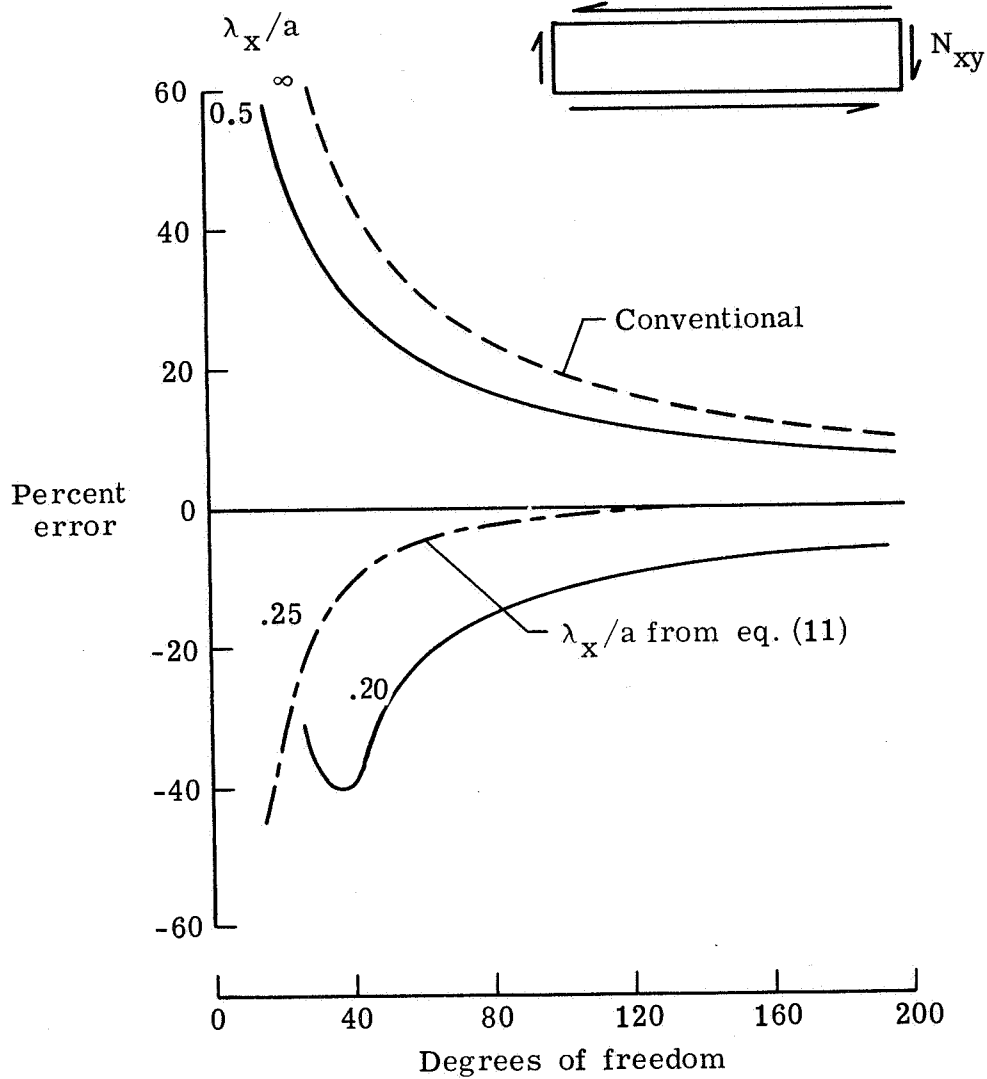
$\lambda_y/\lambda_x = \beta = 1.5$. From reference 17, $\bar{N}_x \approx 10.074$.

Figure 17.- Continued.



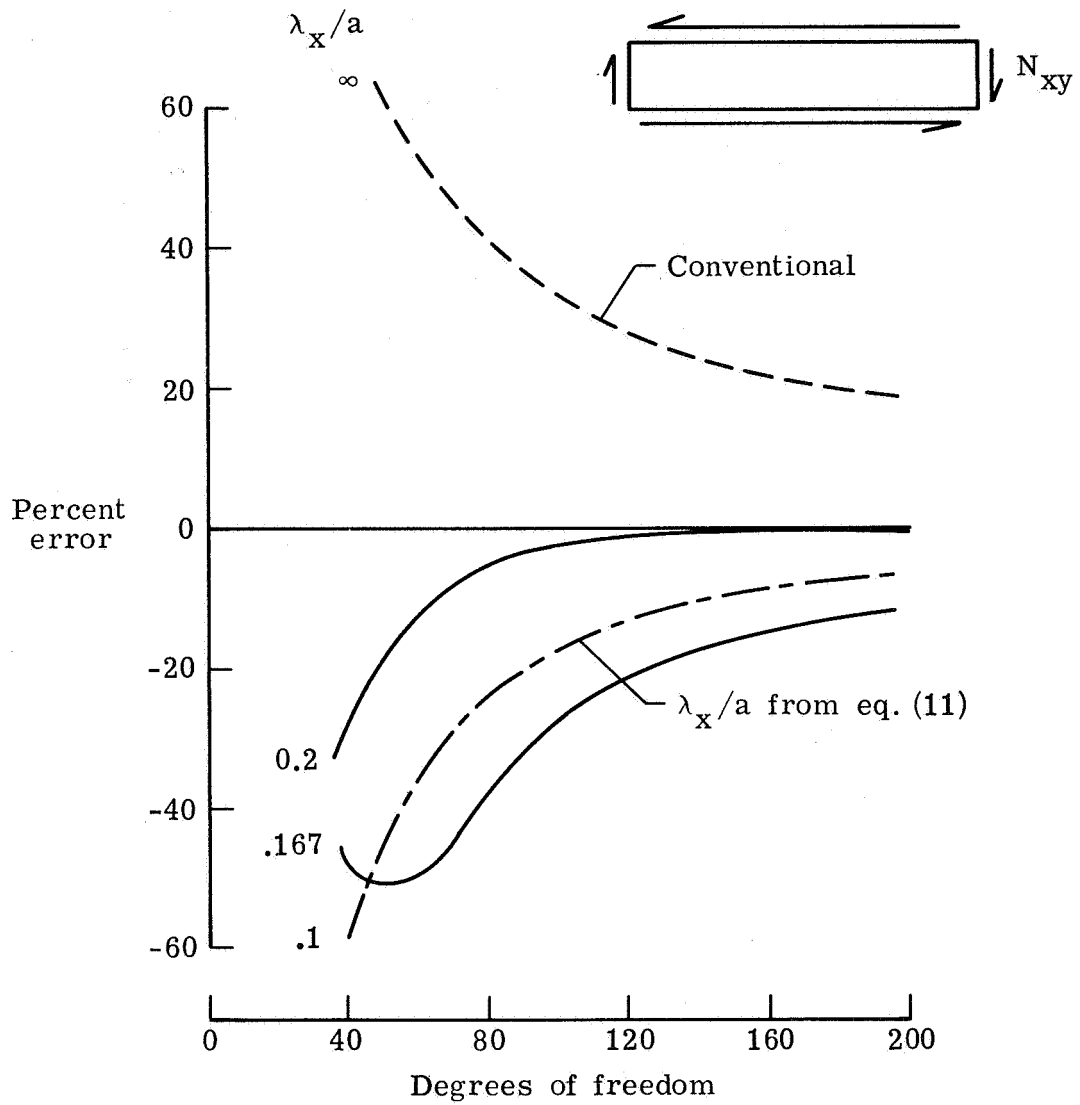
(d) Convergence for the compressive buckling of isotropic clamped 5×1 panels.
 $\lambda_y/\lambda_x = \beta = 1.5$. From reference 16, $\bar{N}_x \approx 7.0$.

Figure 17.- Continued.



(e) Convergence for the shear buckling of isotropic simply supported 5×1 panels.
 $\lambda_y/\lambda_x = \beta = 0.8$. From reference 1, $\bar{N}_{xy} \approx 5.55$.

Figure 17.- Continued.



(f) Convergence for the shear buckling of isotropic clamped 5×1 panels.
 $\lambda_y/\lambda_x = \beta = 1.2$. From reference 1, $\bar{N}_{xy} \approx 9.3$.

Figure 17.- Concluded.

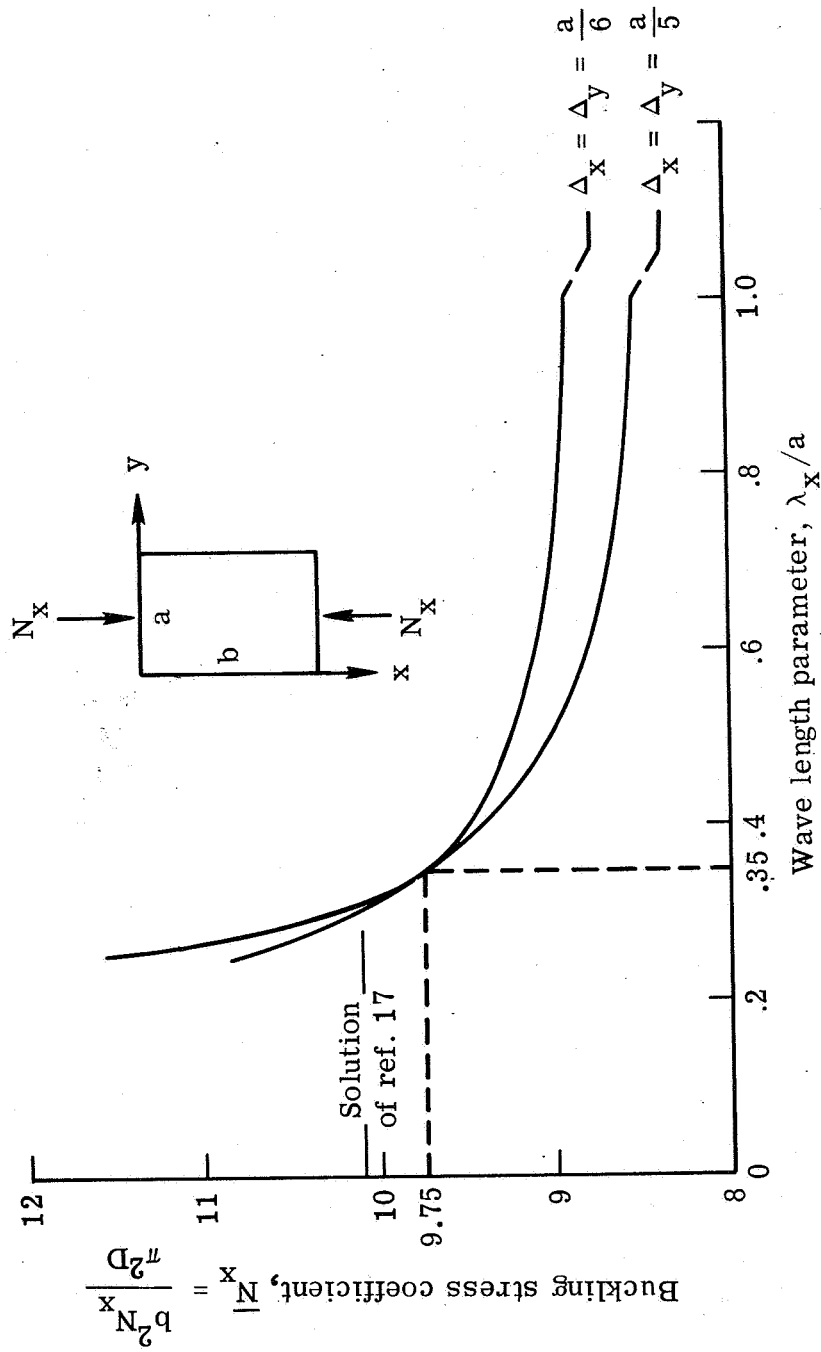


Figure 18.- Variation of buckling stress coefficient \bar{N}_x with trigonometric wavelength parameter λ_x/a for the compression buckling of a clamped square isotropic panel.

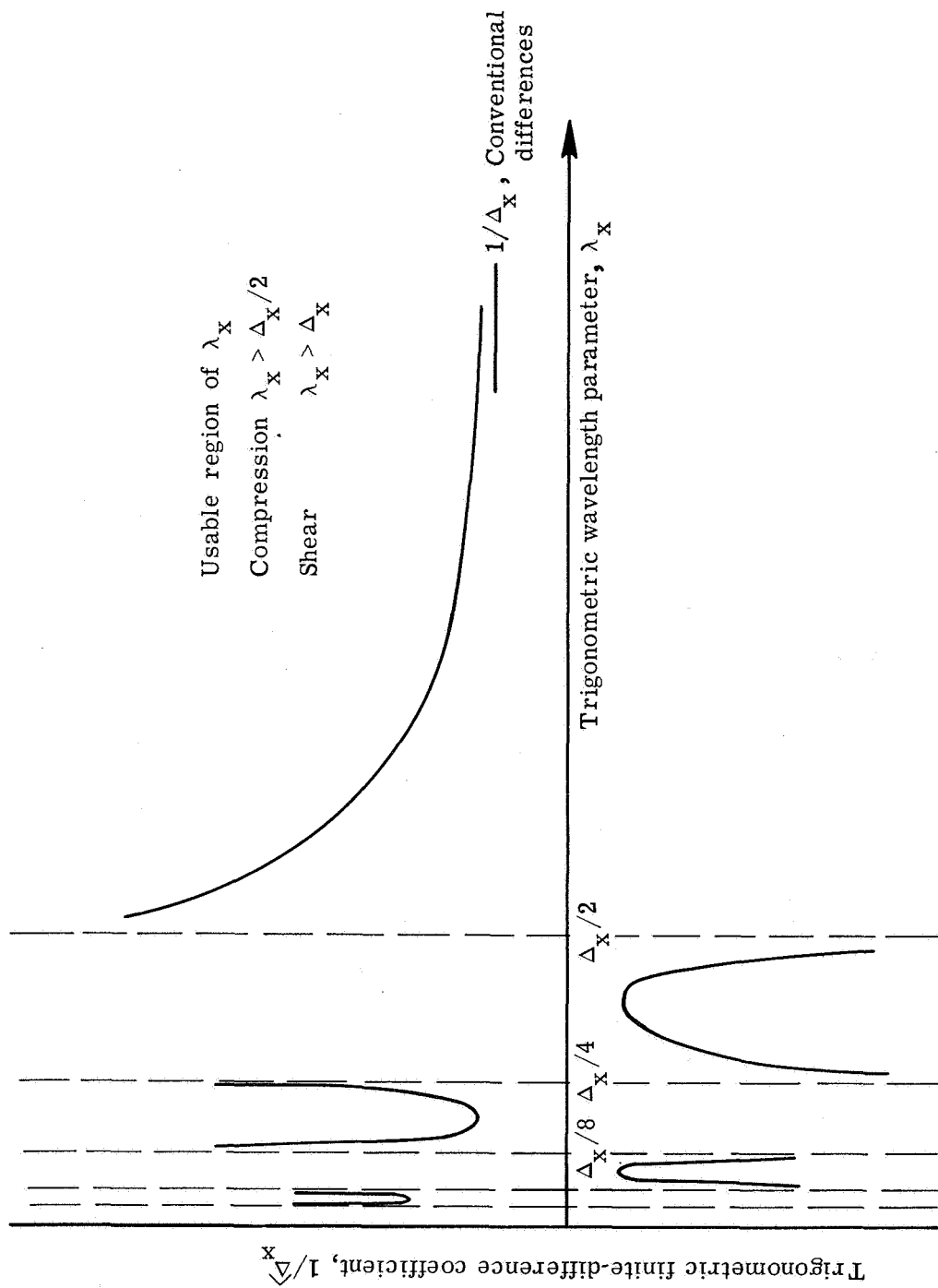


Figure 19.- Variation of $1/\Delta_x$ with trigonometric wavelength parameter λ_x .